2 mil

NASA TECHNICAL NOTE

NASA TN D-7474

NASA TN D-7474

WIND-TUNNEL TESTS OF A FULL-SCALE MODEL OF A LIGHT TWIN-ENGINE AIRPLANE WITH FIXED AUXILIARY AIRFOIL OR LEADING-EDGE SLOT

by Marvin P. Fink, James P. Shivers, and Lucy C. White

Langley Research Center
Hampton, Va. 23665

NATIONAL AERONAUTICS AND SPACE ADMINISTRATION • WASHINGTON, D. C. • APRIL 1974

For sale by the National Technical Information Service, Springfield, Virginia 22151

1. Report No.	2. Government Accession No.	3. Recipient's Catalog No.
NASA TN D-7474		

4. Title and Subtitle	5. Report Date
WIND-TUNNEL TESTS OF A FULL-SCALE MODEL OF A LIGHT TWIN-ENGINE AIRPLANE WITH FIXED AUXILIARY AIRFOIL OR LEADING-EDGE SLOT	April 1974
	6. Performing Organization Code

7. Author(s)	8. Performing Organization Report No.
Marvin P. Fink, James P. Shivers, and Lucy C. White	L-9225
	10. Work Unit No. 760-60-01-16
9. Performing Organization Name and Address	11. Contract or Grant No.
NASA Langley Research Center Hampton, Va. 23665	
	13. Type of Report and Period Covered
12. Sponsoring Agency Name and Address	Technical Note
National Aeronautics and Space Administration Washington, D.C. 20546	14. Sponsoring Agency Code

15. Supplementary Notes

16. Abstract

An investigation has been conducted by means of wind-tunnel tests of a full-scale mockup of a light twin-engine airplane configuration to determine the effects of outboard partial-span slots and of auxiliary airfoils ahead of the leading edge of the wing in improving aerodynamic characteristics at high angles of attack. Both of the stall-control devices gave considerable improvement in high angle-of-attack characteristics with the auxiliary airfoil giving the more favorable results, but neither device performed as well as might have been expected.

17. Key Words (Suggested by Author(s))	18. Distribution Statement
Light airplane Stalling Slats	Unclassified – Unlimited STAR Category 02

19. Security Classif. (of this report)	20. Security Classif. (of this page)	21. No. of Pages	22. Price
Unclassified	Unclassified	117	$4.50

WIND-TUNNEL TESTS OF A FULL-SCALE MODEL OF A LIGHT TWIN-ENGINE AIRPLANE WITH FIXED AUXILIARY AIRFOIL OR LEADING-EDGE SLOT

By Marvin P. Fink, James P. Shivers,
and Lucy C. White
Langley Research Center

SUMMARY

An investigation has been conducted by means of wind-tunnel tests of a full-scale mockup of a light twin-engine airplane configuration to determine the effects of outboard partial-span slots and of auxiliary airfoils ahead of the leading edge of the wing in improving aerodynamic characteristics at high angles of attack. Small-scale tests of full-span models of such leading-edge stall-control devices many years ago had indicated an increase in the stall angle of the airfoil of about 8°, with a very minimal increase in minimum drag, which would be of paramount interest for high-speed cruise. The object of the present investigation was to determine the extent of the improvements that could be obtained in the three-dimensional case of application of these devices only on the outboard part of the wing. Tests were made for a range of power settings for both flaps-up and flaps-down conditions.

Both of the stall-control devices gave considerable improvement in high angle-of-attack characteristics with the auxiliary airfoil giving the more favorable results, but neither device performed as well as might have been expected. The slot delayed the stall of the outboard part of the wing about 5° or 6°, flattened or extended the top of the lift curve, and caused the ailerons to maintain full effectiveness to about 5° higher angle of attack. But the slot increased the minimum drag of the model about 10 percent and did not diminish the large asymmetric rolling moments at the stall. The auxiliary airfoil also provided a flat-topped lift curve and improved aileron effectiveness at high angles of attack; it actually decreased the value of minimum drag slightly; and it reduced by about one-half the large asymmetric rolling moments at the stall. Tuft tests, however, indicated little delay in the stall of the outboard part of the wing, so that it might be questioned whether damping in roll would be maintained at the higher angles of attack.

INTRODUCTION

Stall/spin accidents constitute a sizable percentage of all accidents of general-aviation airplanes. Part of the problem is simply a matter of stalling and losing lift at an altitude so low that the airplane cannot gain sufficient speed to recover before striking the ground. Another part of the problem is one of serious roll-off at the stall due to roll asymmetry, unstable damping in roll, or loss of aileron effectiveness, which results in a much larger loss of altitude than a symmetrical stall, and may result in a spin. Stall-control devices such as wing slots and slats were researched extensively with considerable success by NACA (NASA), and others, during the 1920's and 1930's by means of flight tests and small-scale wind-tunnel tests. Hence, it was decided to investigate the application of some of the results of this research to a modern, twin-engine, light, general-aviation airplane as part of a current ongoing program of full-scale wind-tunnel research at the NASA Langley Research Center. The particular configuration chosen was one which had been found in previous full-scale wind-tunnel tests, reported in references 1 and 2, to have a rather rapid stall progression and decided aerodynamic asymmetry at the stall, particularly as a result of unsymmetrical stalling induced by rotation of the propeller slipstream.

The philosophy behind the investigation was to put on the outboard section of the wing simple fixed-geometry slots or auxiliary airfoils designed for low drag in the cruise condition and to determine the extent of the aerodynamic improvements at the stall. The improvements to be expected were a delay in the stall of the outboard part of the wing with the following beneficial effects:

(1) Root stall occurring markedly before stall of the outboard part of the wing should give a strong, early stall warning.

(2) Delay in stall of the outboard part of the wing would be expected to provide damping in roll and good aileron effectiveness beyond maximum lift.

(3) Possibly, resistance to spread of the asymmetric stalling may be caused by slipstream rotation to the outboard parts of the wing, with attendant reductions in asymmetric rolling and yawing moments at the stall.

One device tested was a fixed slot based on the low-drag slot research of references 3 and 4 which had been conducted, at small scale in one case and with a two-dimensional model in the other, using the Clark Y and NACA 23012 airfoil sections typical of the 1930 time period. Of course, the slot had to be reconfigured somewhat to fit the more modern NACA 6-series airfoil of the test airplane. Even though this slot was designed for low drag, the data of references 3 and 4 indicated an increase in minimum airfoil section drag of about 100 percent, which would correspond to an increase in minimum wing drag of about 40 percent for a partial-span slot or to an increase of about 8 percent in minimum drag of the complete airplane in the cruise condition. This increase in drag would result

in a reduction in cruise speed of about 2.5 percent, or 4 knots, for the test airplane. In return for this reduction in cruise performance, the data of reference 1 indicated an increase in the angle of attack for stall of 9° or 10° for the slotted part of the wing.

Although the cruise performance penalty for the slot was not high, it seemed that it might be eliminated altogether by the use of an auxiliary airfoil such as one of those investigated in references 5 and 6. These auxiliary airfoils were located much higher and farther ahead of the leading edge of the wing than conventional slats are; and the data of references 5 and 6 indicated that they could be located to give substantially no increase in drag, or perhaps even a small decrease in minimum drag, and would give almost as great an increase in airfoil stall angle (about 8°) as the slot.

It should be realized that the same type of improvements at high angles of attack could be expected, but to a lesser degree, from the use of wing twist, or washout, or from increased leading-edge camber toward the tip. The object of the present investigation, however, was to try to effect a much larger improvement than would ordinarily be expected from twist or camber distribution with simple fixed-geometry devices which would have low cruise drag.

The investigation was run on a full-scale model in the Langley full-scale tunnel at values of Reynolds number on the order of 2×10^6 to 3×10^6. The tests were made with the leading-edge devices extending from the nacelle to the wing tip, and with lesser spans of the stall-control devices by removing the inboard ends of the slot or auxiliary airfoils. Tests were made for both flap-up and flap-down conditions for a range of engine power settings (i.e., thrust coefficients).

SYMBOLS

Figure 1 shows the wind-axis system used in the presentation of the data and the positive direction of forces, moments, and angles. The data are computed about the moment center shown in figure 2 which is at 10 percent of the mean aerodynamic chord and 0.30 m (1.0 ft) below the reference line.

Measurements and calculations for this investigation were made in the U.S. Customary Units. They are presented herein in the International System of Units (SI) with the equivalent values in the U.S. Customary Units given parenthetically. Physical constants and conversion factors relating the two system of units used in this paper may be found in reference 7.

b	wing span, 10.97 m (35.98 ft)
C_D	drag coefficient, Drag/qS
C_L	lift coefficient, Lift/qS

C_l rolling-moment coefficient, Rolling moment/qSb

C_m pitching-moment coefficient, Pitching moment/qS$\bar{c}$

C_n yawing-moment coefficient, Yawing moment/qSb

C_Y side-force coefficient, Side force/qS

c wing chord, m (ft)

$\bar{c}$ wing mean geometric chord, 1.53 m (5 ft)

q free-stream dynamic pressure, N/m^2 (lb/ft^2)

S wing area, 16.54 m^2 (178 ft^2)

T effective thrust at $\alpha = 0^o$,
$(Drag)_{propellers\ removed} - (Drag)_{propellers\ operating}$

T'_c thrust coefficient, T/qS

V free-stream velocity, m/sec (ft/sec)

α angle of attack of fuselage reference line, deg

δ_a aileron deflection (right aileron only), positive when trailing edge is down

δ_f flap deflection, positive when trailing edge is down, deg

θ vertical angularity of tunnel airstream, positive values indicate upwash, deg

$C_{l_{\delta a}} = dC_l/d\delta_a$

$C_{n_{\delta a}} = dC_n/d\delta_a$

$\Delta C_{l,a} = C_{l(\delta_a=15)} + C_{l(\delta_a=-19)}$

Subscripts:

max maximum

min minimum

MODEL

The model tested was a full-scale mockup of a light twin-engine low-wing monoplane. The basic model was the same as that previously tested in reference 2; and the configuration was the same as that tested in reference 1, although the actual model was not the same. Figure 2 presents a three-view drawing of the model and gives the principal dimensions; and figure 3 presents photographs showing the model mounted in the tunnel. The model had a wing span of 10.97 m (35.98 ft), a wing area of 16.54 m^2 (178 ft^2), and a mean geometric chord of 1.53 m (5 ft) based on projection of the outboard leading edge of the wing through the fuselage. The wing section was a modified NACA 64_2A215 airfoil. The wing was designed to have 5° dihedral, no twist, and a 2° positive incidence with respect to the fuselage reference line. The wing had a constant-chord single-slotted flap of 0.355 m (1.16 ft) chord. The thrust axes were parallel to the fuselage reference line. For these tests the horizontal tail and the rudder were fixed at zero deflection. The ailerons were rigged such that the left aileron was locked at zero deflection and only the right aileron was movable. The right aileron had a deflection range from -19° to 15°.

The wing section was modified to incorporate the fixed leading-edge slot as shown in figure 4(a). The design of the slot was based on data of reference 4. These data were at odds with data of reference 3 as to what design features were optimum for low drag, so the design of the present slot was based on the tests of reference 4 which were run at effectively full scale. Provision was made for sealing and fairing over the slot, and also for mounting an auxiliary airfoil as shown in figure 4(b). The slot was faired over with 0.032-thick sheetmetal and sealed for tests with the basic leading edge and for tests with the auxiliary airfoil. Similarly, the mounting brackets for the auxiliary airfoil, except the one beside the nacelle, were removed for tests with the basic leading edge or with the slot. The auxiliary airfoil had a chord of 0.15c and an NACA 0008 airfoil section. A symmetrical section was chosen for the auxiliary airfoil on the basis of data from reference 6, which shows that symmetrical sections resulted in lower values of minimum drag and higher values of $C_{L_{max}}^2/C_{D_{min}}$ than did cambered sections. The auxiliary airfoil could be located at heights above the wing chord of 3, 6, 9, and 12 percent chord and at distances of 5, 10, and 15 percent chord ahead of the wing leading edge. It could also be adjusted in incidence relative to the wing chord to angles of 2.5°, 0°, -2.5°, -5.0°, and -7.5° (positive angles being nose up). The trailing edge of the auxiliary airfoil was the reference point for vertical and horizontal location and was the pivot point of the angular settings. As will be explained later, a location for the auxiliary airfoil of 0.15c ahead of and 0.12c above the leading edge of the wing, and an incidence of -5°, were selected during preliminary tests and were maintained during the remainder of the tests, including all tests for which data are presented herein. Both the slot and the auxiliary airfoil extended outboard from the engine nacelle to the wing tip and were divided into three sections as

shown in figure 4(c). The various spanwise configurations tested are designated herein by their span, the 0.21b/2 device being only the outboard segment, the 0.41b/2 device being the outboard two segments, and the 0.58b/2 device being all three segments.

TESTS

The tests were made in the Langley full-scale tunnel, which is described in reference 8. Conventional static force tests were made to determine the force and moment characteristics of the model, and tuft tests were made to study the stall progression.

The test program was set up to investigate the effects of the slot and the auxiliary airfoil in providing improved aerodynamic characteristics at and beyond the stall; in particular, to investigate the effects of these stall-control devices in minimizing asymmetric rolling and yawing moments at and beyond the stall, in maintaining aileron effectiveness beyond the stall, and in delaying stall of the outboard sections of the wing. Such delay of the stall, of course, has implications of maintaining damping in roll and yielding a strong stall warning with heavy inboard stall at angles of attack markedly below those for any loss of lift or lateral controllability. Increase in maximum lift was not an objective of the tests since the same undesirable characteristics might simply occur at a higher lift coefficient if the airfoil stall angle were increased uniformly across the span.

Preliminary tests were made with the 0.58b/2 auxiliary airfoil over the full matrix of airfoil location and angle to determine the optimum configuration. These tests were made with propellers removed and covered a range of airfoil angles of 2.5°, 0°, -2.5°, -5.0°, and -7.5° at each horizontal position (5, 10, and 15 percent chord ahead of the wing leading edge) and each vertical position (3, 6, 9, and 12 percent chord above the wing chord) of the auxiliary airfoil. The criteria used in selection of an optimum configuration were: (1) maximum increase in angle of attack achieved before the stall, as indicated by tuft tests, progressed outboard of the 0.57b/2 spanwise station, and (2) minimum increase in drag at cruise lift coefficient $\left(C_L \text{ of } 0.2 \text{ to } 0.3\right)$. The variation of these parameters with vane position gave a broad range of near-optimum positions; and a vane position of 0.15c ahead of and 0.12c above the wing leading edge, with a vane angle of -5°, was selected.

With the auxiliary airfoil position selected in the preliminary tests, the main body of the tests was made with various spanwise segments of the auxiliary airfoil over an angle-of-attack range of -4° to 24° at thrust coefficients of 0, 0.20, and 0.44 for both the flap-up and flap-down conditions. For all flap-down tests the landing gear was also down. The thrust coefficients of 0, 0.20, and 0.44 represent flight conditions of low power or high speed (where the thrust coefficient approaches zero), normal climb at about 90 percent power, and climb at a lower speed with full power as in take-off or wave-off conditions, respectively.

For the leading-edge slot tests, the auxiliary airfoil was removed; and basically the same test conditions that were run for the auxiliary airfoil were repeated, except that propeller-on tests were made only for a 0.41b/2 slot span because of the limited test time available.

A propeller-blade-angle setting of 20° was used for all the tests. The thrust coefficient was set by adjusting the propeller speed to obtain the required thrust for the test condition at $\alpha = 0^{\circ}$, and this propeller speed was maintained as α was varied. All the tests, except those at a thrust coefficient of 0.44, were made at a tunnel speed of 28.35 m/sec (93 ft/sec) which resulted in a Reynolds number of approximately 2.96×10^6 based on a mean geometric chord of 1.53 m (5 ft). Tests at 0.44 thrust coefficient were made at a tunnel speed of 19.2 m/sec (63 ft/sec) which resulted in a Reynolds number of 2.05×10^6. Prior to the actual tests of the model, a calibration of the tunnel airstream angularity was made. The results of this calibration are given in figure 5.

PRESENTATION OF DATA

The data are presented in the following figures:

The longitudinal data have been corrected for blockage, airstream misalinement, buoyancy effects, mounting strut tares, and wind-tunnel jet-boundary effects. The lift and drag have been corrected for the integrated average airstream misalinement. The lateral data are not corrected for lateral variation of stream angle. It should be pointed out, however, that most of the positive rolling moment noted at the lower angles of attack can be attributed to lateral variation of the tunnel stream angles as shown in figure 5. Calculations of section rolling moments using the spanwise variations of stream angle of figure 5 indicate that the total measured out-of-trim rolling moment could be approximately accounted for by airstream angularity.

The results of the tuft tests were recorded by photographs, but the photographs could not be reproduced in this document with sufficient clarity for analysis. Hence, stall patterns were determined from large glossy prints and plotted in figures 6 to 11 to show areas of stall at each test angle of attack from 12° to 24°. In the shaded areas indicated as being stalled, the tufts had one of the following characteristics:

(1) Tufts indicated a flow forward along the wing,

(2) Tufts were standing up off the surface,

(3) Tufts were waving so violently as to be indiscernible, or

(4) Tufts were limp and curved and indicated essentially no airflow.

It should be noted that the patches of stall on the ailerons near the midspan and inboard end of the ailerons at 12° and 14° angle of attack are behind the slot and auxiliary airfoil support brackets and probably reflect disturbances from these sources. It should also be noted that the paths of unstalled flow generally over the nacelles at high angles of attack involved marked spanwise flow angularity (up to 60°) as though the surface might be being wiped by a vortex; and it also seemed that the flow in these areas had very little energy so that in some senses it might have been effectively stalled.

RESULTS AND DISCUSSION

Stall Progression

The tuft-test results for the basic leading edge (figs. 6(a), 7(a), 10(a), and 11(a)) show the unsymmetrical nature of the stall, starting on the left side of the nacelles, caused by propeller slipstream rotation for the higher power conditions $\left(T_C' = 0.20 \text{ and } 0.44\right)$. For these power-on conditions, especially with flaps down, the stall progressed far outboard on the left wing before there was significant outboard stall of the right wing. This characteristic was observed in reference 1 and was identified as the cause of large asymmetric rolling moments at the stall.

The data of figures 6 to 11 show that the slot had a pronounced effect in delaying the stall of the outer part of the wing, principally that behind the slot or ahead of the ailerons. This was qualitatively the effect sought from the slot, but the quantitative effect of the slot was less than that indicated by the tests of references 3 and 4 with a full-span slot. In the reference tests, an increase of about 9° or 10° in angle of attack for the stall was obtained with the slot. Study of the results of the present tuft tests, however, shows an increase of about 6° or 7° $\left(\text{actually only } 3^{\circ} \text{ for the } \delta_f = 27^{\circ}, T_C' = 0.44 \text{ condition}\right)$ in the angle of attack for stall of the slotted portion of the wing was obtained. Such an effect is to be expected because the low-aspect-ratio partial-span nature of the slotted part of the present wing lets stall from the adjacent part of the wing influence, and creep onto, the slotted part of the wing.

Although the tuft-test results for the slotted wing were encouraging, those for the auxiliary-airfoil configurations were discouraging. The auxiliary airfoils generally provide only about a 3° or 4° delay in the angle of attack for stall of the outboard part of the wing (the part ahead of the ailerons); and, indeed, this delay was only 1° for the 0.41b/2 slat with $\delta_f = 27^{\circ}, T_C' = 0.44$. This rather small delay in the stall was markedly less than the approximately 8° delay indicated by the tests of references 5 and 6 with a full-span auxiliary airfoil.

There is an implication in the foregoing results that the auxiliary airfoil might be less effective than the slot in maintaining damping in roll at high angles of attack. Most of the other aerodynamic characteristics at high angles of attack that one might desire to

analyze can be determined from the force tests, in which case the tuft tests are an aid in analysis; but the stall patterns are the principal indication as to whether the lift-curve slope of the outer parts of the wing, and consequently the damping in roll, was maintained at high angles of attack.

Longitudinal Characteristics

Basic leading edge.- The longitudinal aerodynamic characteristics of the basic leading-edge configuration are presented in figures 12 and 13. These data compared with the results of reference 2 show good agreement, which indicates that the modification to the leading edge of the wing did not significantly affect the basic characteristics of the model.

Slots.- The effects of the leading-edge slots on longitudinal characteristics are shown in figures 14 to 17. Figure 17 is a replot of lift data from figures 13 and 16 for direct comparison of data for the basic leading edge and the 0.41b/2 slot for power-on conditions. The data show very little effect of the slots on pitching moment, as would be expected. They generally show only small, and in some cases inconsistent, effects on lift at low angles of attack (up to 10° or 12°). Close study of the lift data at high angles of attack, however, generally shows that with the slots there are pronounced breaks in the lift-curve slopes at the same angle of attack at which the stall occurred with the basic leading edge. At higher angles of attack, however, the slotted configurations generally produced more lift than the basic wing, with the result that, in general, there was no significant loss in lift until the angle of attack was 5° to 10° higher than that for the stall of the basic wing. The fact that the lift curves all showed a pronounced break at the same angle of attack as the maximum lift, or stall, of the basic wing was probably due to the fact that the stall started inboard on the wing for both slotted and unslotted configurations, as shown by the tuft test results of figures 6 to 11. The effect of the slots in delaying stall of the outer parts of the wing influenced by the slots, which constitutes less than one-half the wing area, adds a small increment of lift at angles of attack above the normal stall angle. Depending on the span of the slot system, and its effectiveness, this additional lift sometimes causes the total lift to increase and sometimes only prevents a loss in lift, that is, gives a more flat-topped lift curve.

The enlarged plots of drag data presented in figure 15 show that the slot caused an increase in minimum drag, as expected on the basis of the data of references 3 and 4. The magnitude of the increase in drag, however, was slightly greater than that expected, with the result that the use of the 0.41b/2 slot caused a 10-percent increase in total model drag, which would correspond to a reduction in cruise speed of about 5 knots, rather than the 2 to 4 knots anticipated. The reason for this higher drag increment due to the slot was not established.

With regard to the effect of the slots on drag at higher angles of attack, the data of figure 14 show that the slots caused no increase in drag and that the longer span slots actually gave a small reduction in drag.

Auxiliary airfoils.- The effects of the auxiliary airfoils on longitudinal characteristics are shown in figures 18 to 21. The data show that the auxiliary airfoils had generally the same effects on lift and pitching moment as the slots. Quantitatively, however, the effect of the auxiliary airfoils in increasing lift at high angles of attack was less than that of the slots. This result is in agreement with the results of the tuft tests presented in figures 6 to 11 which showed that the auxiliary airfoils were less effective in delaying stall of the outboard parts of the wing.

The enlarged drag plots presented in figure 19 show that, in general, the larger auxiliary airfoils caused a small decrease in drag at angles of attack of 0° to -1°, which correspond to the cruise condition. If the decrease in drag seems surprising, one should keep in mind the fact that the auxiliary airfoils are operating in the upwash ahead of the wing so that it is possible for their lift vector to be tilted forward to offset their profile drag. The particular order of the curves in figure 19 requires some explanation. The basic-leading-edge configuration included the inboard auxiliary-airfoil bracket, right beside the nacelle. All the remaining auxiliary-airfoil brackets and the 0.21b/2 auxiliary airfoil were added; and the result was an increase in drag (because of the drag of the brackets). When the 0.41b/2 auxiliary airfoil was added, there were no extra brackets as compared with the basic-leading-edge configuration; and there was a small net reduction in drag as compared with the basic-leading-edge configuration. The 0.58b/2 auxiliary airfoil was added (again there were no extra brackets) and there was a larger net reduction in drag. These results indicate that the auxiliary airfoils produced a forward component of force; but, in the case of the 0.21b/2 auxiliary airfoil, it was not large enough to offset the drag of the extra auxiliary-airfoil mounting bracket.

With regard to drag at the higher angles of attack, the data of figure 18 show that the auxiliary airfoils caused a small increase in drag. This increase in drag might be largely the result of stall of the auxiliary airfoil itself which the tuft tests showed occurred between 8° and 10° angle of attack.

Lateral Characteristics

The basic lateral data are presented in figures 22 to 29, and the rolling-moment coefficient data from these figures are replotted in the summary figures 41 to 46 for convenience in comparison.

Basic leading edge.- The data for the basic-leading-edge configuration are presented in figures 41 and 42. The results of these tests are not in good agreement with those of references 1 and 2, particularly for the flap-down power-on conditions. The data of refer-

ences 1 and 2 show a very abrupt buildup of unsymmetrical rolling moment over an angle-of-attack range of only 1° or 2° at the stall; whereas, the present data show a much more gradual buildup (over 6° or 8°) to about the same value of unsymmetrical rolling moment. The data of figure 41 show that with the propellers removed, the rolling moments for both the flap-up and flap-down configurations are essentially constant over the angle-of-attack range, even through the stall which occurs at 12° to 14°. This result indicates symmetrical wing stall, and observation of tufts on the wing during the tests confirmed these findings.

With power on, the rolling moments presented in figure 42 showed considerable variation with angle of attack; and they became fairly large and showed abrupt changes at the stall ($\alpha = 16^{\circ}$ to 18°) for the flap-down configuration at $T_C' = 0.20$ and 0.44. These large asymmetric rolling moments were one of the principal concerns that led to the present investigation. The maximum values of rolling-moment coefficient of -0.03 or -0.04 would correspond approximately to complete stall of about three-fourths of the left wing outboard of the nacelle with no corresponding stall of the right wing. Or, in other terms, the asymmetric rolling moments were about as large as, or in some cases larger than, could be produced by full aileron deflection. The result of such a situation is that the wings could not be kept level at the stall, even with full aileron deflection in straight (zero sideslip) flight.

Slots.- A comparison of the rolling-moment coefficients of the various leading-edge slot configurations with those for the basic leading edge with propellers removed is presented in figure 43 for the flap-up and flap-down conditions. These data show that the rolling moments were small and the slots had no significant effect on the rolling moments over the angle-of-attack range.

Figure 44 presents a comparison of the 0.41b/2 leading-edge slot and the basic-leading-edge configurations for power-on conditions. These data show that for most cases the rolling moments, and rolling-moment variations with α, are no less for the slotted configurations than for the basic configuration. In fact, in some cases they are greater. This result is surprising, particularly in view of the fact the tuft test results of figures 6 to 11 showed the outer parts of the wing, which would be expected to make the major contribution to the rolling moments, to remain unstalled to an angle of attack of 22°, and in some cases 24°. It would not seem that unsymmetrical stalling of the inboard part of the wing could account for the large rolling moments measured for the model with slots. Hence, no explanation for this result can be offered.

Auxiliary airfoils.- The data for the auxiliary-airfoil configurations are presented in figure 45 for the propeller-removed condition. These data show that with the propeller removed the rolling-moment coefficients are generally small and not appreciably affected by the various spanwise segments of the auxiliary airfoil over the angle-of-attack range.

The data for the power-on conditions are presented in figure 46. Figure 46(a) shows that with flaps up the rolling moments are generally small and only at the highest thrust coefficient $T_c' = 0.44$ does the auxiliary airfoil have any significant effect on the rolling moments.

With the flaps deflected and power on, the 0.21b/2 and 0.58b/2 auxiliary airfoils markedly reduced the rolling moments at the stall for all the thrust coefficients of the test. The 0.41b/2 auxiliary airfoil, however, did not result in any significant reduction in rolling moments as compared with those for the basic leading edge.

Aileron effectiveness.- The basic aileron effectiveness data are presented in figures 30 to 40 and are summarized in figures 47 to 53 for convenience in analysis. It must be pointed out again that the aileron data are for one control; that is, only the right aileron was moved. The left aileron was fixed at zero deflection. Figures 47 to 52 present slope values $C_{l_{\delta a}}$ and $C_{n_{\delta a}}$ for small aileron deflections, and figure 53 presents the difference in rolling moment between full-up and full-down aileron deflection. This value of $\Delta C_{l,a}$ would correspond to the rolling moment due to full aileron deflection if the effectiveness of the right and left aileron were the same. The values of $\Delta C_{l,a}$ for the basic leading edge were taken from reference 1 and are for a slightly smaller aileron deflection than that used in the present investigation, 14° down and 18° up instead of the present values of 15° down and 19° up.

Individual data points are somewhat erratic, as rolling-moment data generally are, especially near the stall; but the data, especially those of figure 53, generally show that both the slot and the two larger span auxiliary airfoils caused the aileron effectiveness to be maintained to significantly higher angles of attack than was the case for the basic leading edge. With these stall-control devices, the ailerons generally maintained full control effectiveness of $\Delta C_{l,a}$ approximately -0.04 up to about 18° or 19° angle of attack as compared with about 13° or 14° angle of attack for the basic leading-edge configuration.

With regard to aileron yawing moments, the data of figures 47 to 52 show that the ailerons produced increasing adverse yawing moments with increasing angle of attack and that there was no significant effect of the leading-edge stall control device on this adverse yawing moment.

With regard to damping in roll, the fact that aileron effectiveness was maintained to high angles of attack without undue increase in adverse yawing moments might be taken to indicate that the outer parts of the wing maintained lift-curve slope up to these same high angles of attack and would, consequently, maintain damping in roll. It should be noted, however, that the aileron effectiveness at high angles of attack with the auxiliary airfoils was less than that with the slots. This result is in agreement with the results of the tuft tests which showed more stalling of the outboard parts of the wing with the auxiliary air-

foils and might be taken to indicate that damping in roll would be maintained at high angles of attack by the auxiliary airfoils, but to a lesser degree than by the slots.

CONCLUSIONS

A full-scale wind-tunnel investigation was made to determine the effect of partial-span fixed leading-edge slots and auxiliary airfoils in improving the aerodynamic characteristics of a mockup of a light twin-engine airplane at high angles of attack with a minimum penalty in cruise performance. Neither of the stall-control devices performed as well as might have been expected, but the auxiliary airfoil gave the more favorable results. Specifically, the results with regard to the various problems investigated showed the following effects of the leading-edge stall-control devices:

1. Tuft tests showed that the slot provided an increase of about 6° or 7° in the angle of attack at which the outboard part of the wing, essentially that ahead of the ailerons, stalled. The auxilairy airfoils, however, provide only about 3° or 4° increase in the stall angle of this part of the wing. With either device there was extensive stall of the inboard part of the wing long before the tips stalled, which is a desirable result; but there is an implication in the lesser delay in tip stall resulting from use of the auxiliary airfoil that it might be less successful than the slot in maintaining damping in roll at high angles of attack.

2. With either the slot or auxiliary airfoil there was a marked break in the slope of the lift curve as a result of stall of the inboard part of the wing at the same angle of attack at which stall occurred with the basic leading edge. At higher angles of attack, the additional lift provided by the outboard leading-edge stall-control devices caused the lift curves to have much flatter tops than the lift curve of the basic wing, or, perhaps, to actually increase in lift and give a higher maximum lift coefficient.

3. The auxiliary airfoil caused no increase in minimum drag; in fact, it produced a small decrease in drag, evidently because it was operating in the upwash ahead of the wing. The slot, however, caused an increase of about 10 percent in the minimum drag of the whole airplane. This was a slightly greater drag increase than was expected on the basis of small-scale research done many years ago with a different airfoil.

4. With the basic wing leading edge, the model had large asymmetric rolling moments at the stall with flaps down and high thrust settings. The auxiliary airfoil reduced the magnitude of these asymmetric rolling moments by about one-half; but the slot did not cause any such reduction. In fact, the asymmetric rolling moments at the stall were slightly larger with the slot than with the basic leading edge for the power-on conditions.

5. Aileron effectiveness at high angles of attack was markedly improved by the use of either the slot or auxiliary airfoil, full control effectiveness being achieved to about 5° higher angle of attack than with the basic leading edge.

Langley Research Center,
National Aeronautics and Space Administration,
Hampton, Va., December 6, 1973.

REFERENCES

1. Fink, Marvin P.; and Freeman, Delma C., Jr.: Full-Scale Wind-Tunnel Investigation of Static Longitudinal and Lateral Characteristics of a Light Twin-Engine Airplane. NASA TN D-4983, 1969.

2. Fink, Marvin P.; Shivers, James P.; Greer, H. Douglas; and Megrail, James L.: The Effects of Configuration Changes on the Aerodynamic Characteristics of a Full-Scale Mockup of a Light Twin-Engine Airplane. NASA TN D-6896, 1972.

3. Weick, Fred E.; and Wenzinger, Carl J.: The Characteristics of a Clark Y Wing Model Equipped With Several Forms of Low-Drag Fixed Slots. NACA Rep. 407, 1932.

4. Bamber, M. J.: Wind-Tunnel Tests of Several Forms of Fixed Wing Slot in Combination With a Slotted Flap on a NACA 23012 Airfoil. NACA TN 702, 1939.

5. Weick, Fred E.; and Bamber, Millard J.: Wind-Tunnel Tests of a Clark Y Wing With a Narrow Auxiliary Airfoil in Different Positions. NACA Rep. 428, 1932.

6. Weick, Fred E.; and Sanders, Robert: Wind-Tunnel Tests on Combinations of a Wing With Fixed Auxiliary Airfoils Having Various Chords and Profiles. NACA Rep. 472, 1933.

7. Mechtly, E. A.: The International System of Units – Physical Constants and Conversion Factors (Second Revision). NASA SP-7012, 1973.

8. DeFrance, Smith J.: The NACA Full-Scale Wind Tunnel. NACA Rep. 459, 1933.

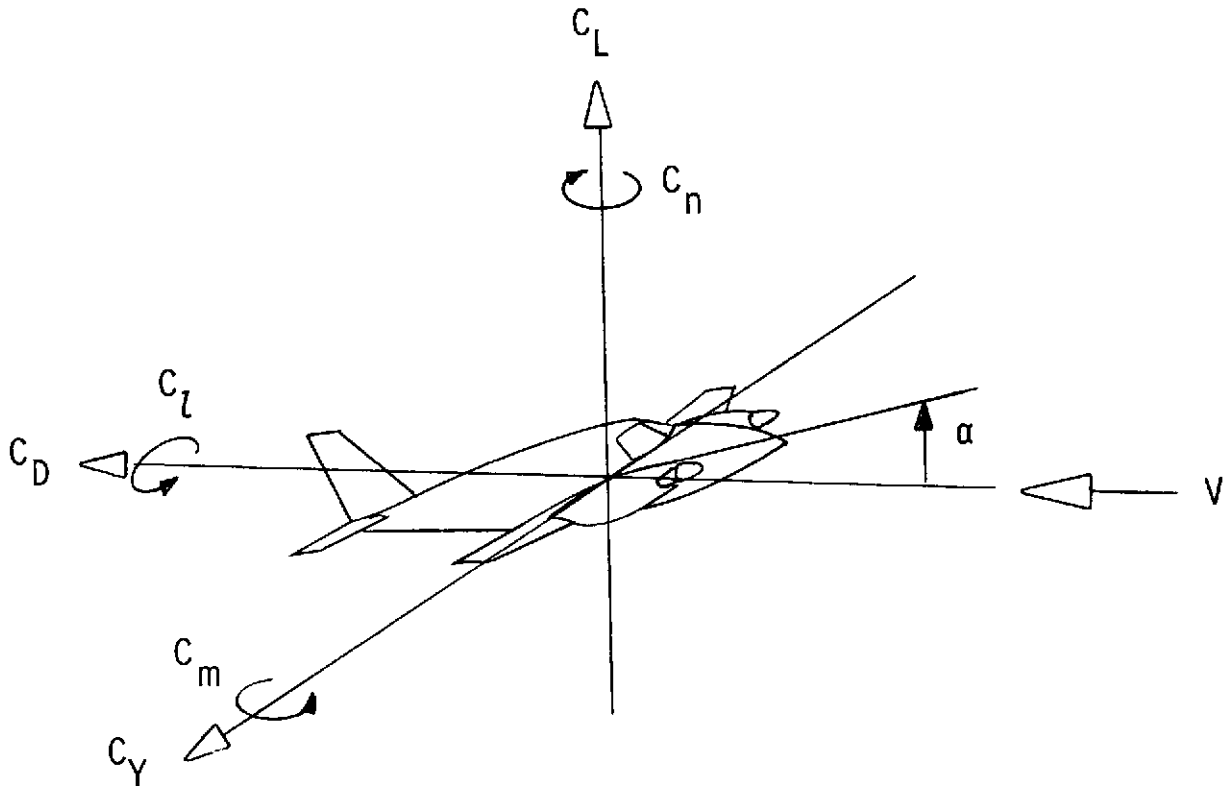

Figure 1.- System of axes and positive sense of angles, forces, and moments.

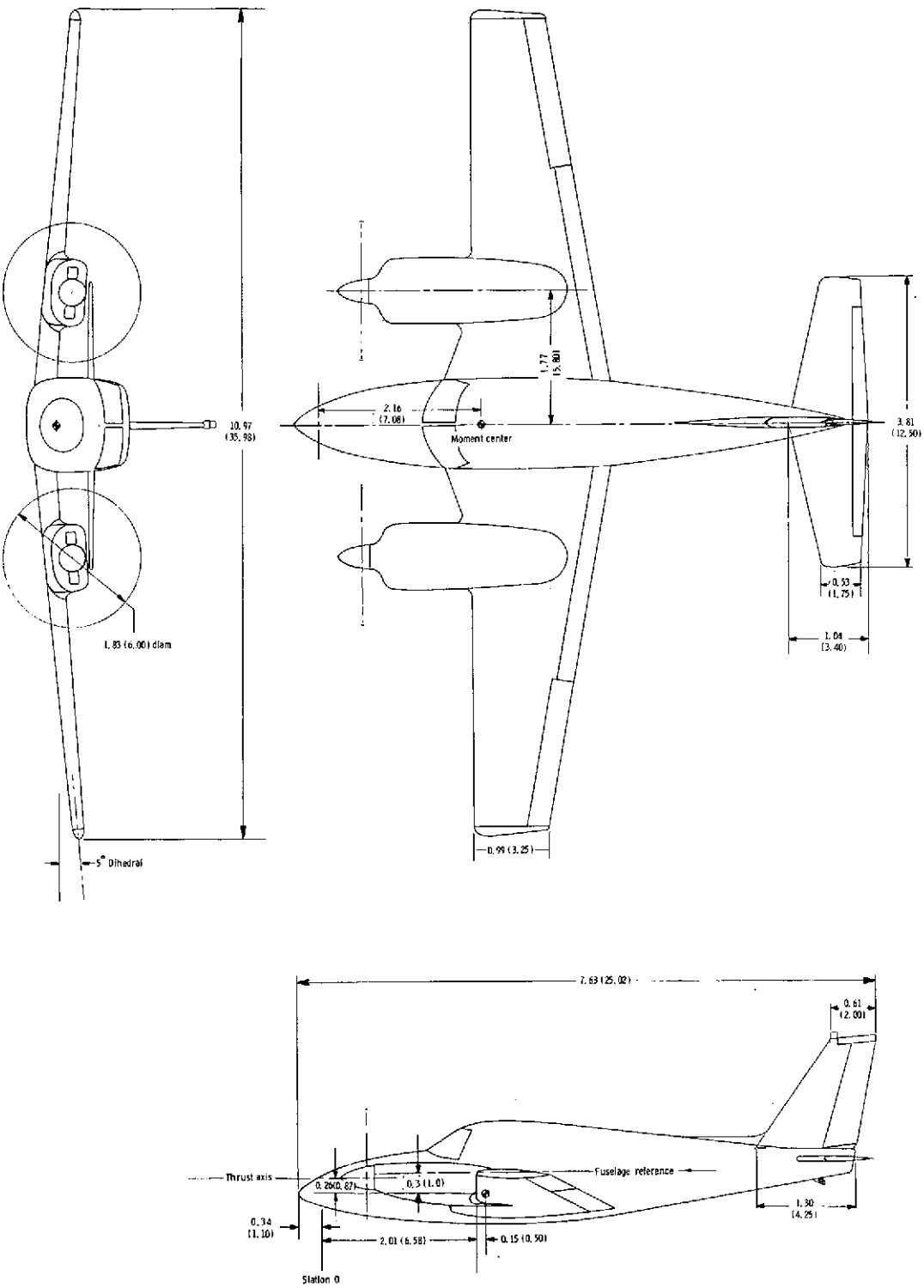

Figure 2.- Three-view drawing of the model. All dimensions are in meters (feet).

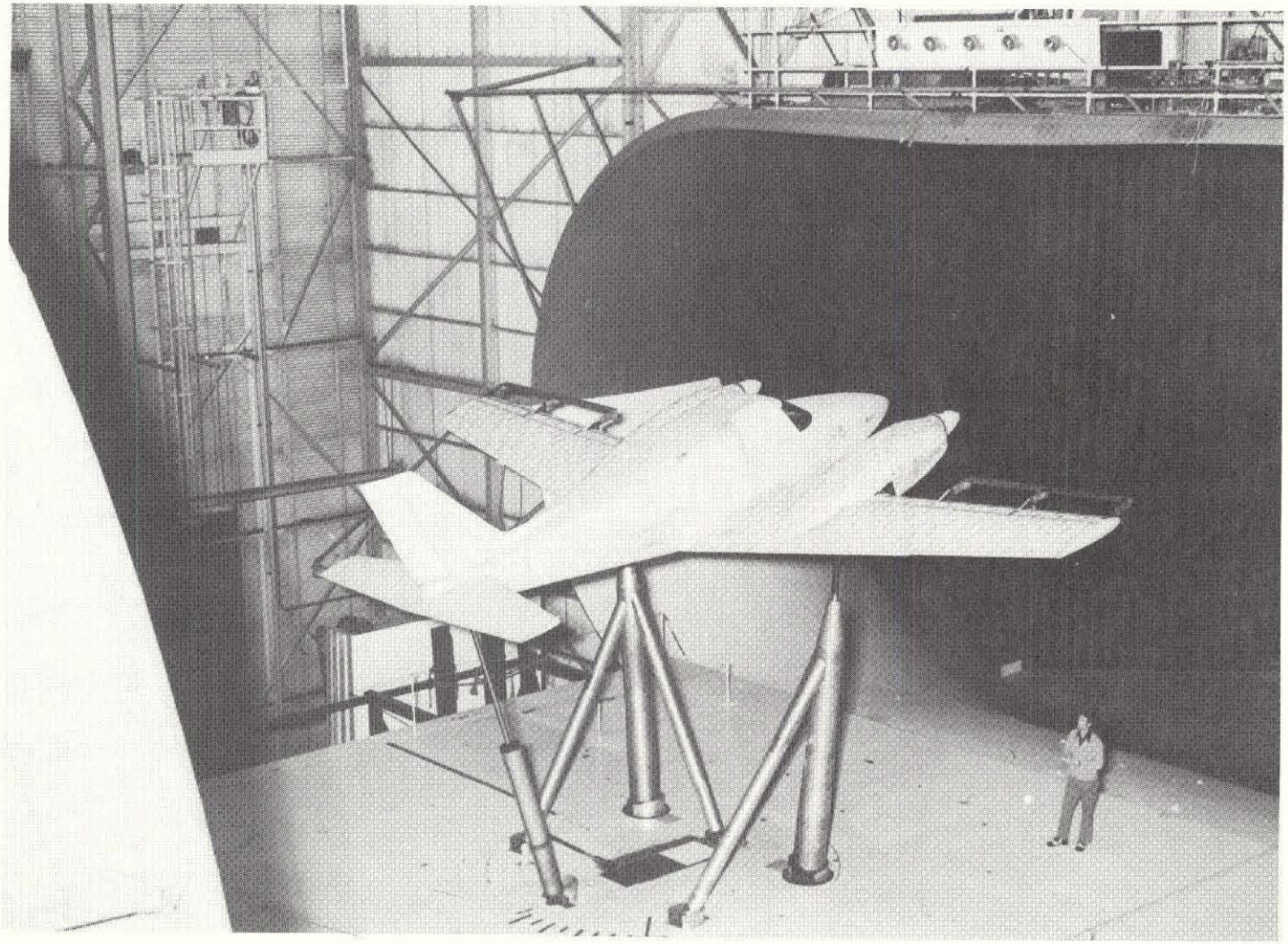

L-73-2094

(a) Three-quarter rear view of model.

Figure 3.- Photograph of model in the tunnel.

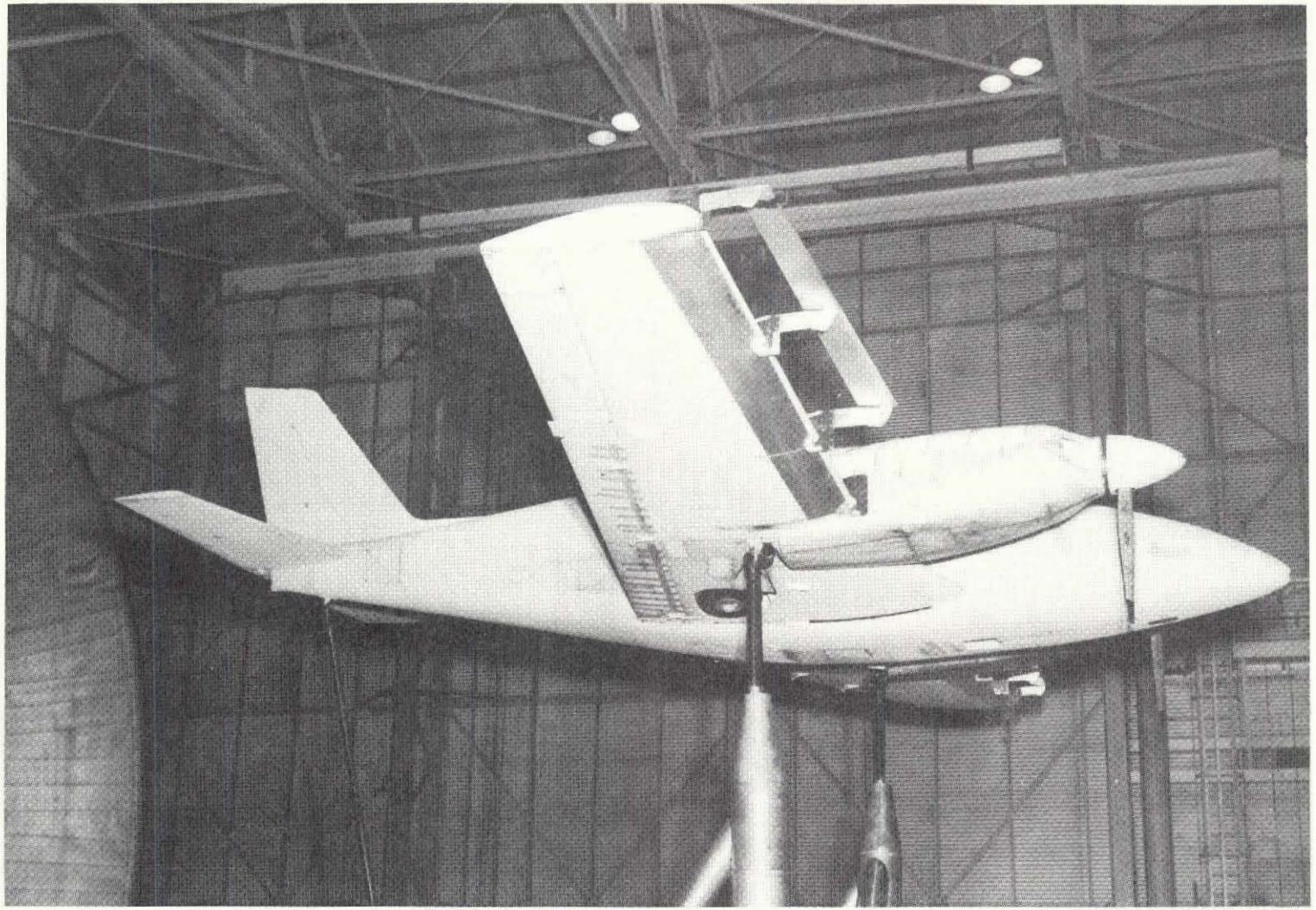

L-73-2091

(b) Side view showing auxiliary airfoil.

Figure 3.- Concluded.

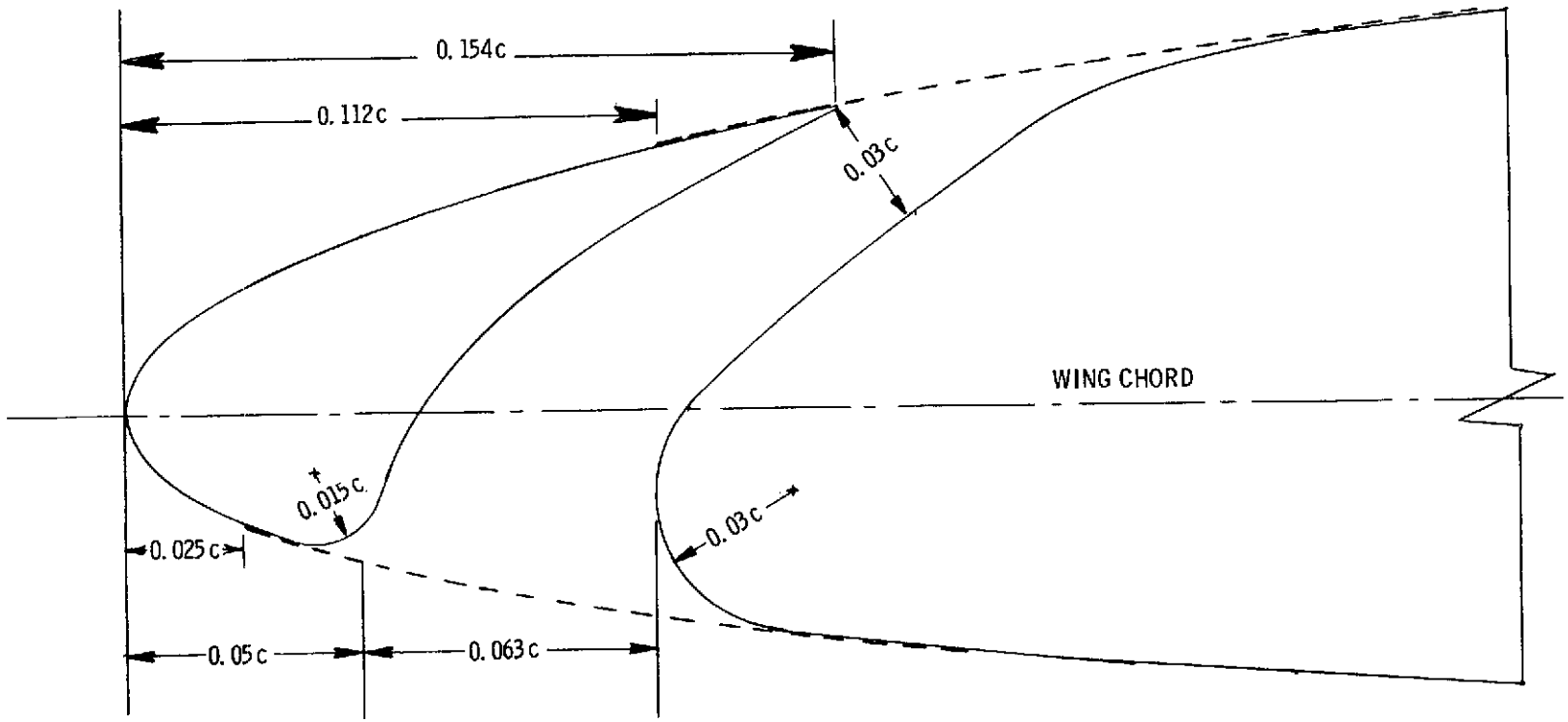

(a) Typical cross section of leading-edge slot.

Figure 4.- Slots and auxiliary airfoils. Dashed lines indicate shape of airfoil with slot sealed over with sheetmetal.

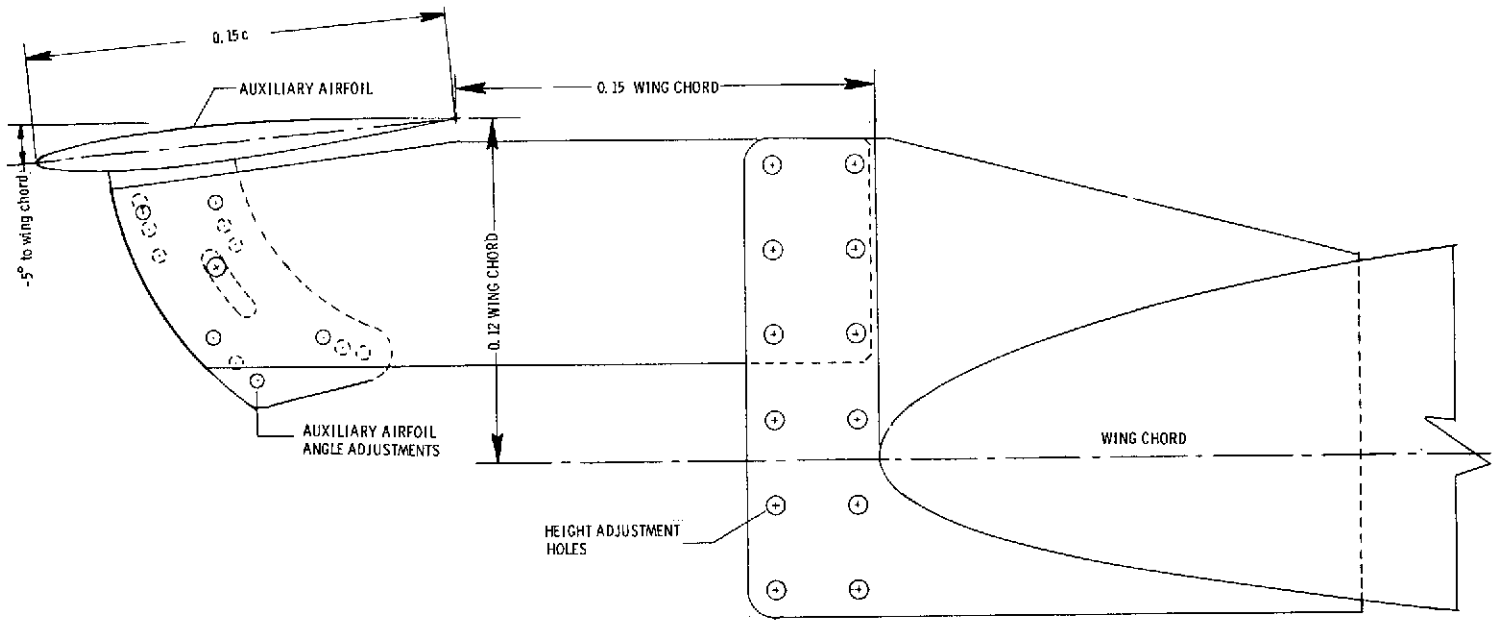

(b) Cross section of auxiliary airfoil arrangement.

Figure 4.- Continued.

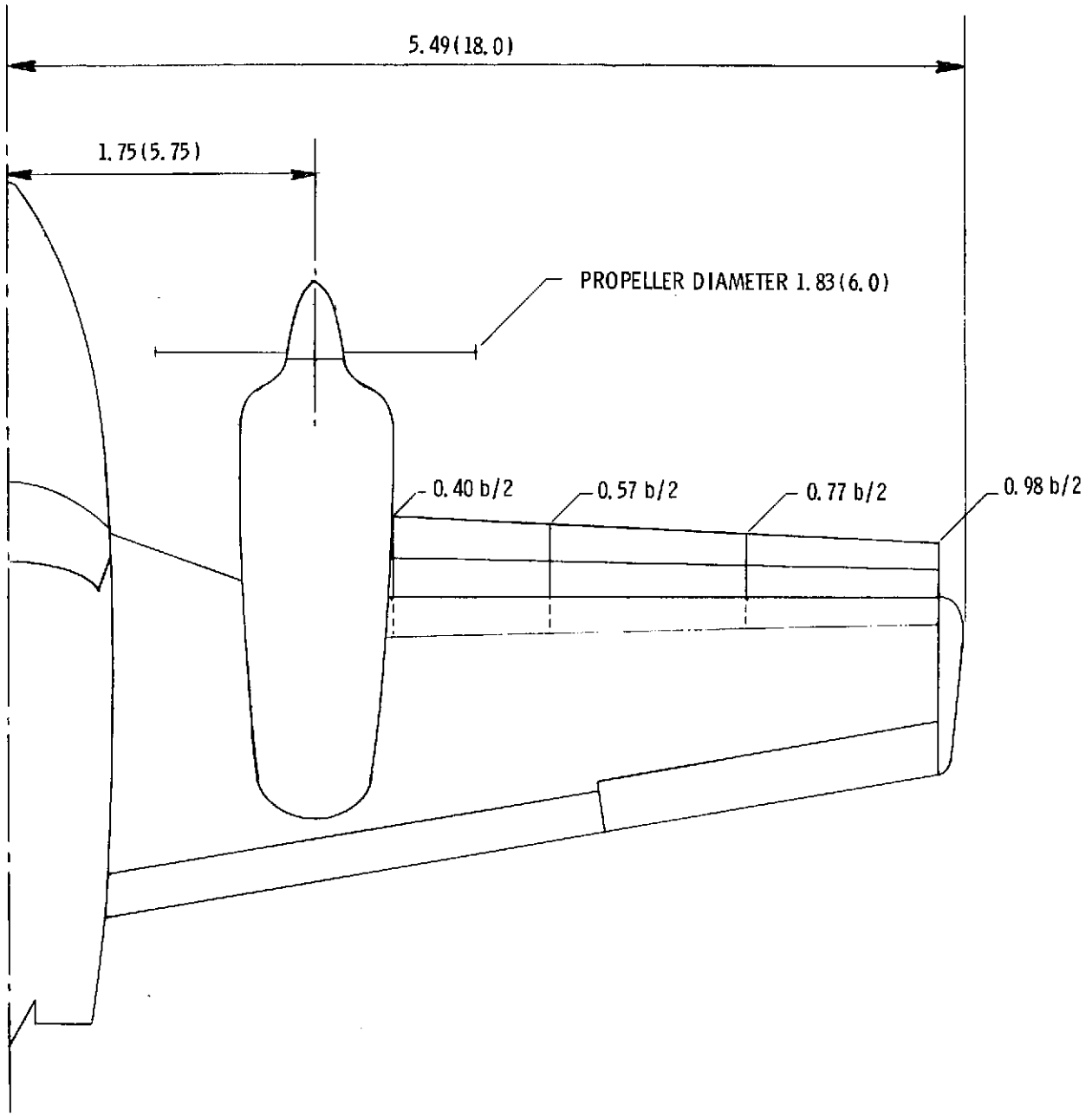

(c) Spanwise segments of auxiliary airfoils and leading-edge slot.

Figure 4.- Concluded.

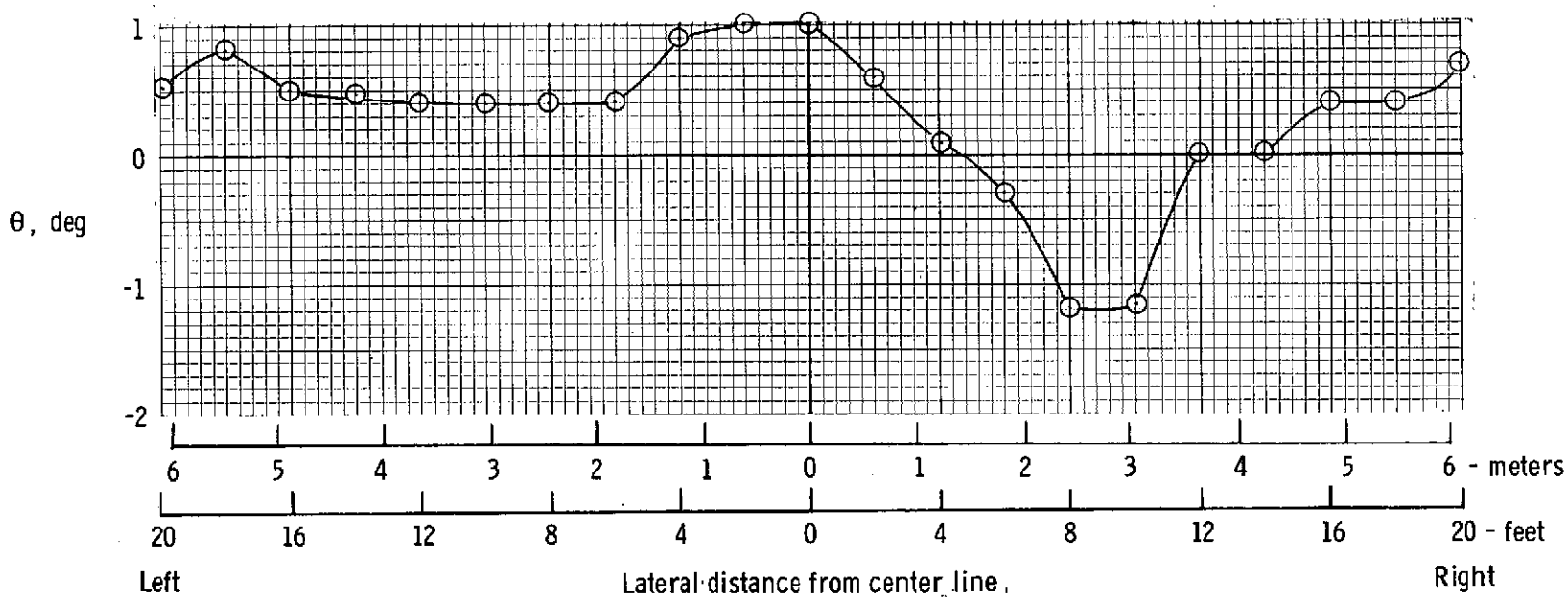

Figure 5.- Lateral variation of airstream angle at the wing location in tunnel.

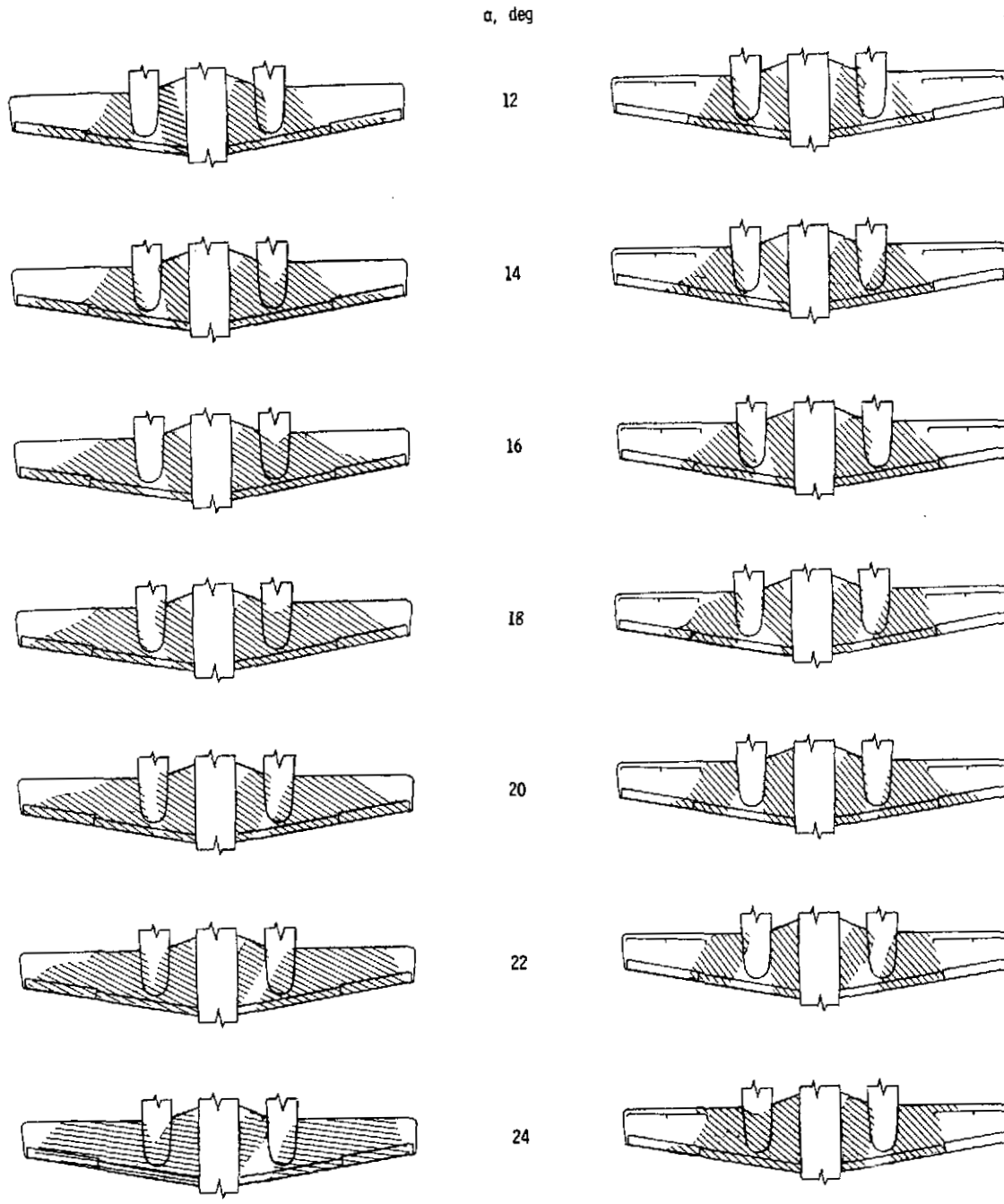

(a) Basic leading edge.

(b) 0.41b/2 slot.

Figure 6.- Stall progression as determined from tuft tests. $\delta_f = 0^o$; $T'_c = 0$

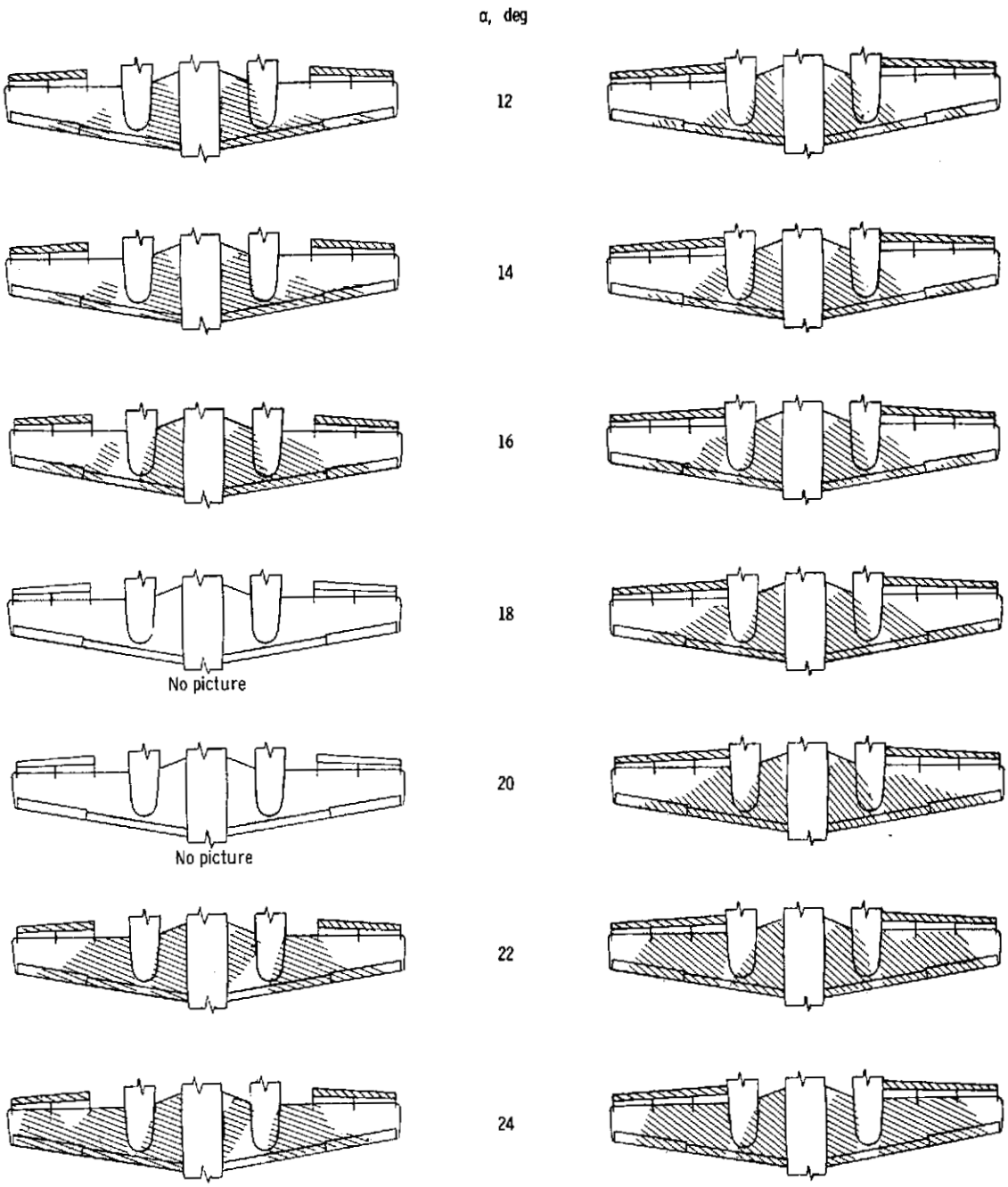

(c) 0.41b/2 auxiliary airfoil.

(d) 0.58b/2 auxiliary airfoil.

Figure 6.- Concluded.

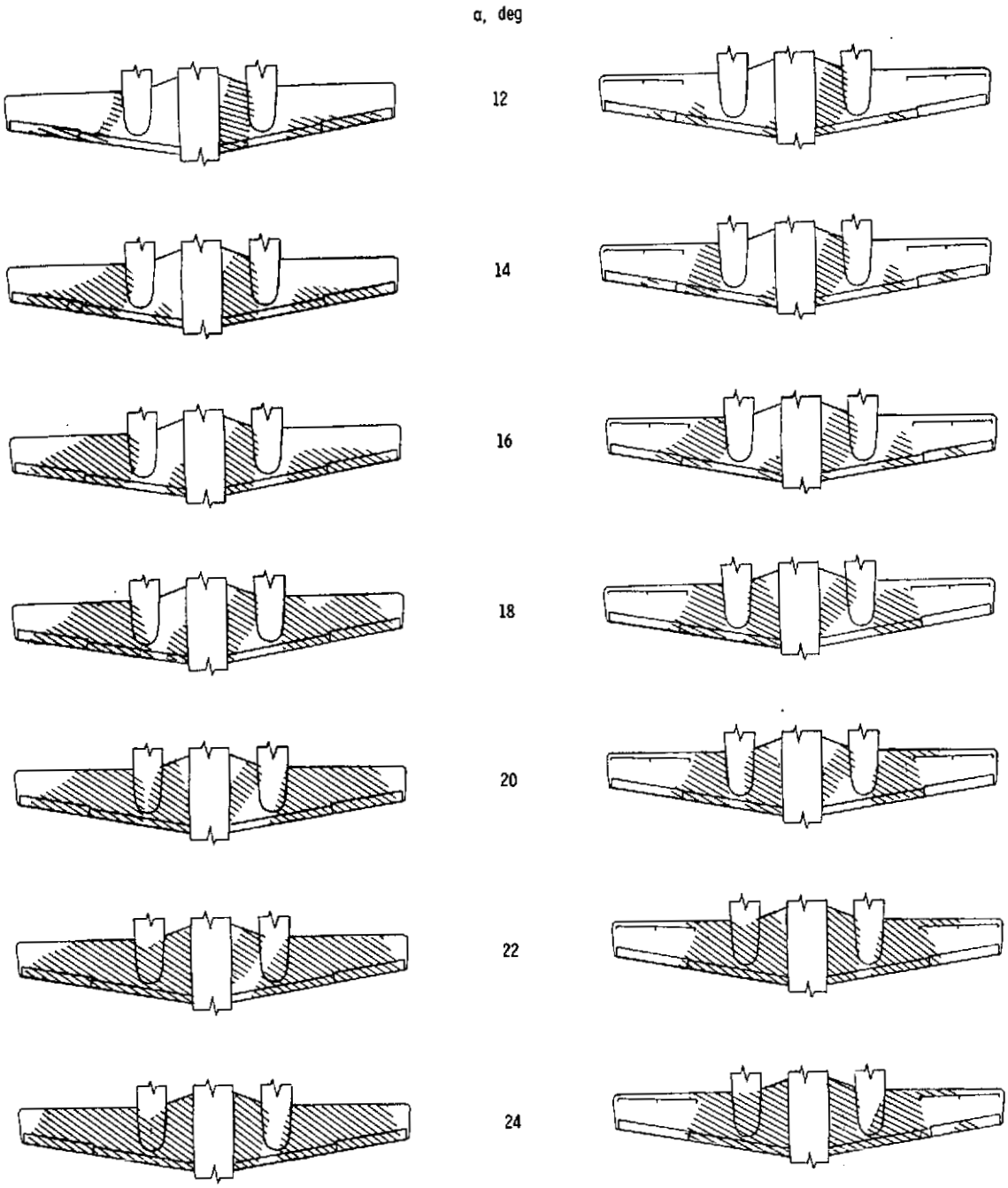

(a) Basic leading edge. (b) 0.41b/2 slot.

Figure 7.- Stall progression as determined from tuft tests. $\delta_f = 0^o$; $T'_c = 0.20$.

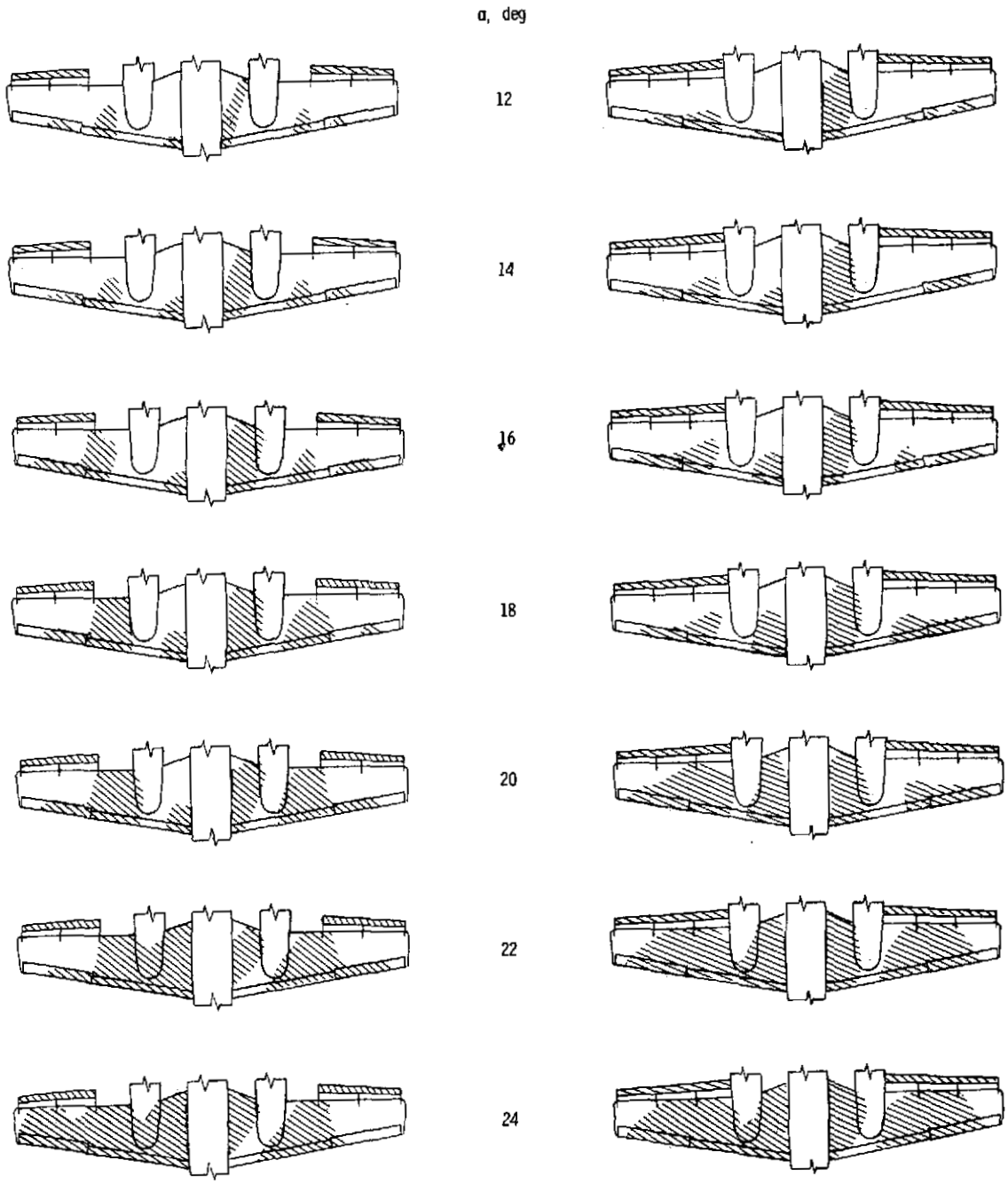

(c) 0.41b/2 auxiliary airfoil.

(d) 0.58b/2 auxiliary airfoil.

Figure 7.- Concluded.

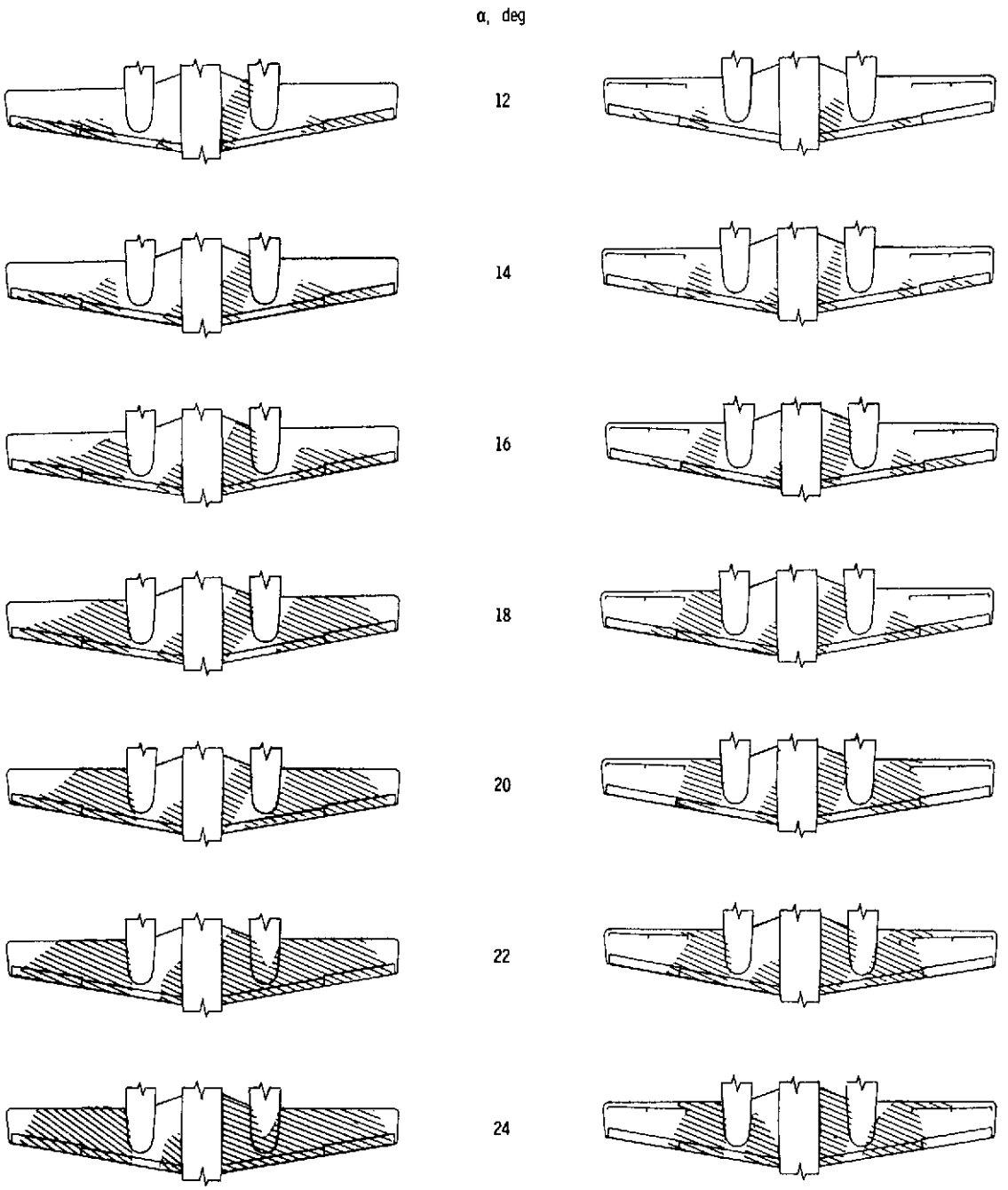

(a) Basic leading edge. (b) 0.41b/2 slot.

Figure 8.- Stall progression as determined from tuft tests. $\delta_f = 0^o$; $T_c' = 0.44$.

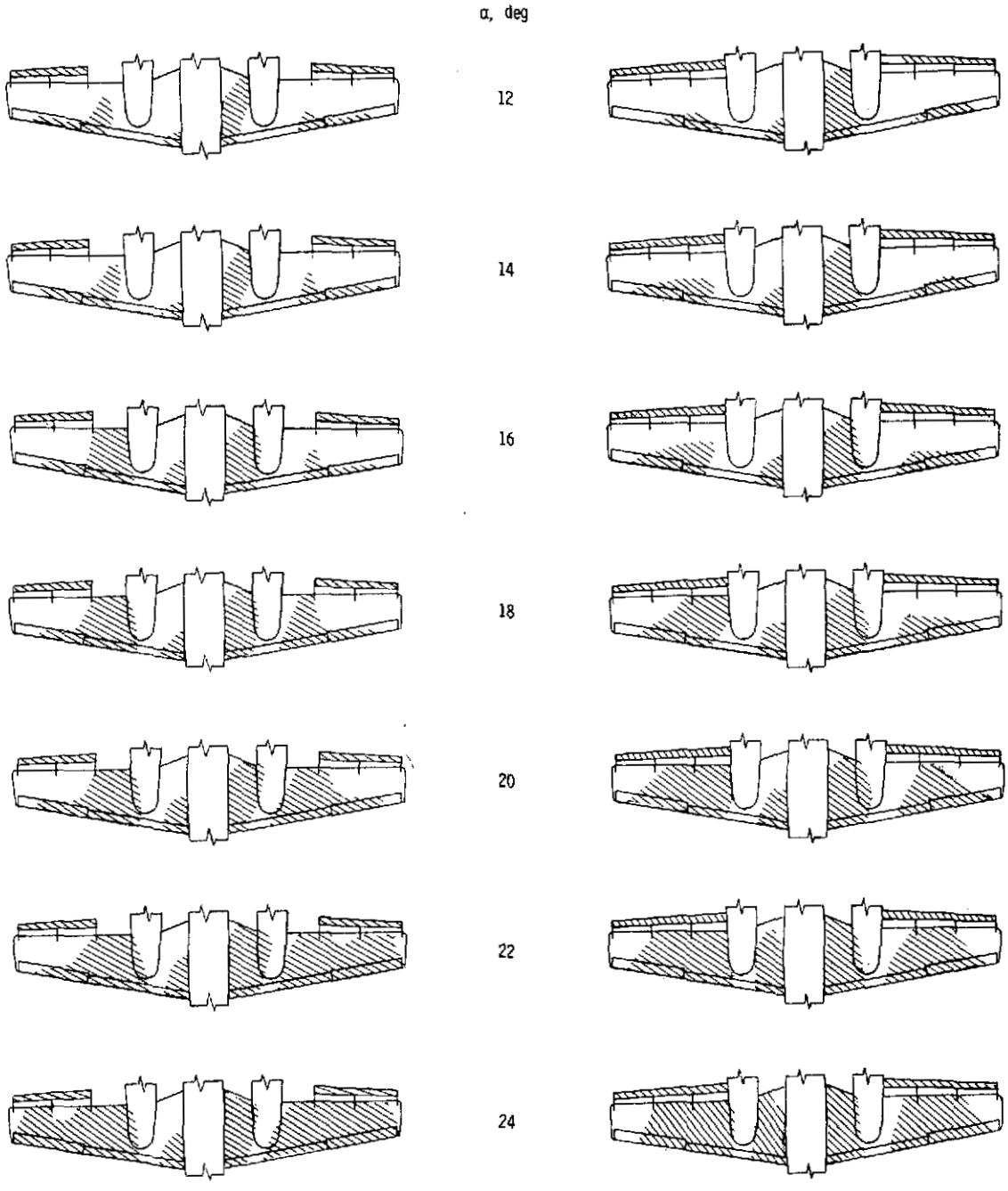

(c) 0.41b/2 auxiliary airfoil.

(d) 0.58b/2 auxiliary airfoil.

Figure 8.- Concluded.

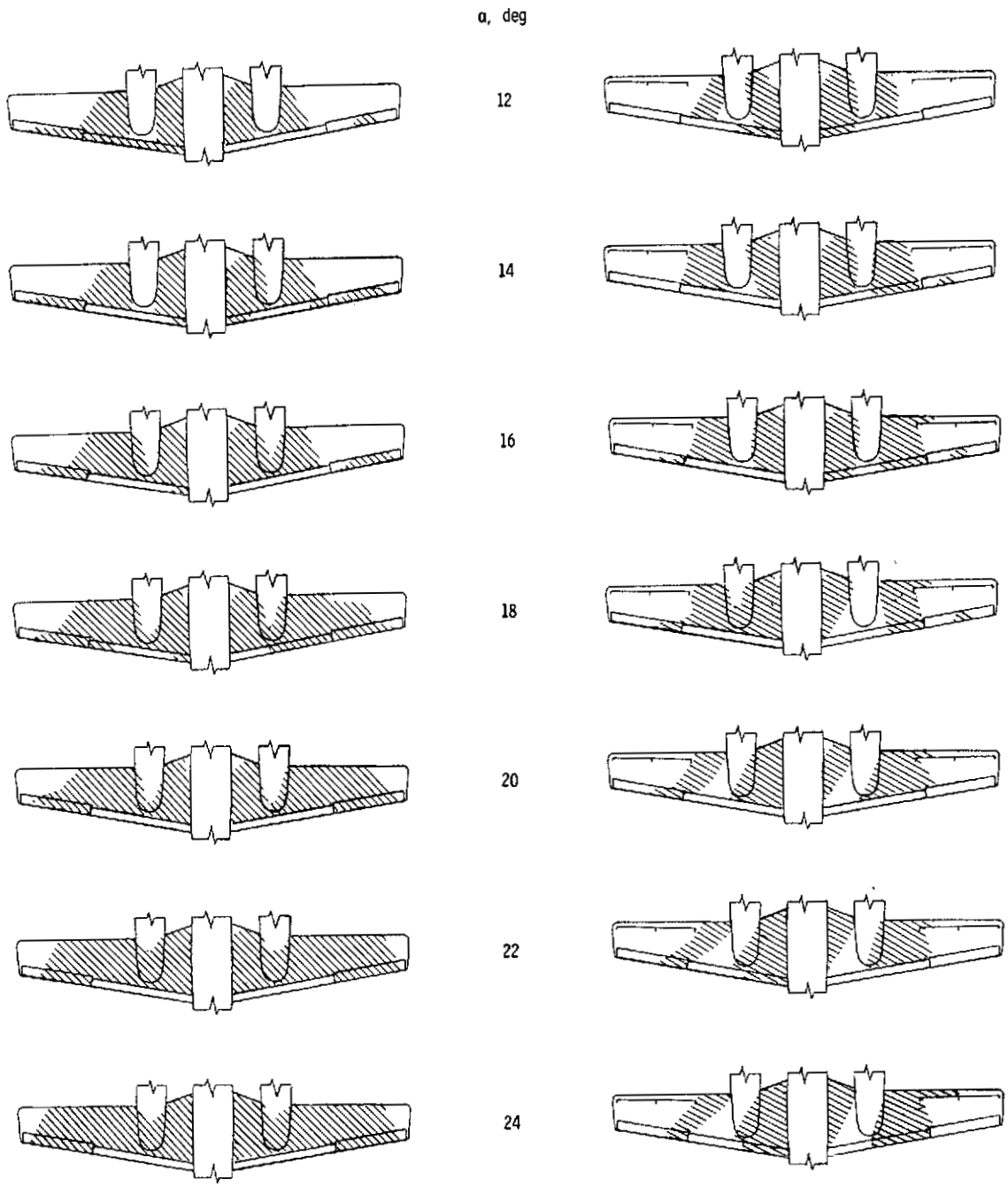

(a) Basic leading edge.

(b) 0.41b/2 slot.

Figure 9.- Stall progression as determined from tuft tests. $\delta_f = 27^o$; $T_c' = 0$.

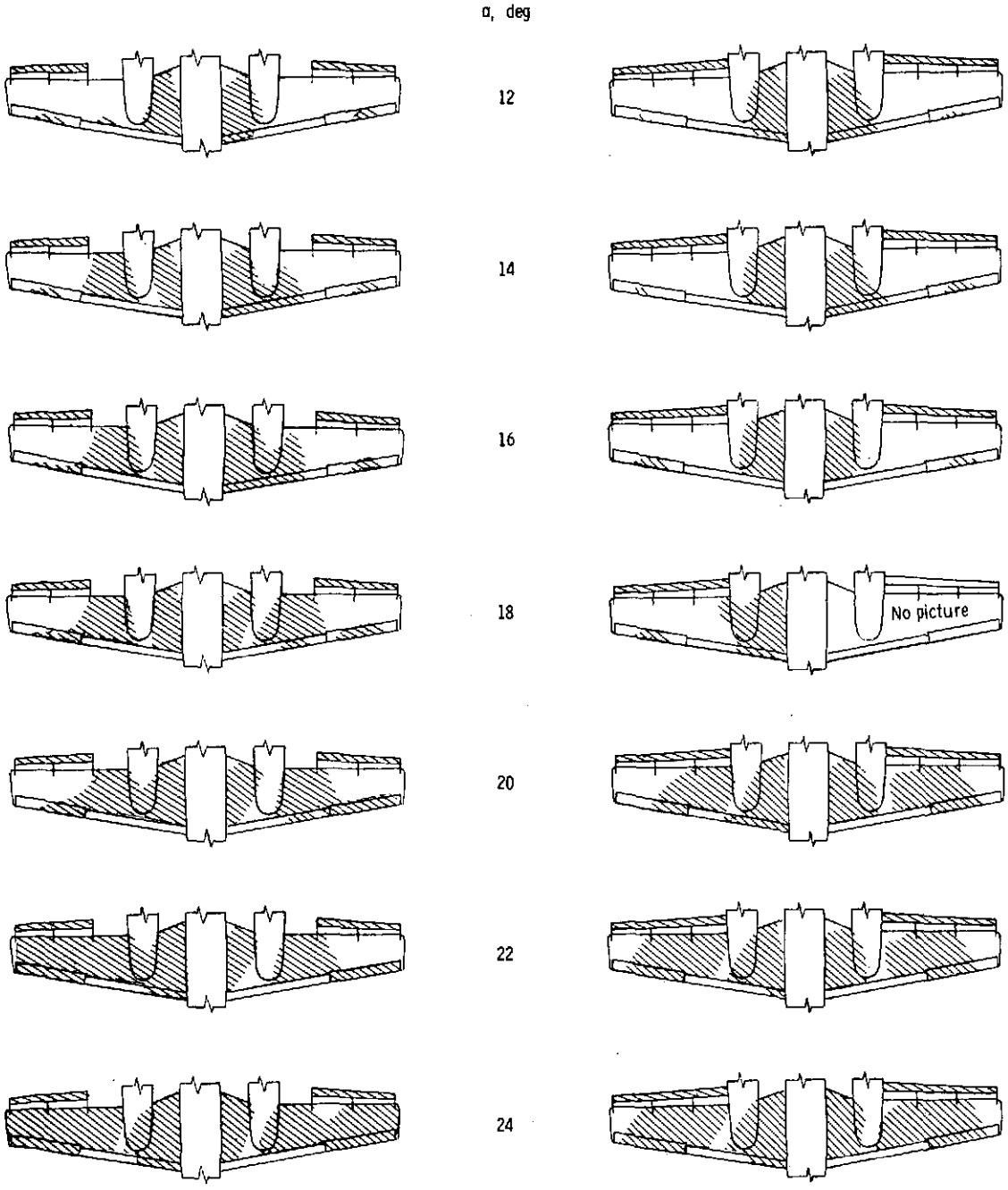

(c) 0.41b/2 auxiliary airfoil.

(d) 0.58b/2 auxiliary airfoil.

Figure 9.- Concluded.

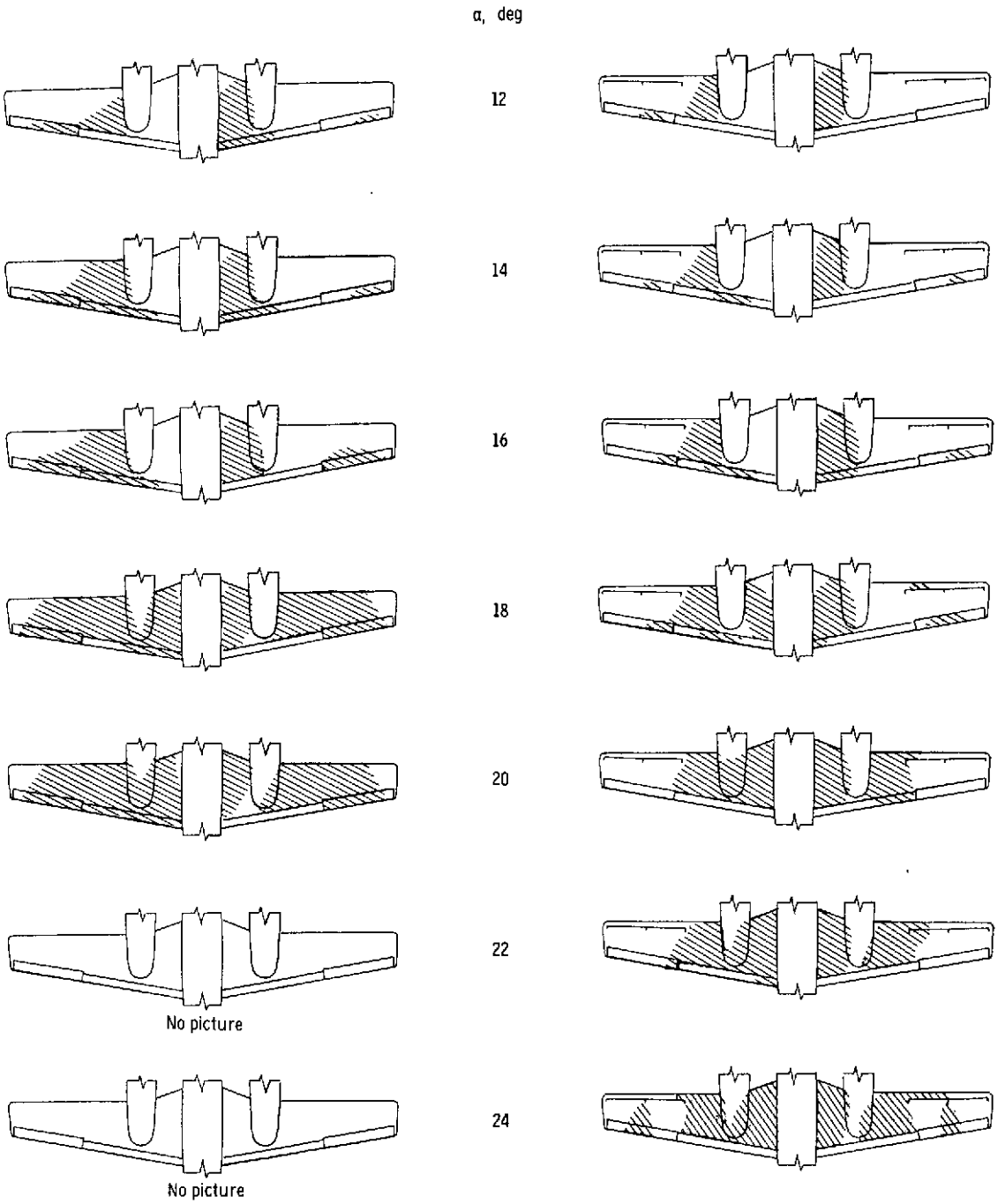

(a) Basic leading edge.

(b) 0.41b/2 slot.

Figure 10.- Stall progression as determined from tuft tests. $\delta_f = 27^o$; $T_c' = 0.20$.

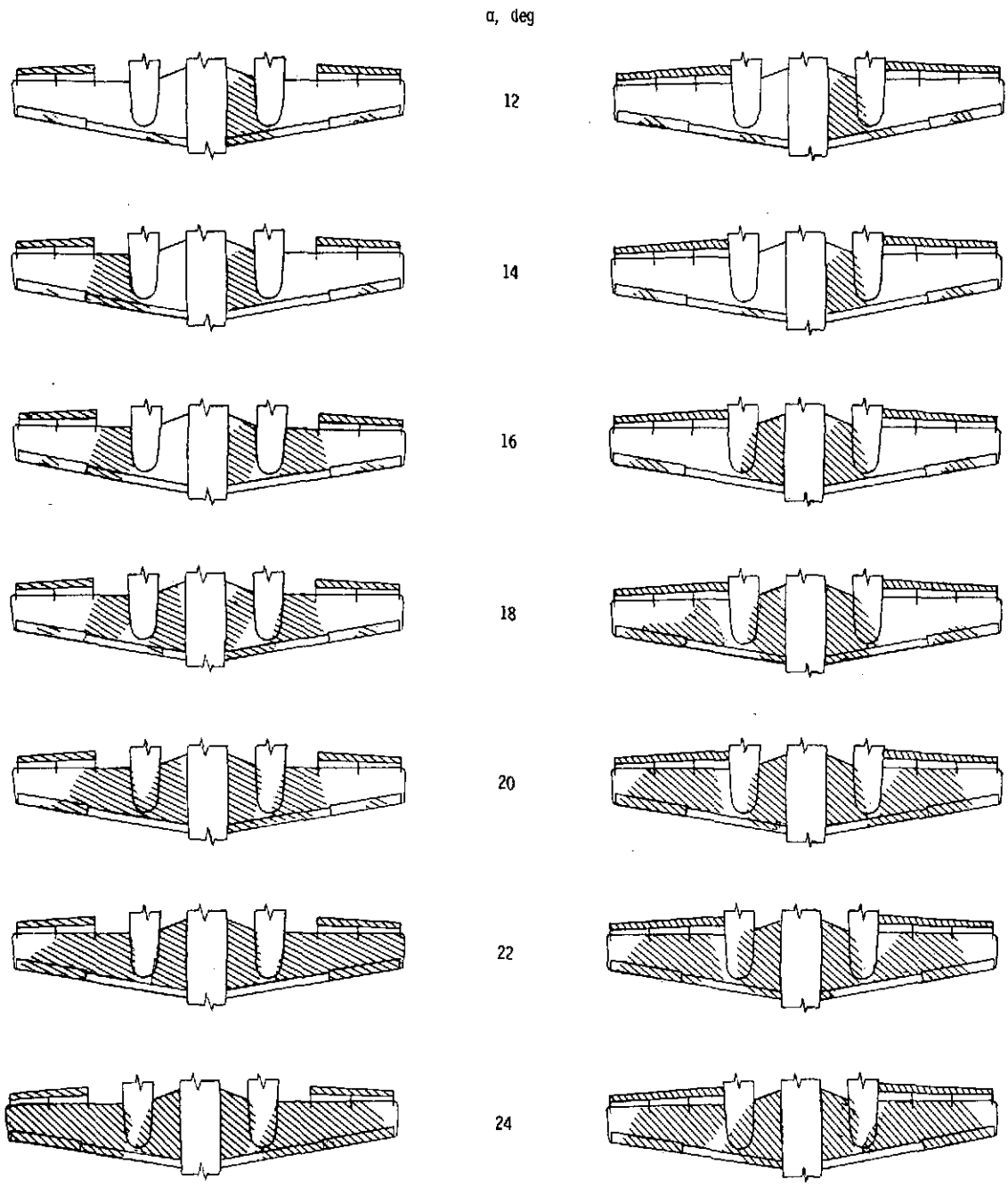

(c) 0.41b/2 auxiliary airfoil.

(d) 0.58b/2 auxiliary airfoil.

Figure 10.- Concluded.

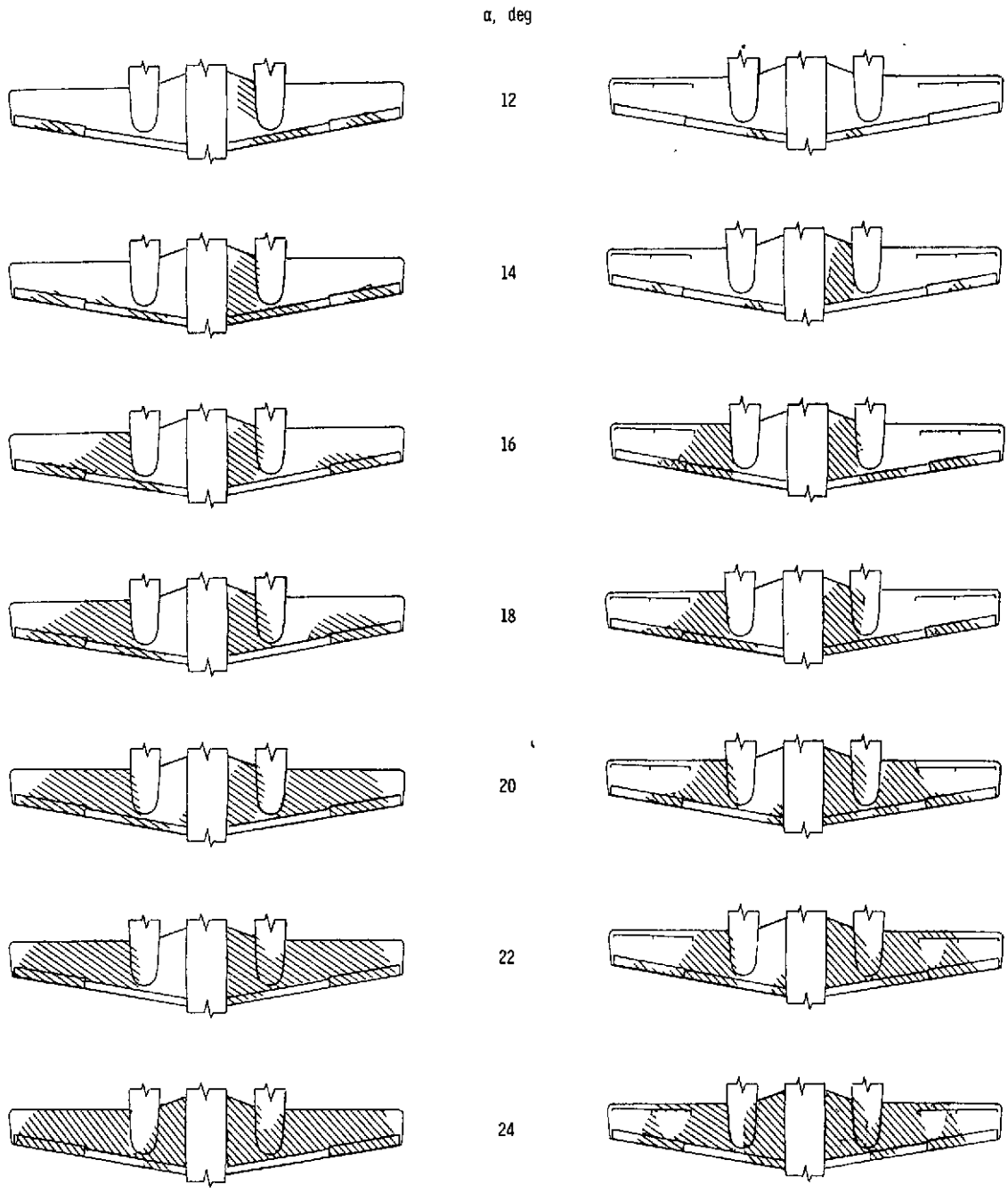

(a) Basic leading edge.

(b) 0.41b/2 slot.

Figure 11.- Stall progression as determined from tuft tests. $\delta_f = 27^o$; $T_c' = 0.44$.

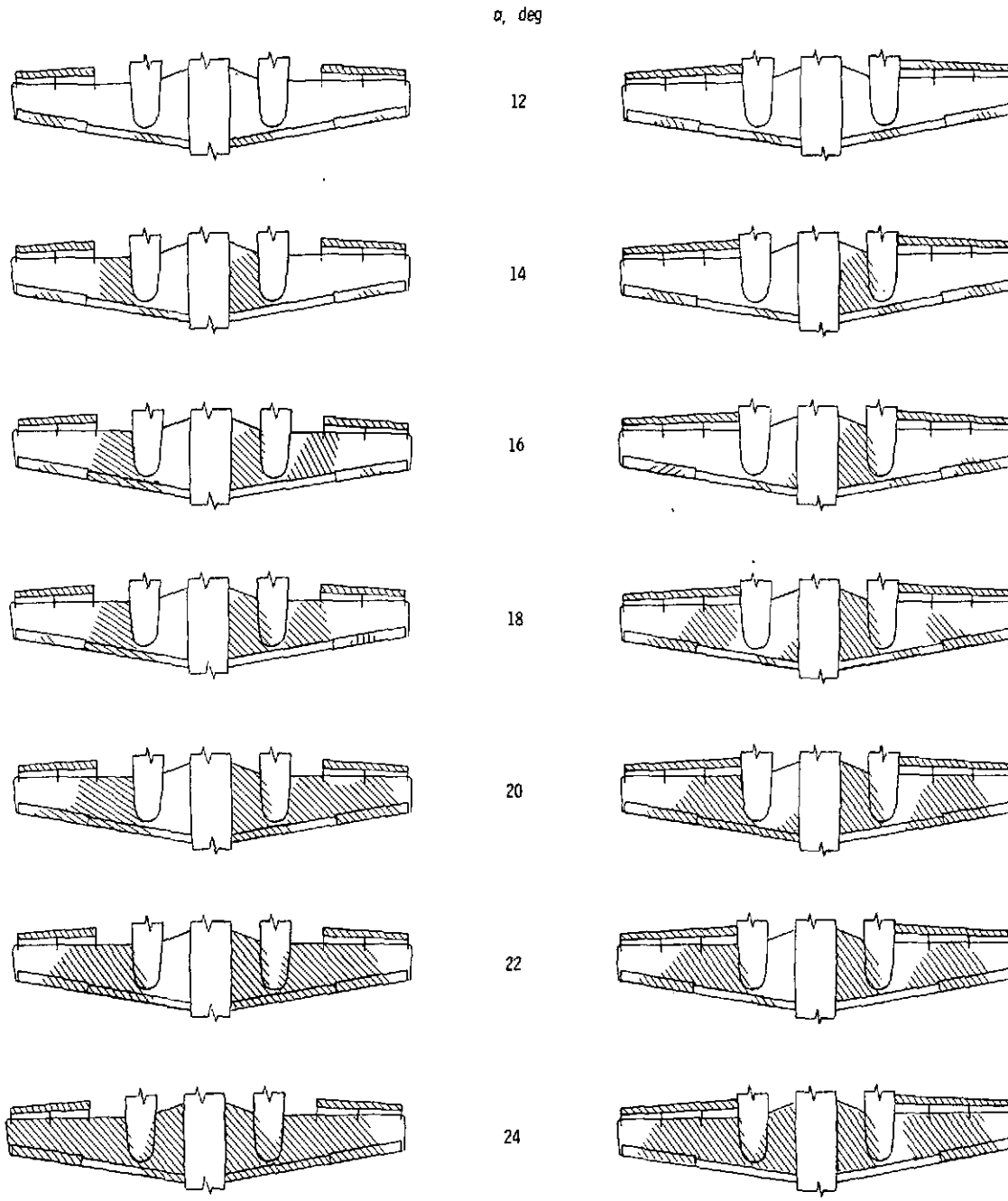

(c) 0.41b/2 auxiliary airfoil.

(d) 0.58b/2 auxiliary airfoil.

Figure 11.- Concluded.

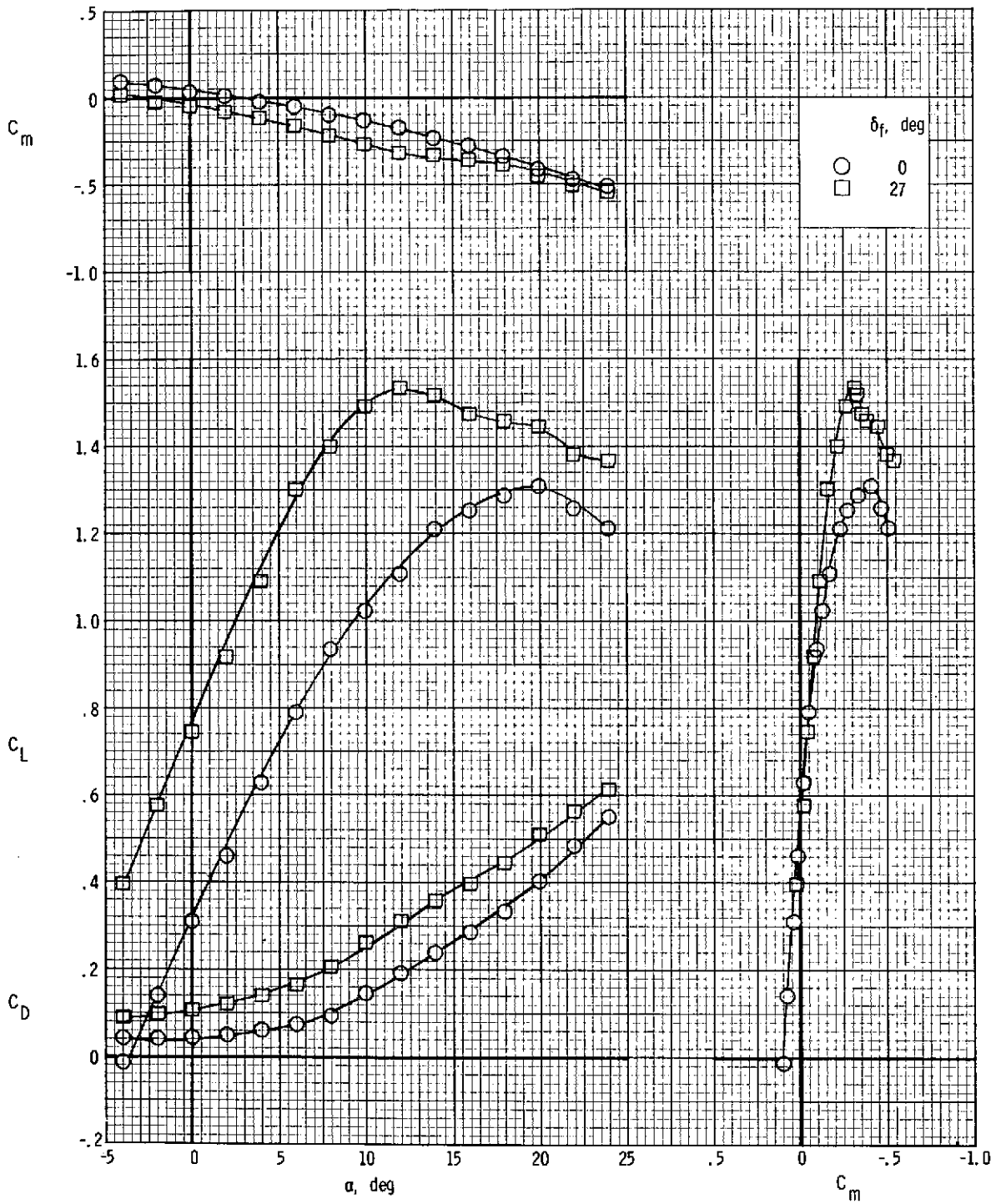

Figure 12.- Longitudinal characteristics for the basic leading-edge configuration with propellers removed.

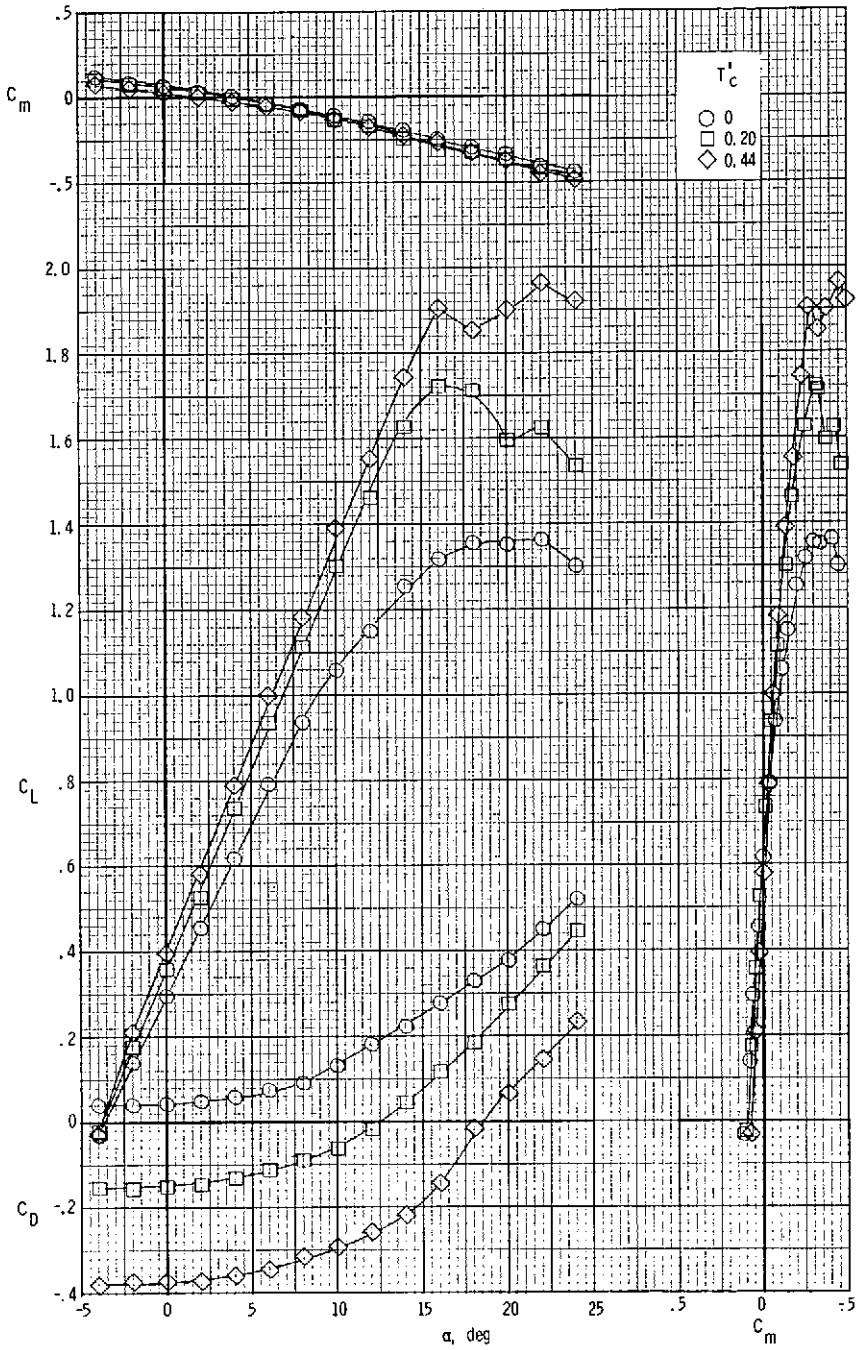

(a) $\delta_f = 0^o$.

Figure 13.- Longitudinal characteristics for the basic leading edge with power.

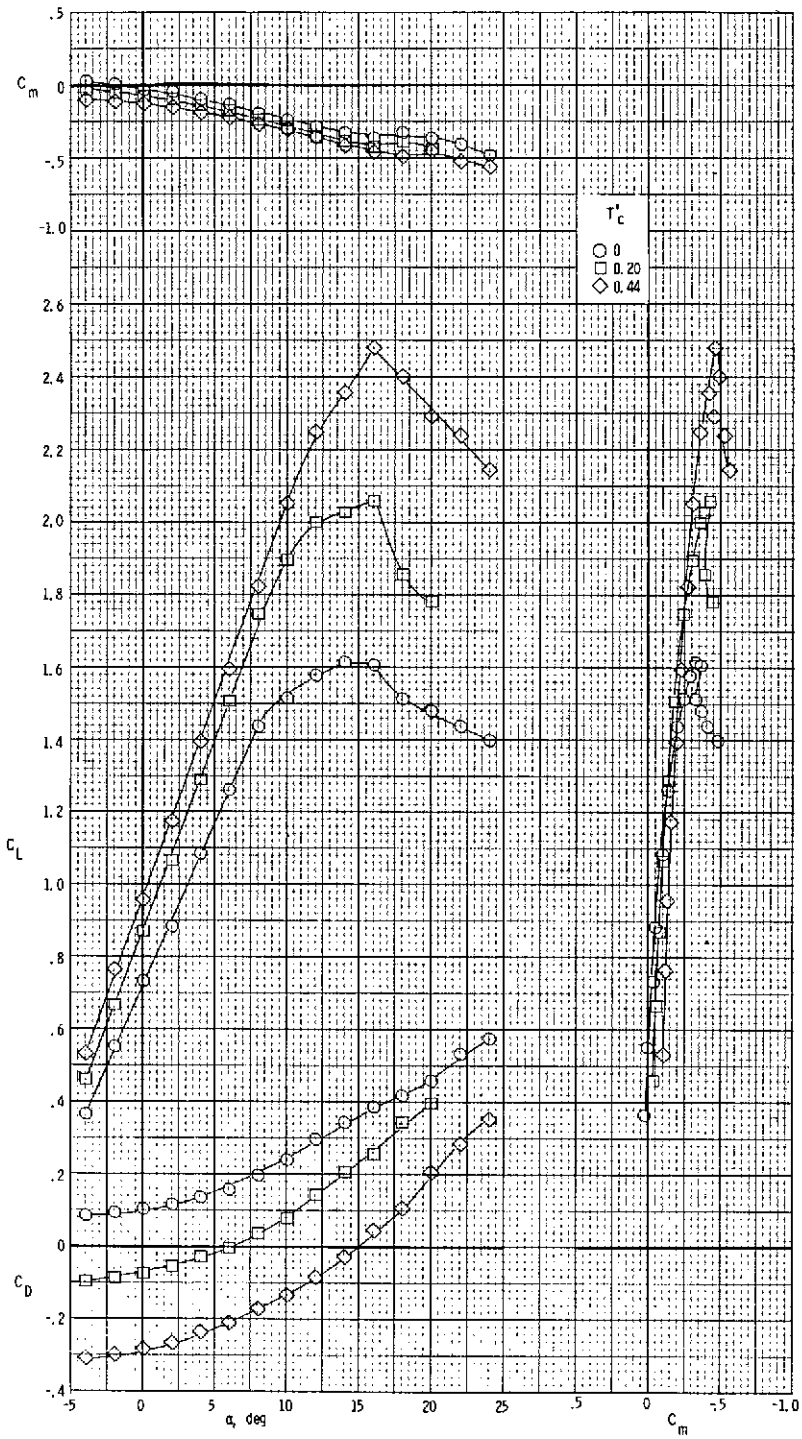

(b) $\delta_f = 27^o$.

Figure 13.- Concluded.

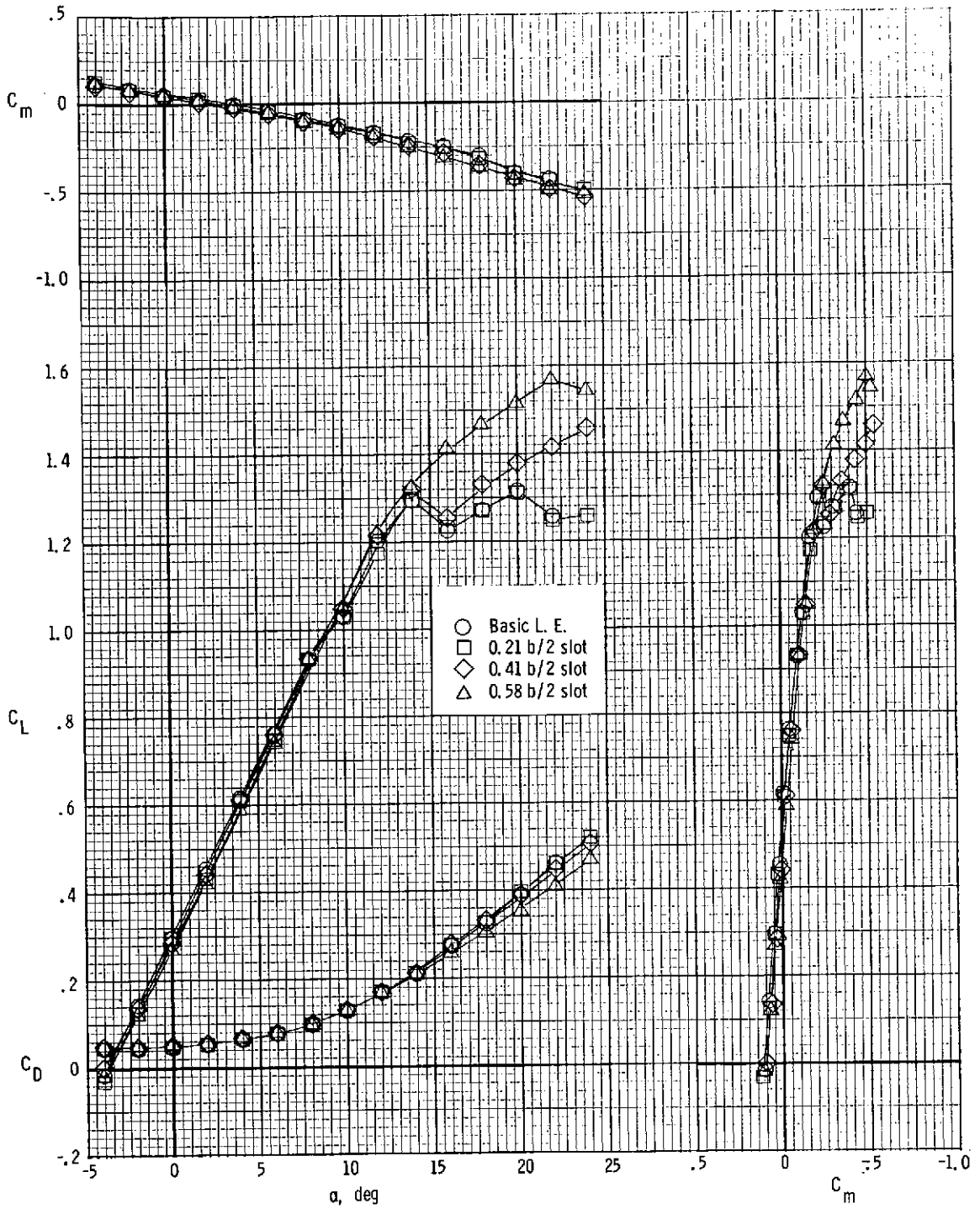

(a) $\delta_f = 0^o$.

Figure 14.- Longitudinal characteristics for leading-edge slots with propellers removed.

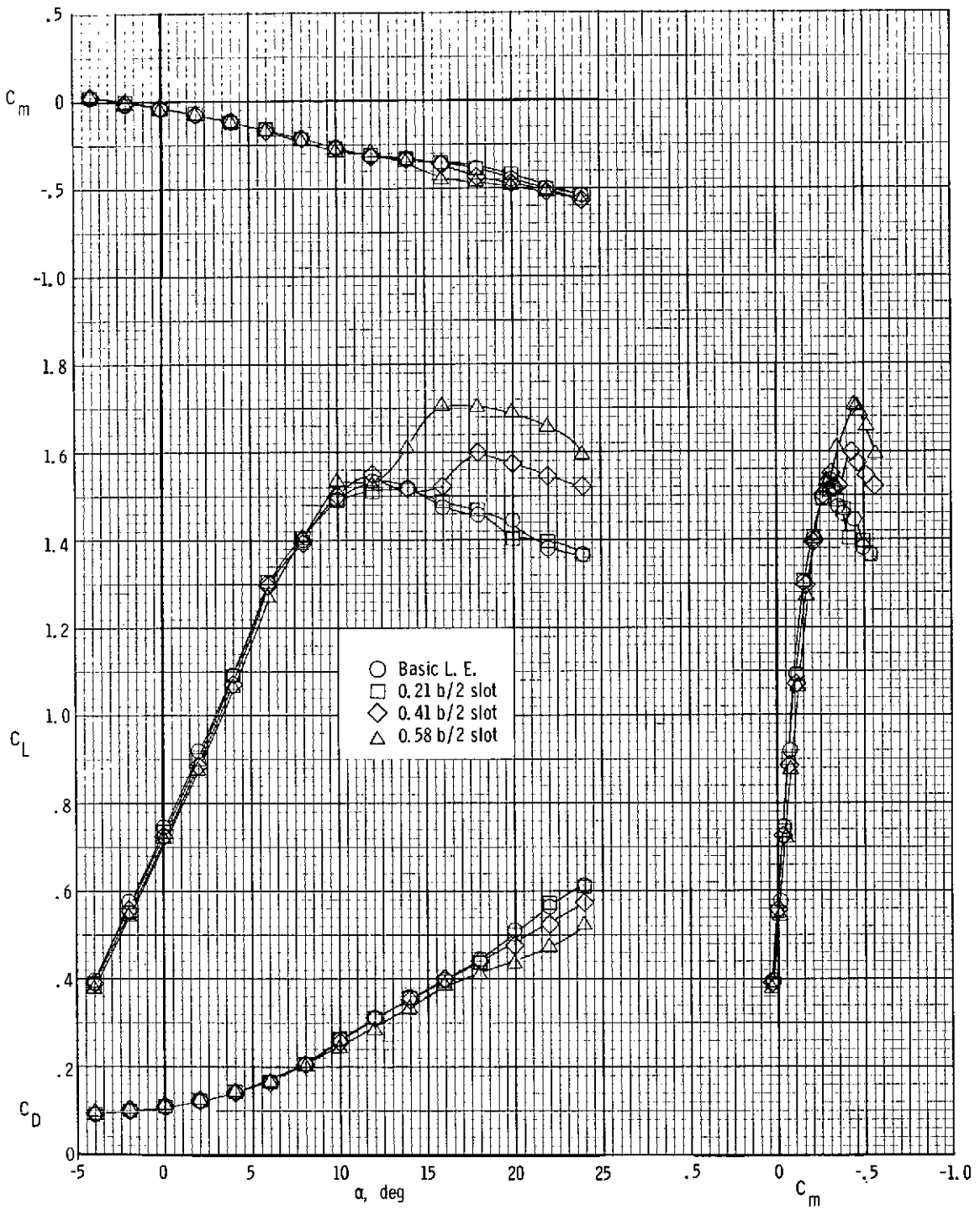

(b) $\delta_f = 27^o$.

Figure 14.- Concluded.

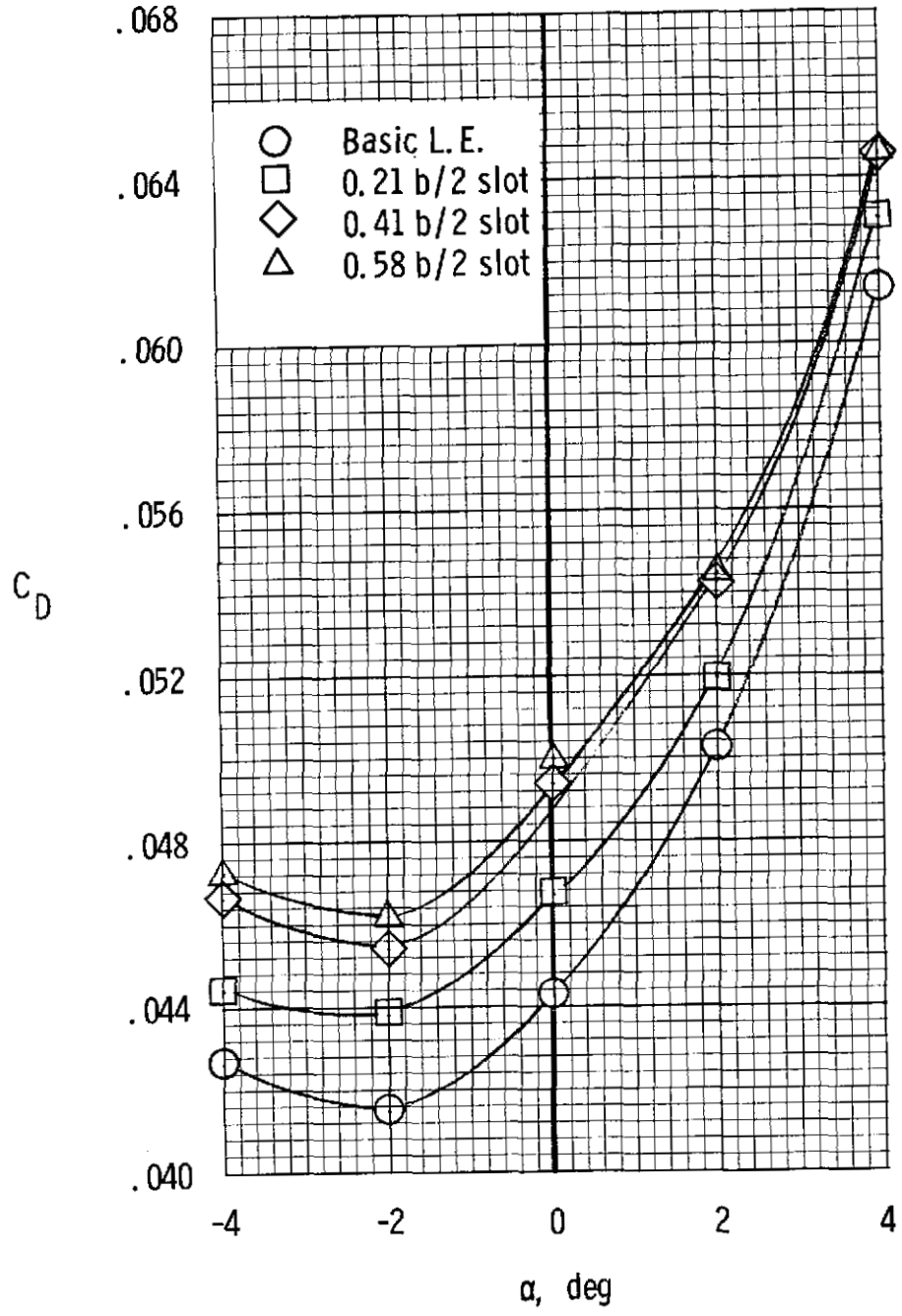

Figure 15.- Comparison of drag coefficients at low angles of attack for leading-edge slot configurations with propellers removed. $\delta_f = 0^o$.

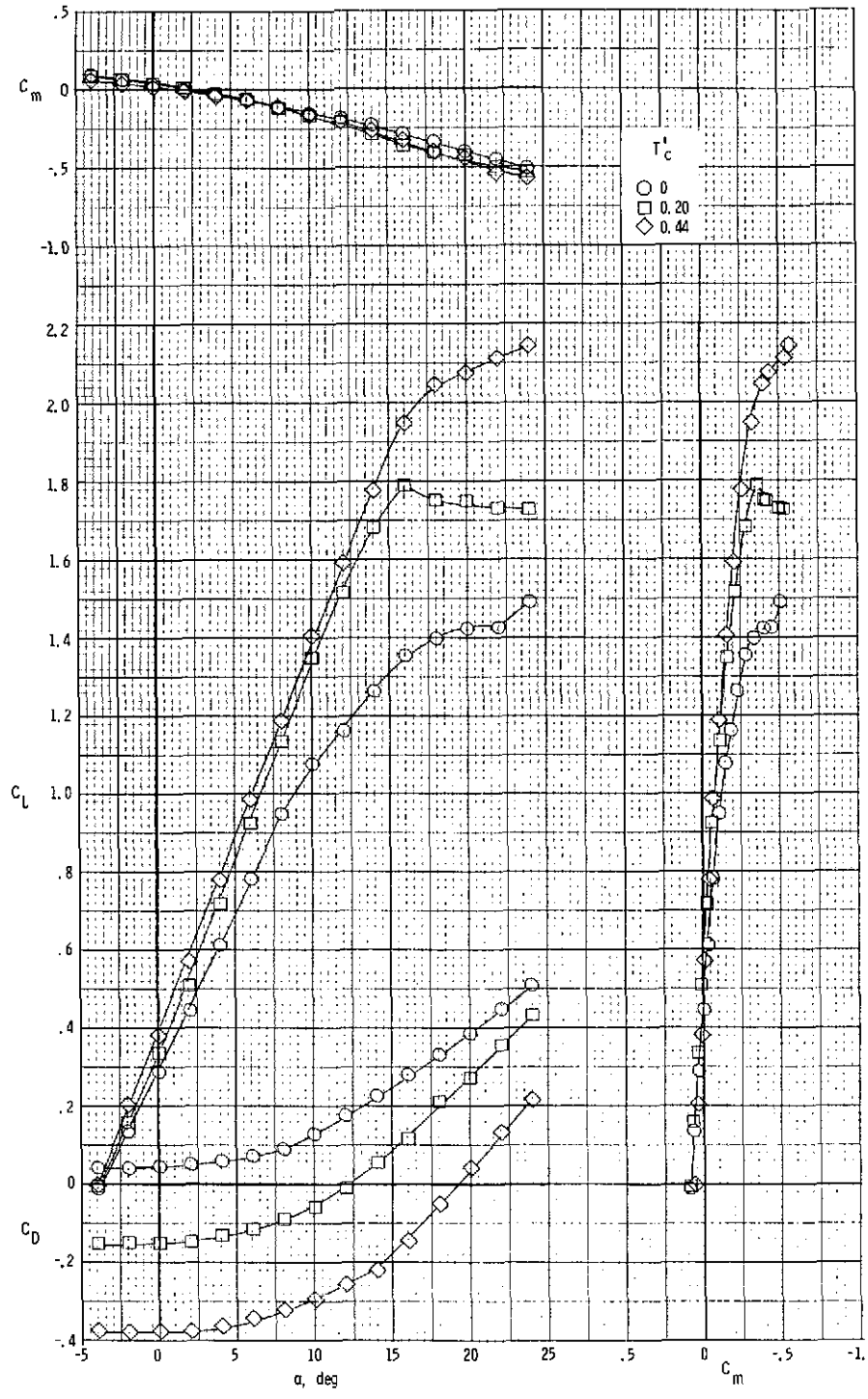

(a) $\delta_f = 0^o$.

Figure 16.- Longitudinal characteristics with 0.41b/2 leading-edge slots with power.

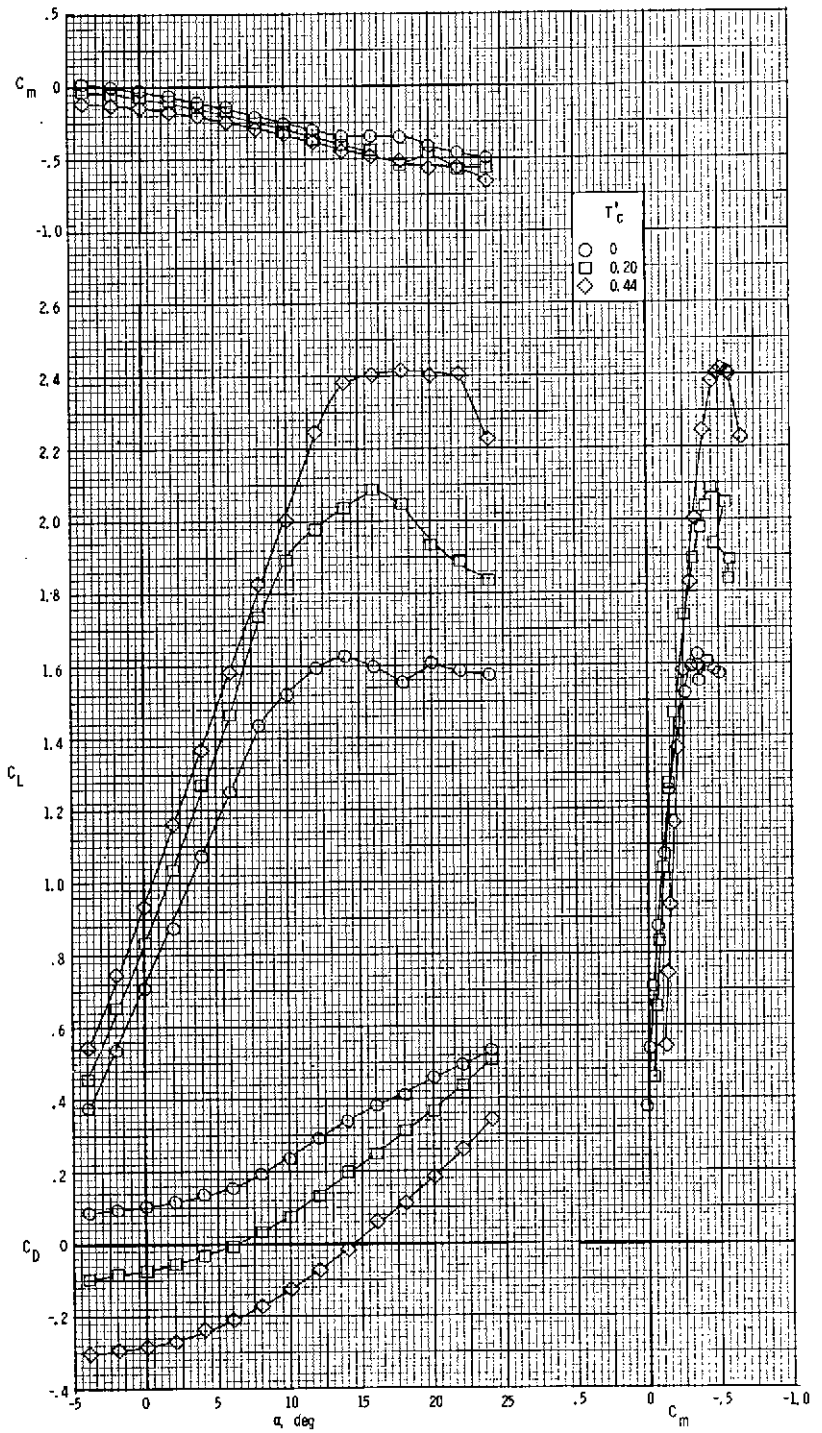

(b) $\delta_f = 27^o$.

Figure 16.- Concluded.

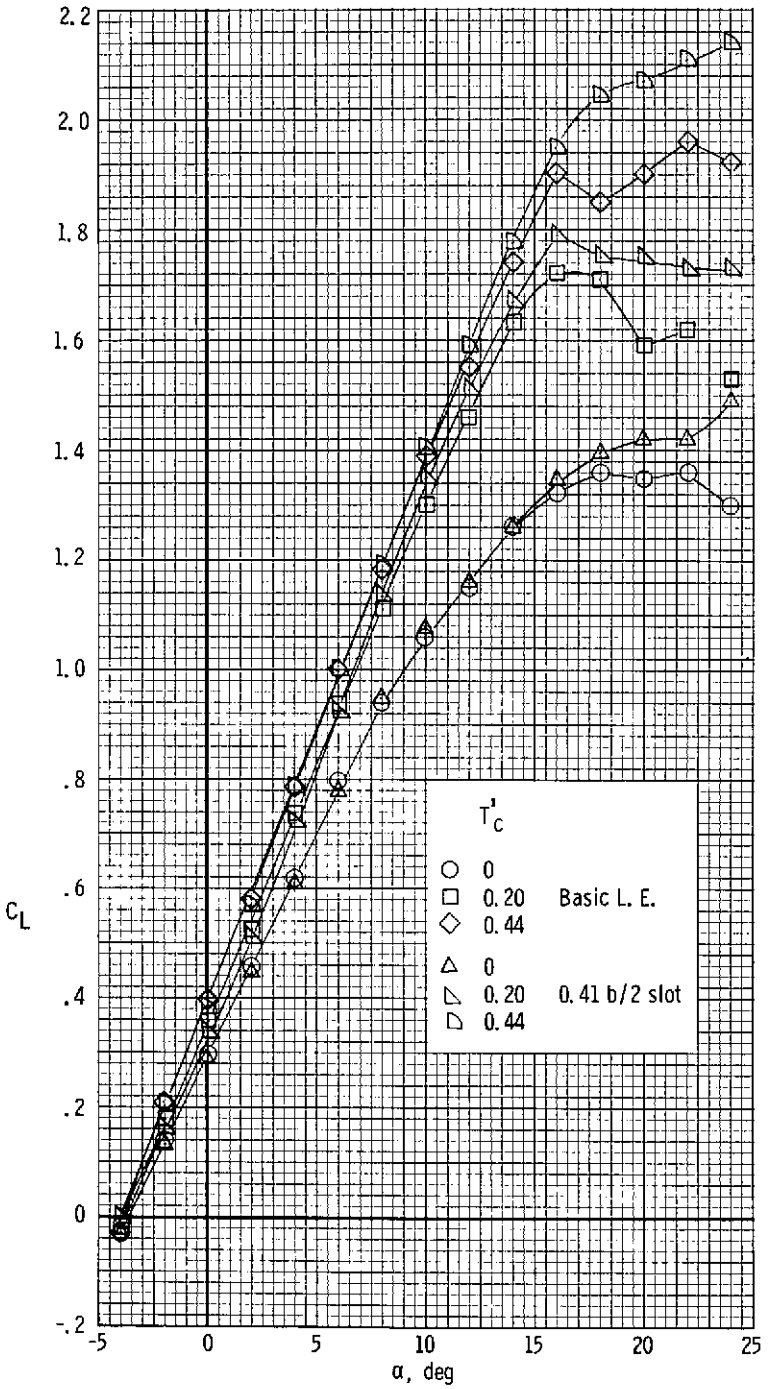

(a) $\delta_f = 0^o$.

Figure 17.- Comparison of lift coefficients of 0.41b/2 leading-edge slot for several power and flap conditions.

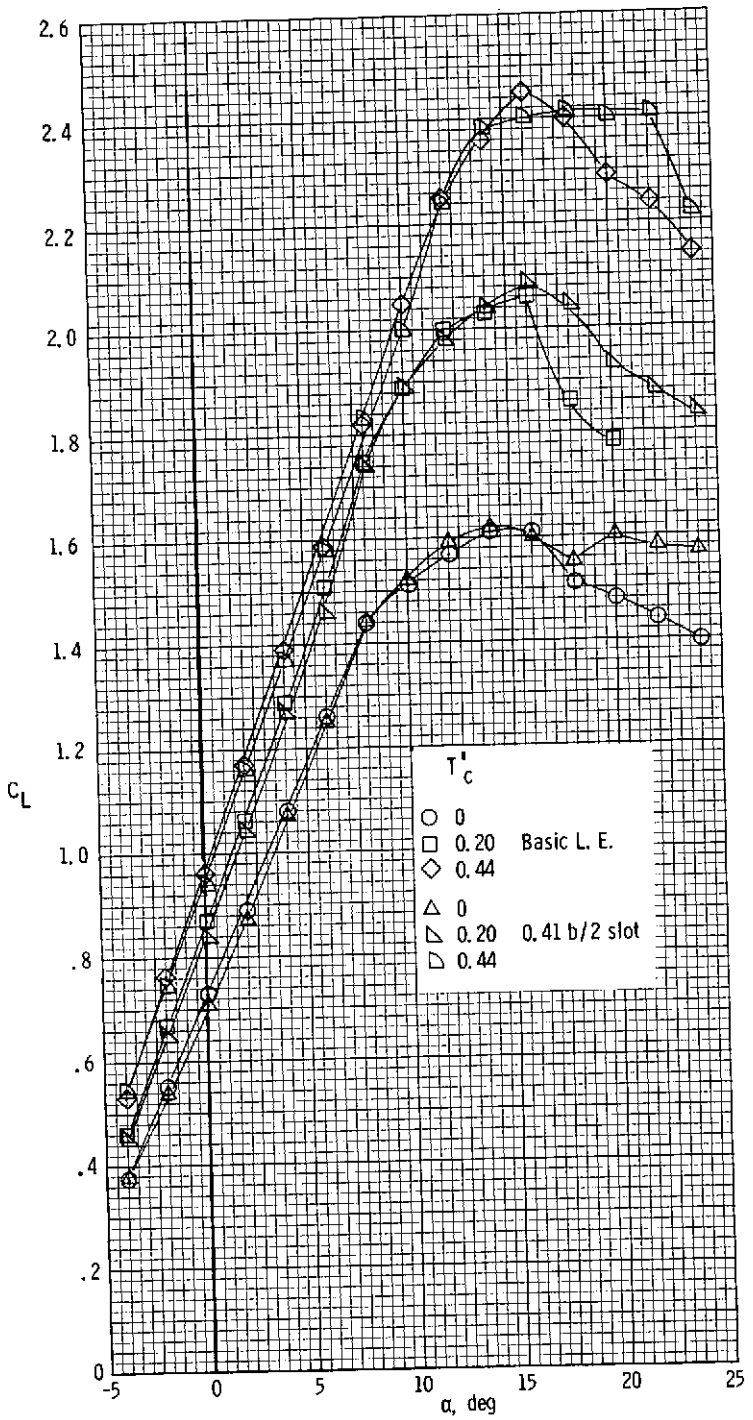

(b) $\delta_f = 27^o$.

Figure 17.- Concluded.

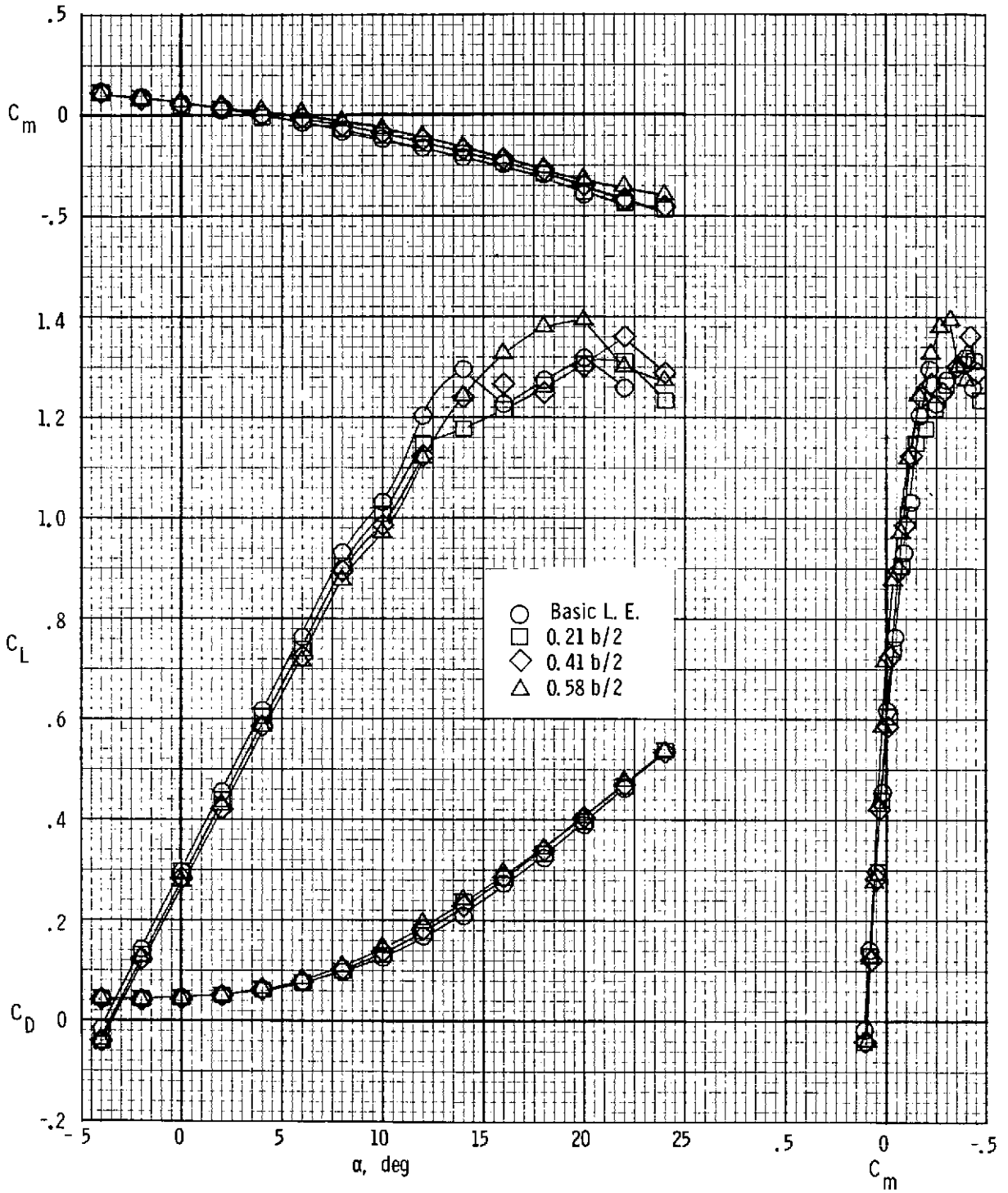

Figure 18.- Longitudinal characteristics for the auxiliary airfoil configurations with propellers removed. $\delta_f = 0^o$.

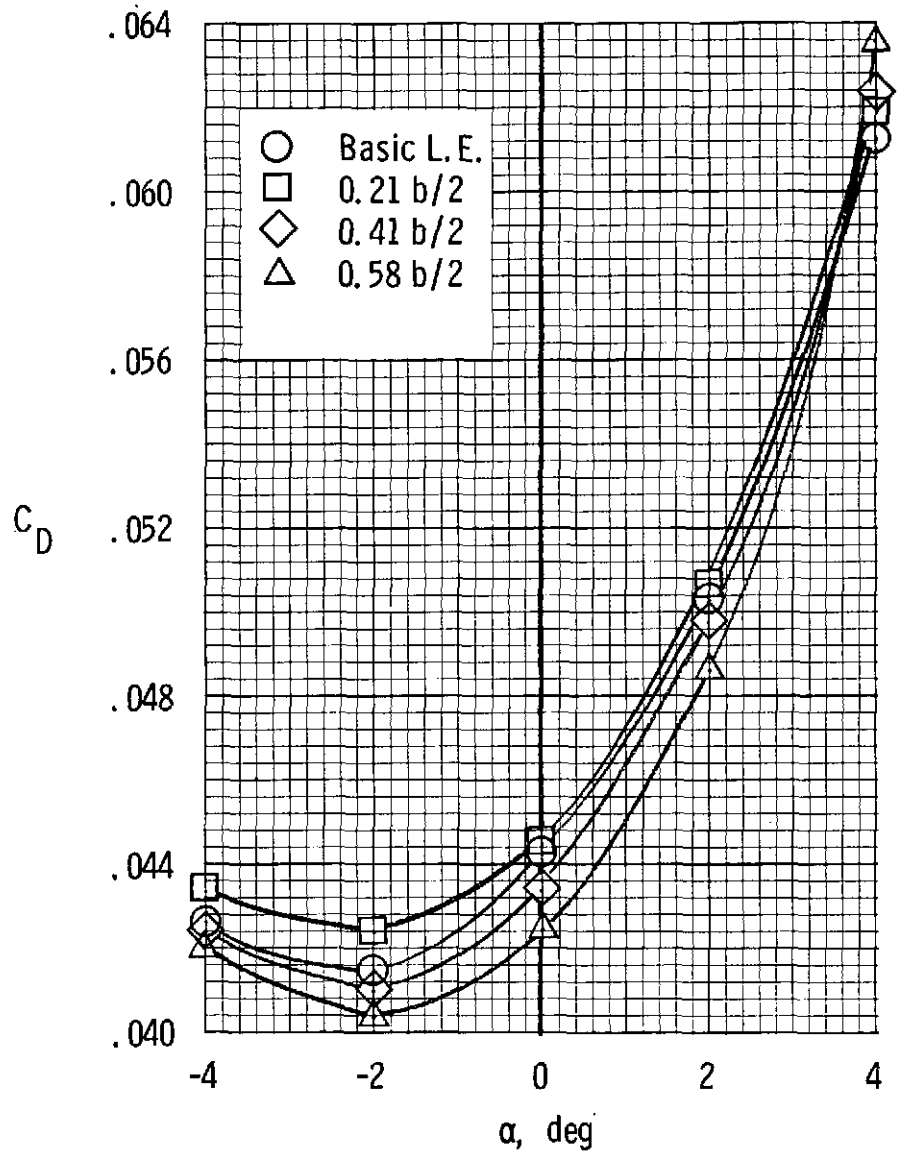

Figure 19.- Comparison of drag coefficients at low angle of attack for the auxiliary airfoil configurations with propellers removed. $\delta_f = 0^o$.

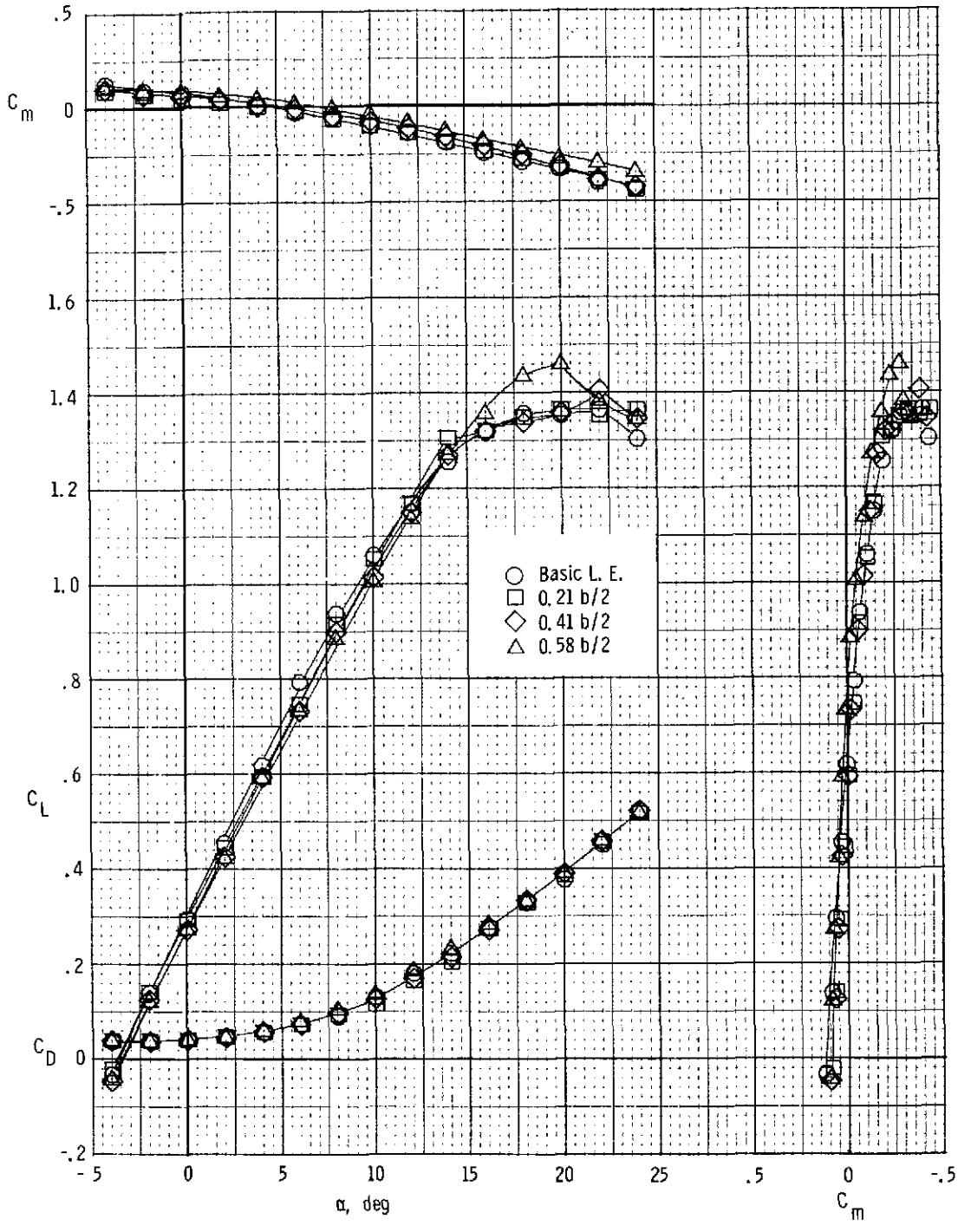

(a) $T_c' = 0$.

Figure 20.- Longitudinal characteristics of the auxiliary airfoil configurations with power. $\delta_f = 0^o$.

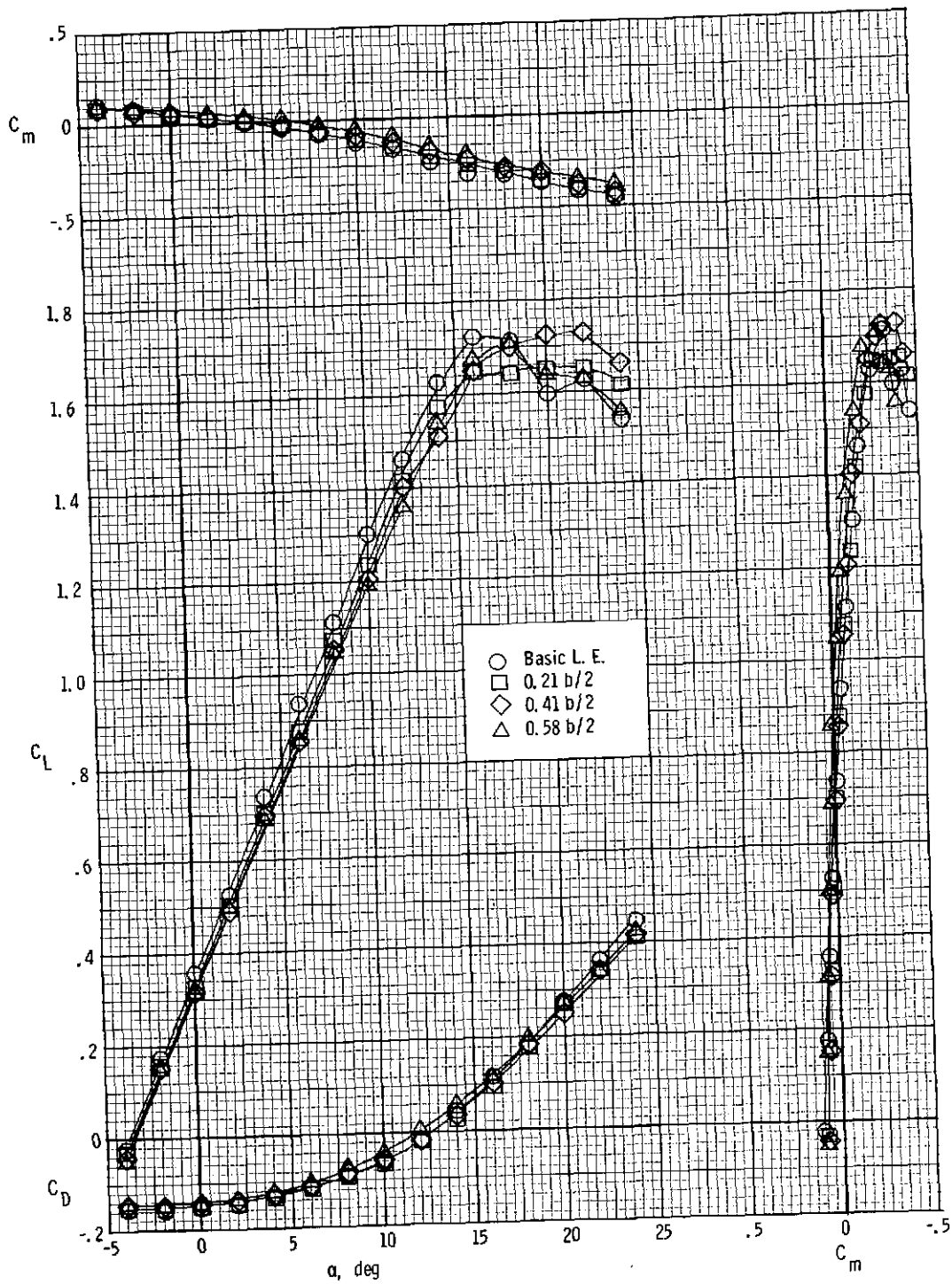

(b) $T_c' = 0.20$.

Figure 20.- Continued.

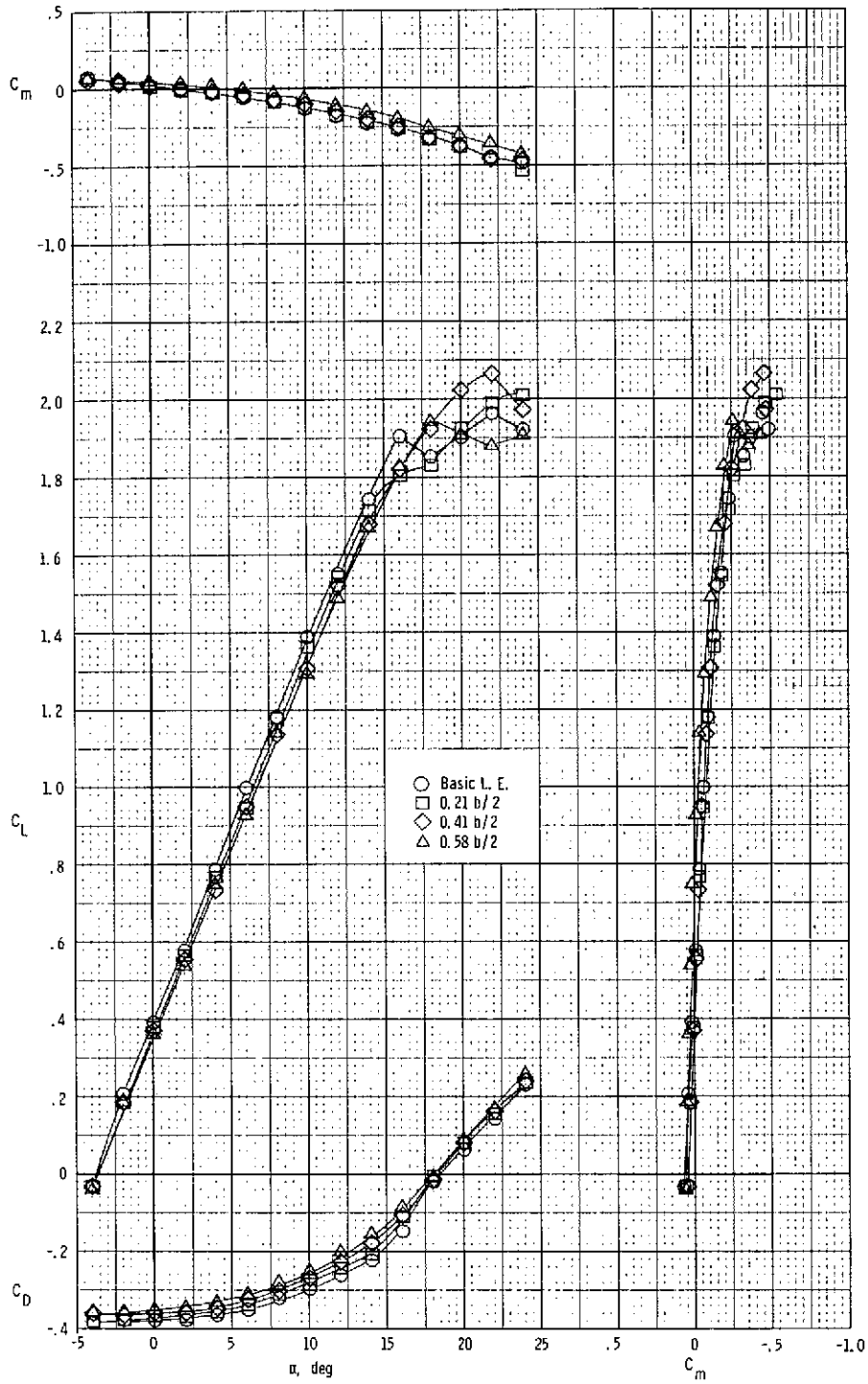

(c) $T_c' = 0.44$.

Figure 20.- Concluded.

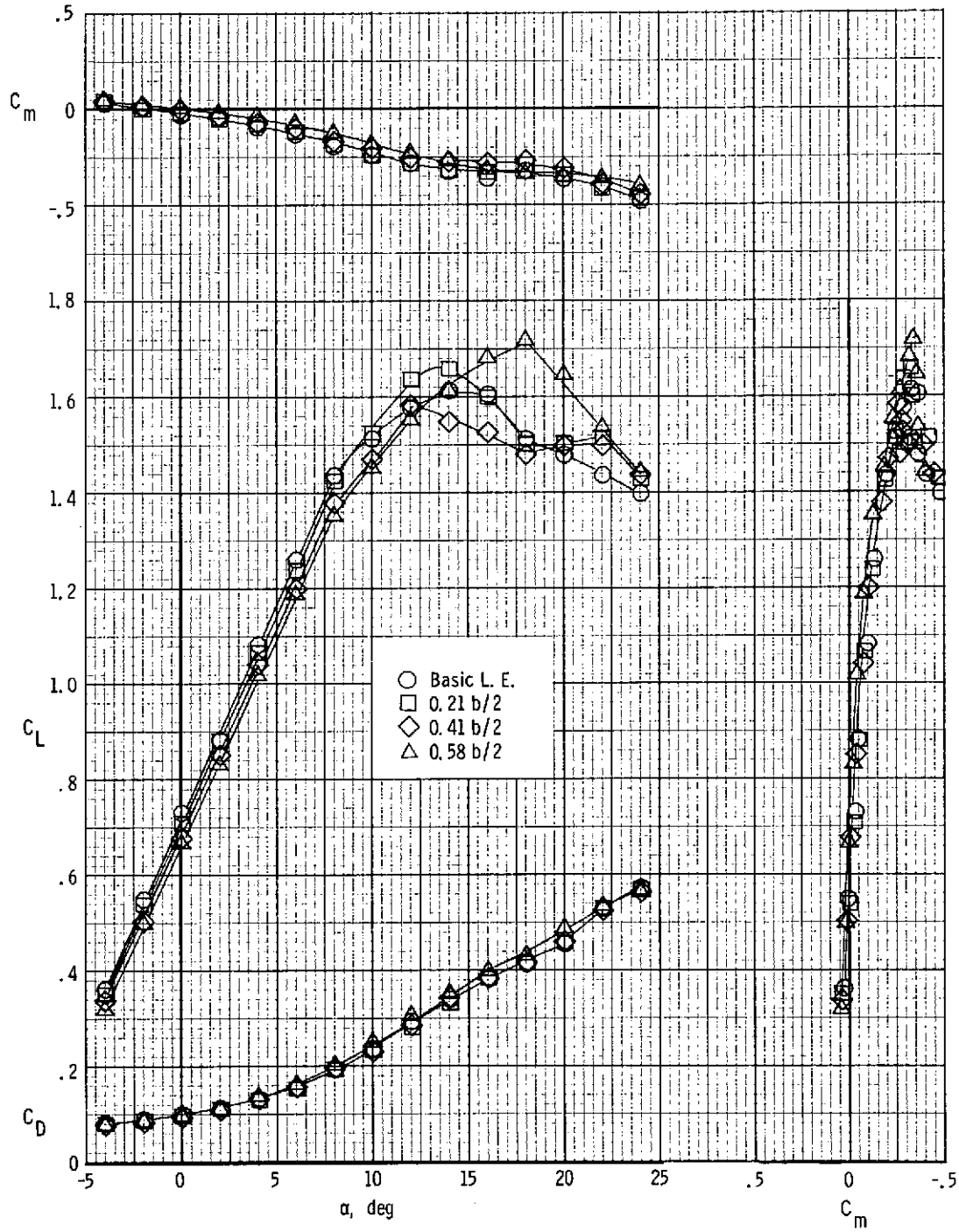

(a) $T_c' = 0.$

Figure 21.- Longitudinal characteristics of the auxiliary airfoil configurations with power. $\delta_f = 27^o$.

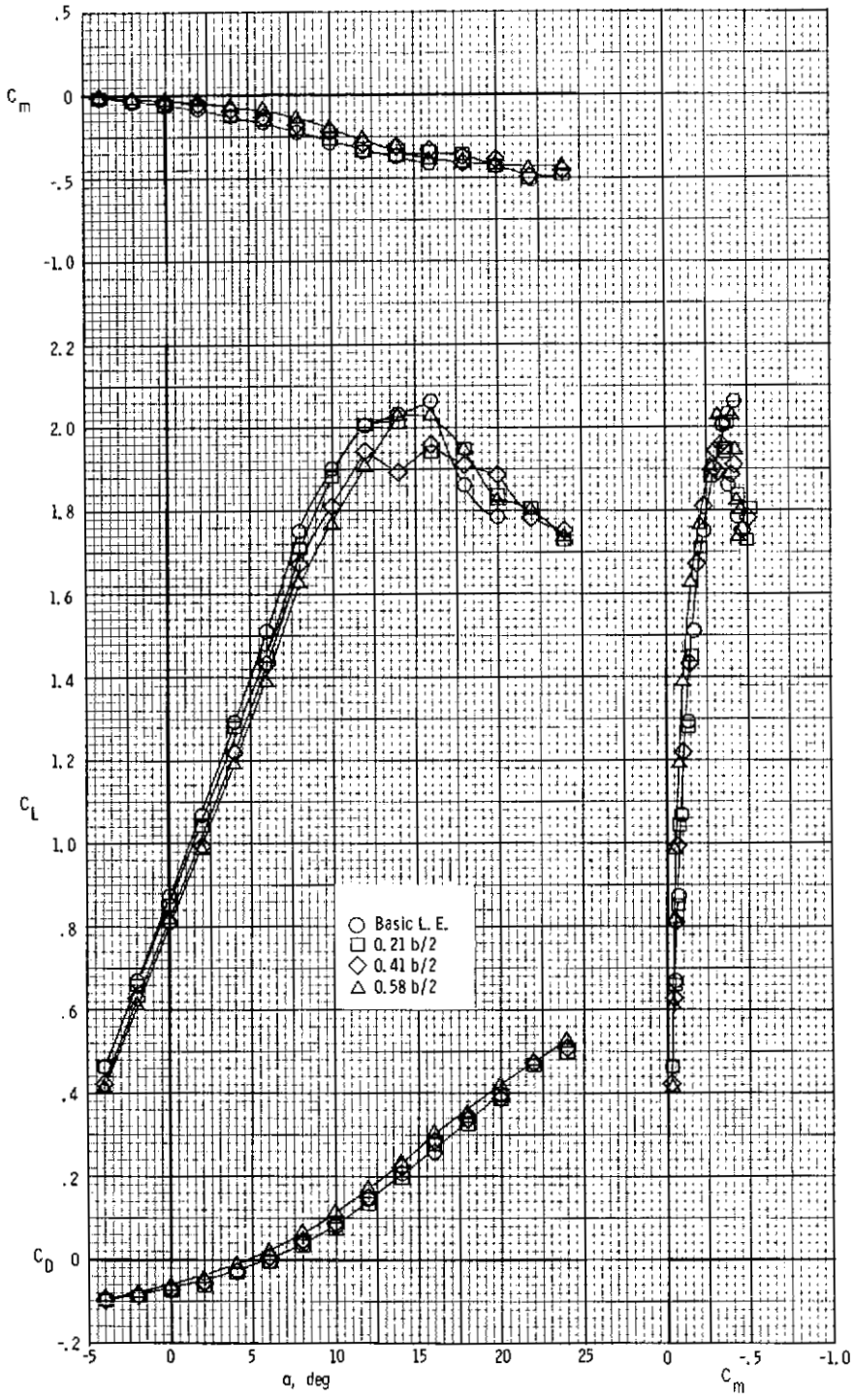

(b) $T_c' = 0.20$.

Figure 21.- Continued.

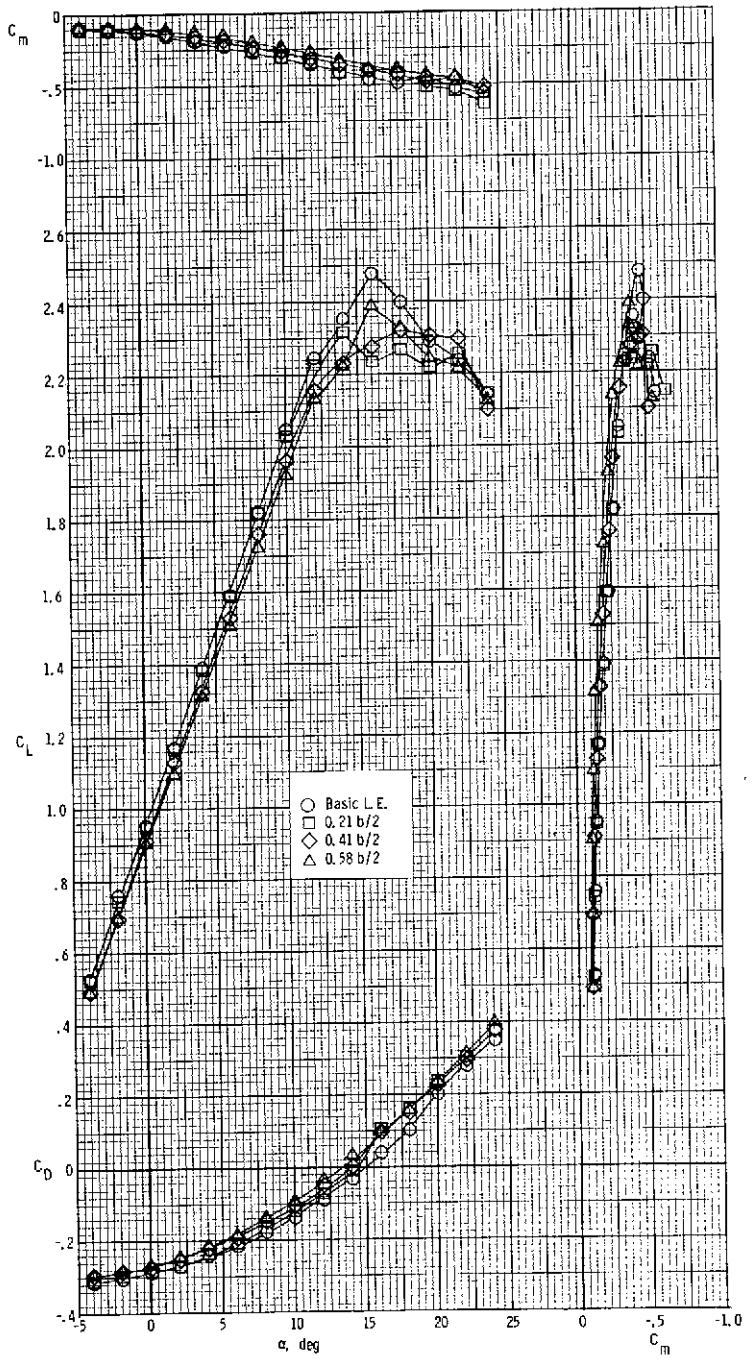

(c) $T_C' = 0.44$.

Figure 21.- Concluded.

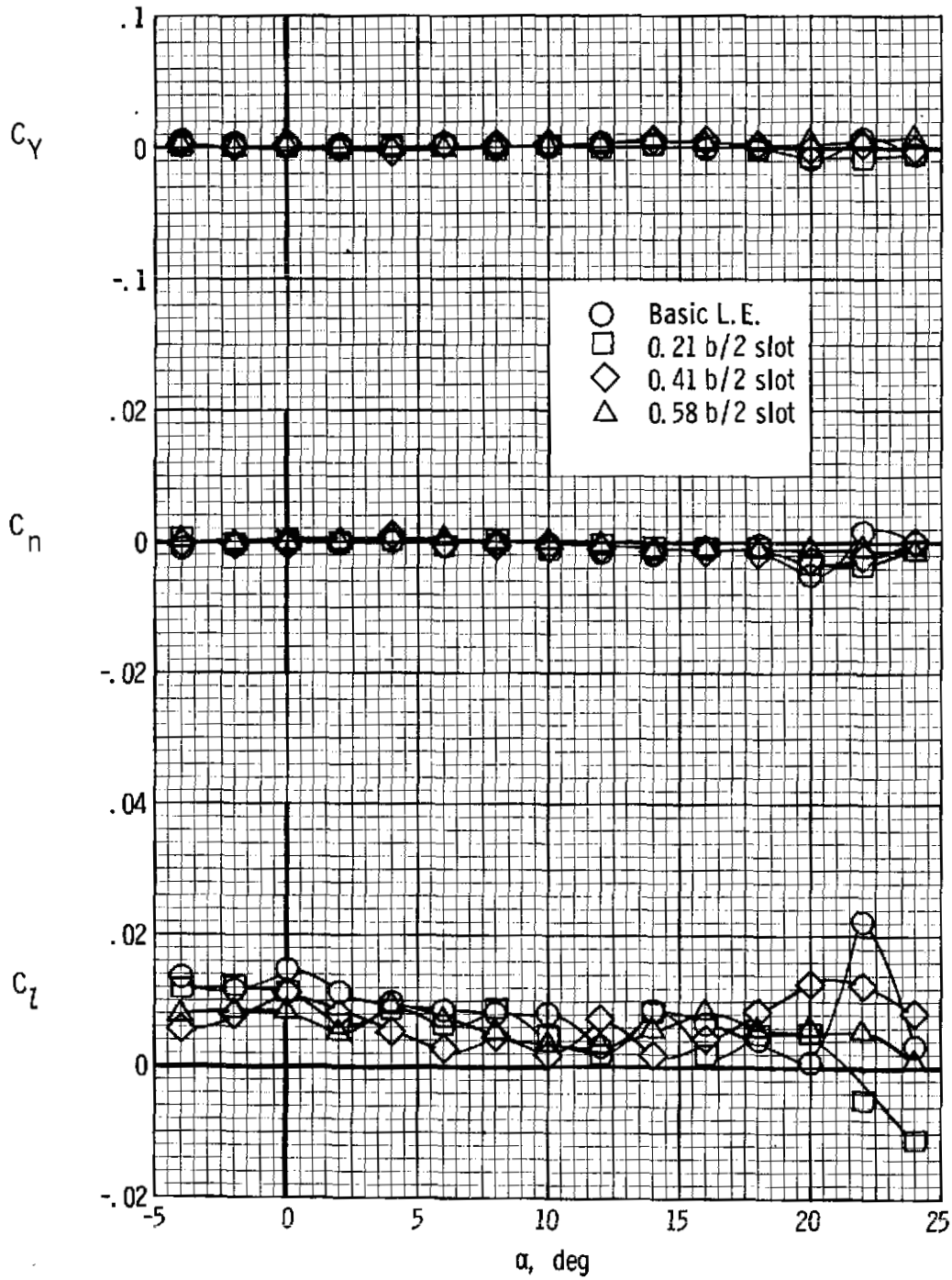

(a) $\delta_f = 0^o$.

Figure 22.- Lateral characteristics for leading-edge slots with propellers removed.

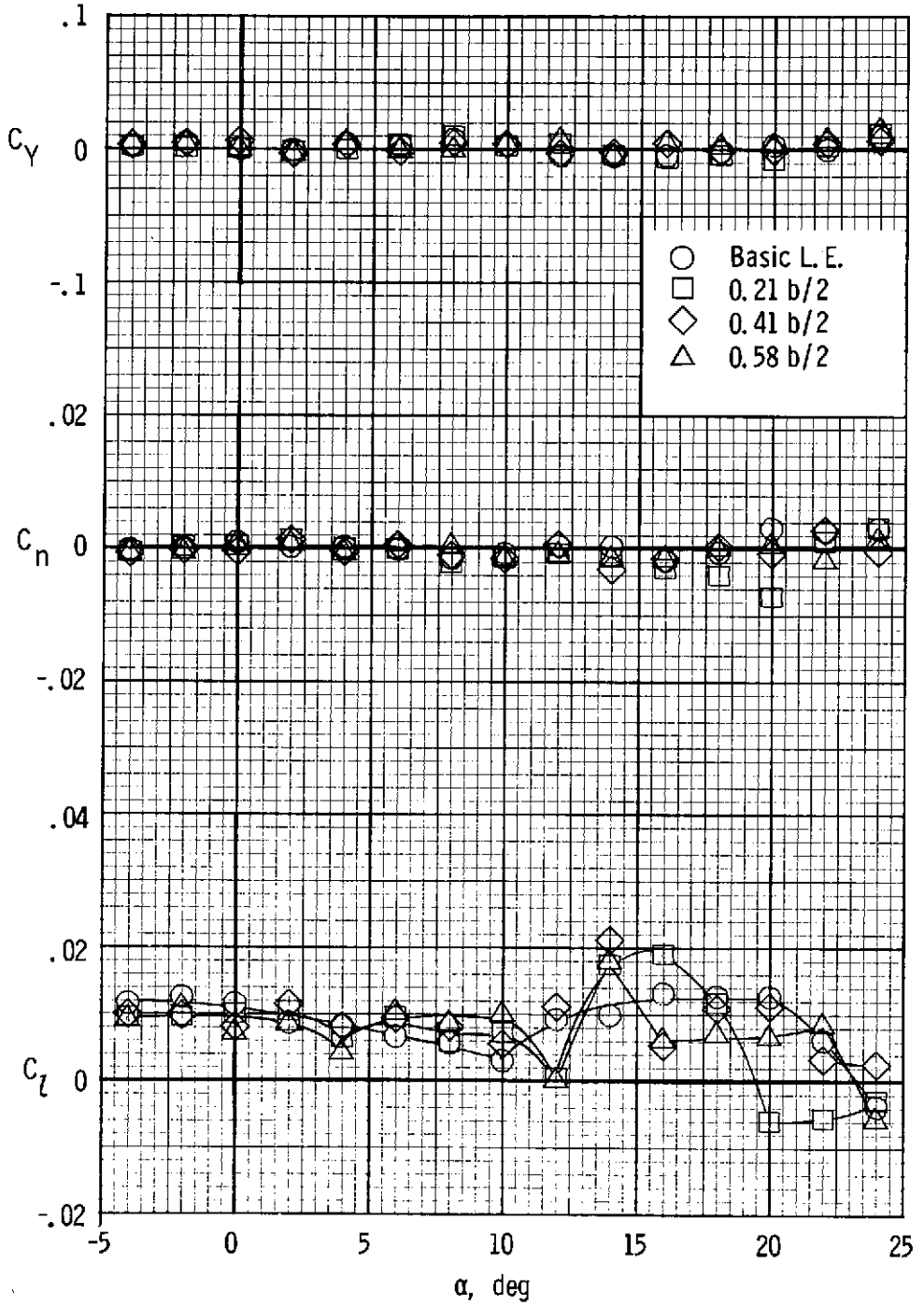

(b) $\delta_f = 27^o$.

Figure 22.- Concluded.

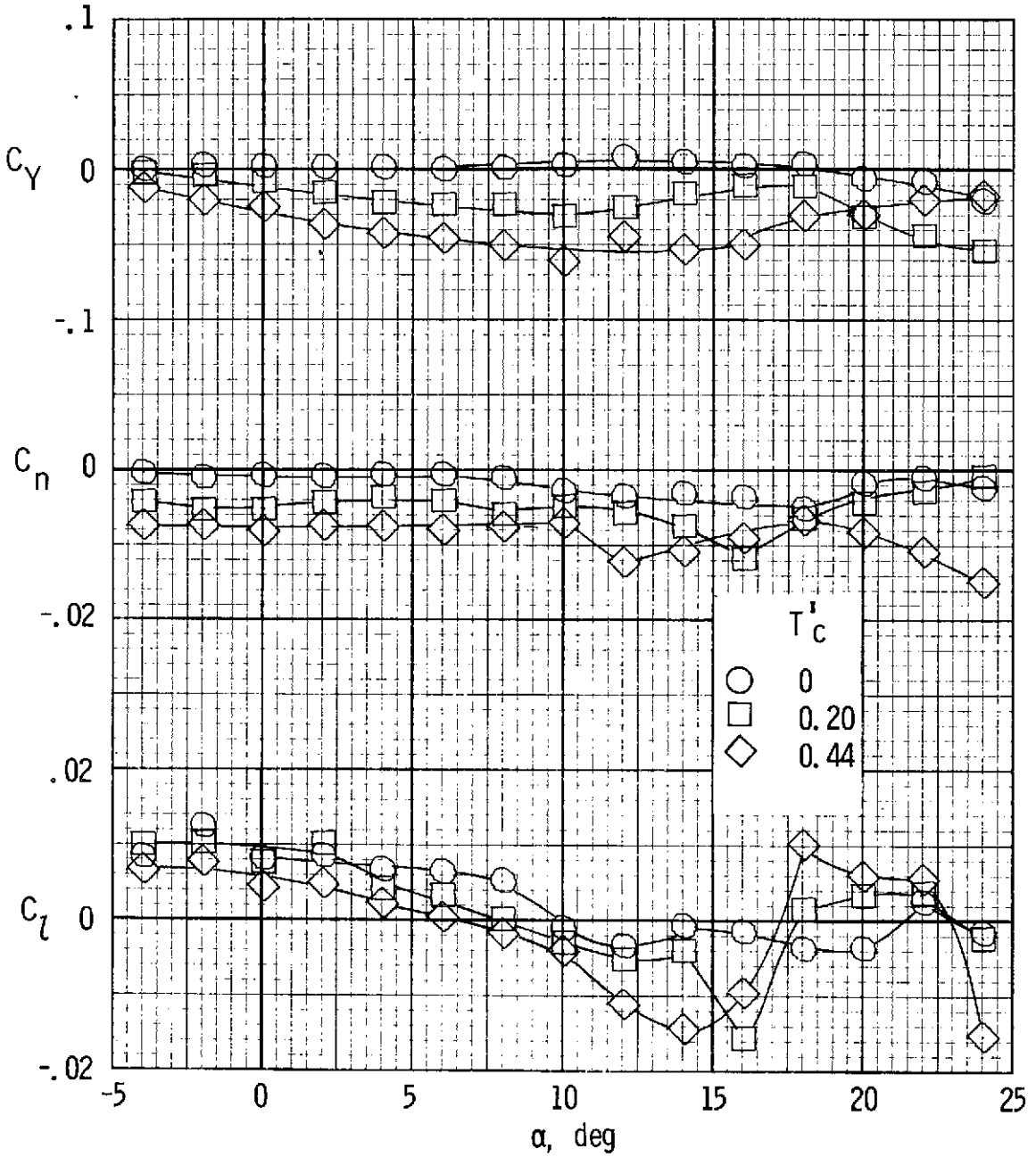

(a) $\delta_f = 0^o$.

Figure 23.- Lateral characteristics of basic leading edge with power.

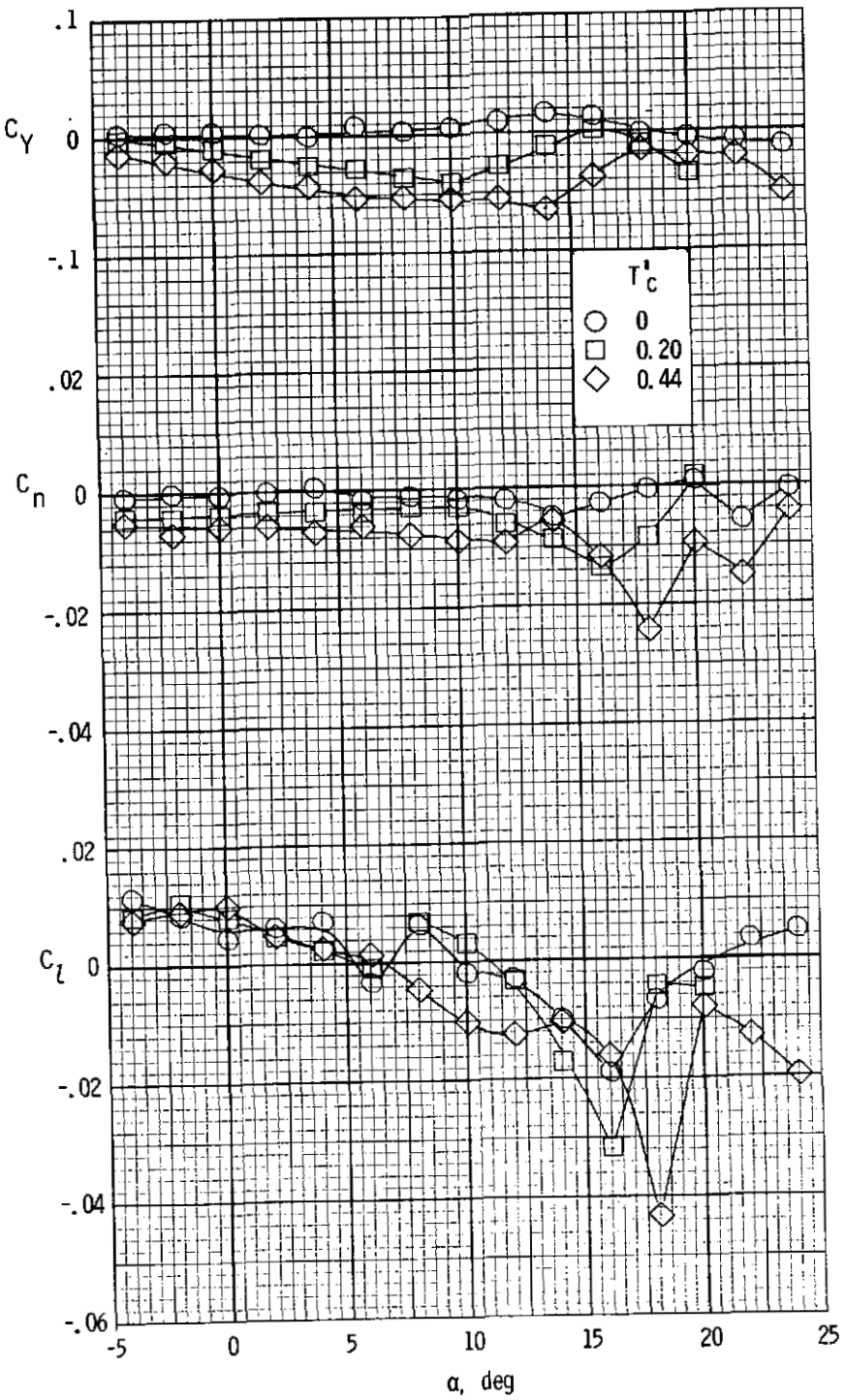

(b) $\delta_f = 27^o$.

Figure 23.- Concluded.

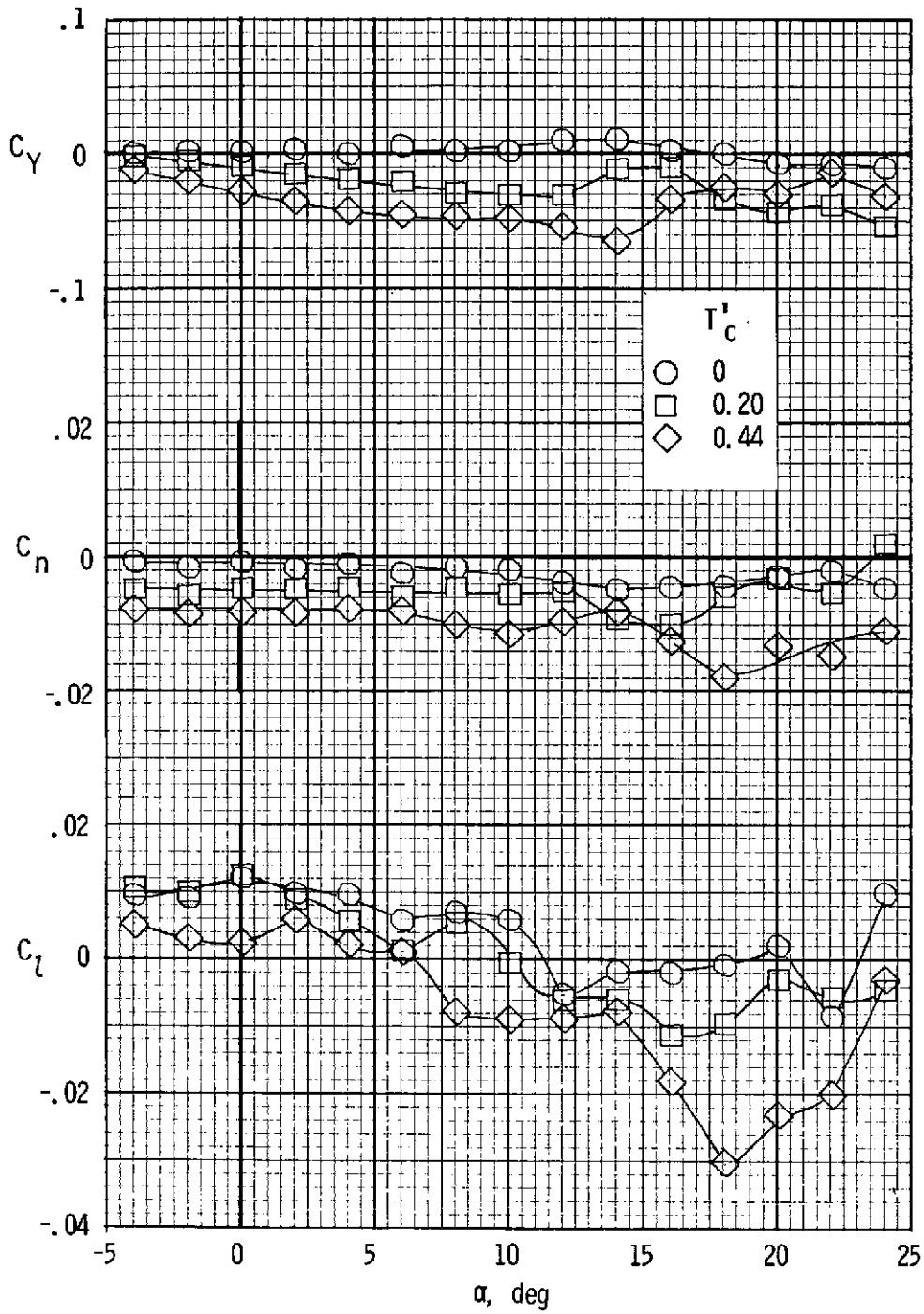

(a) $\delta_f = 0^o$.

Figure 24.- Lateral characteristics of the 0.41b/2 leading-edge slot configuration with power.

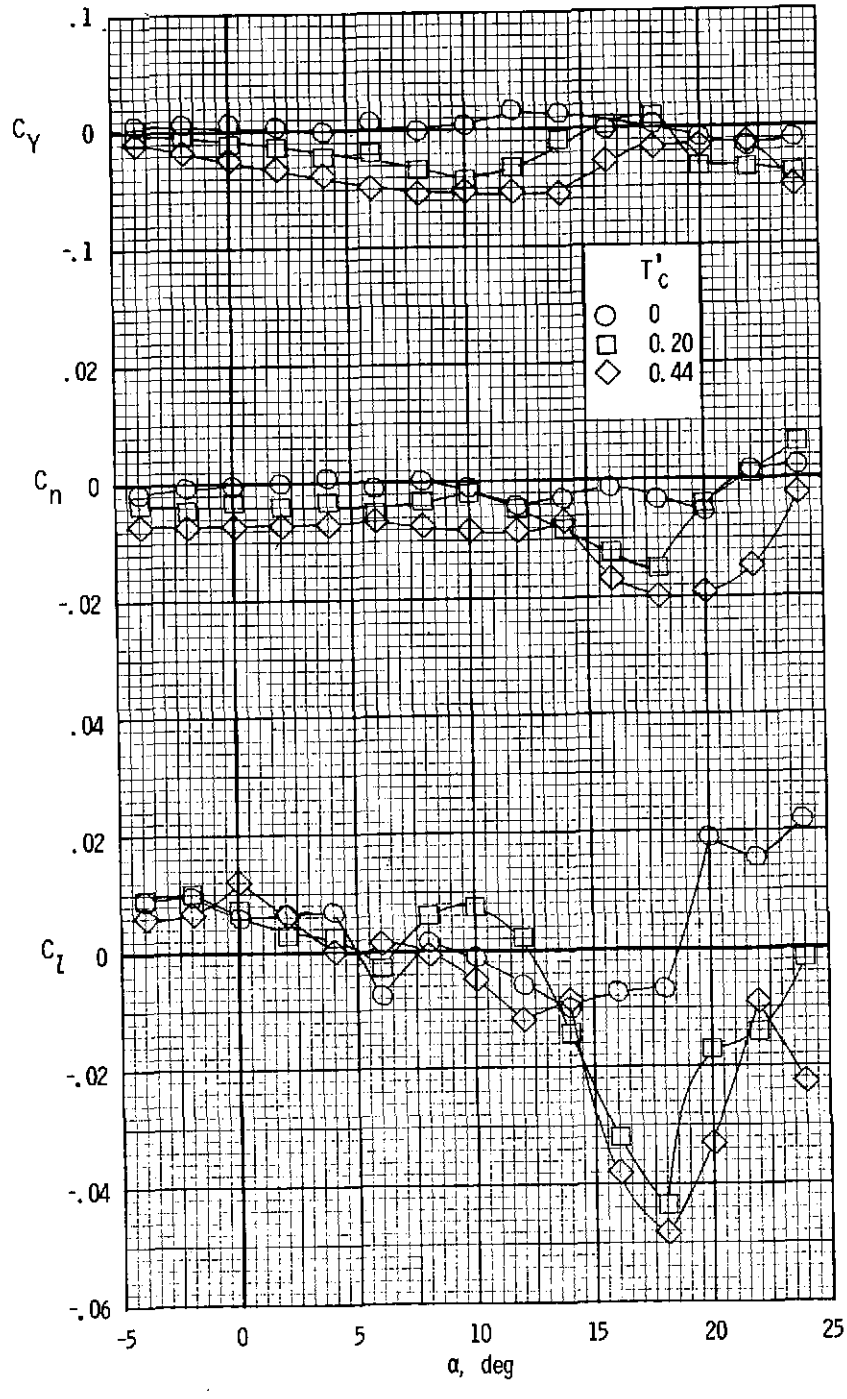

(b) $\delta_f = 27^o$.

Figure 24.- Concluded.

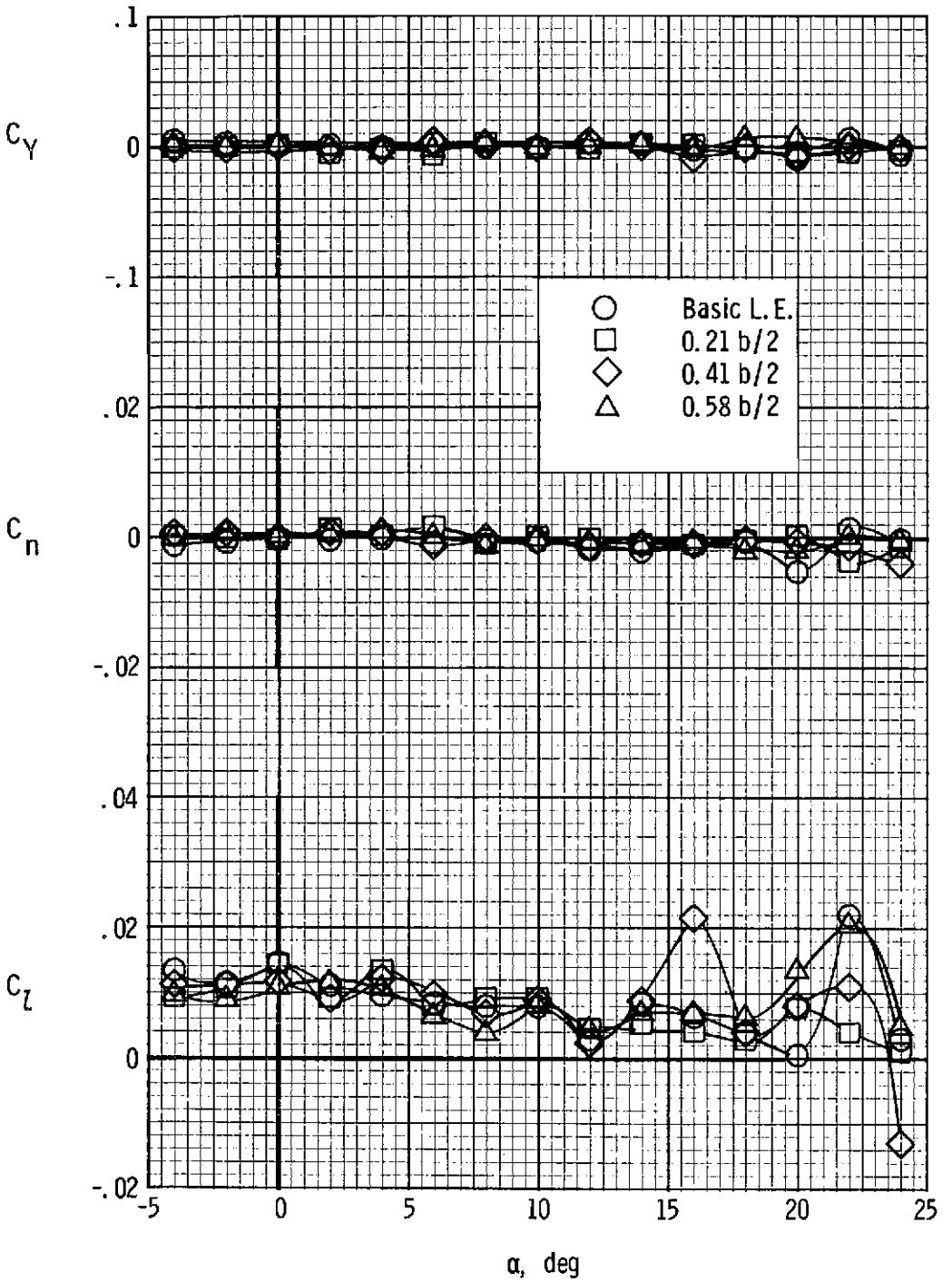

Figure 25.- Lateral characteristics for the various auxiliary airfoil configurations with propellers removed. $\delta_f = 0^o$.

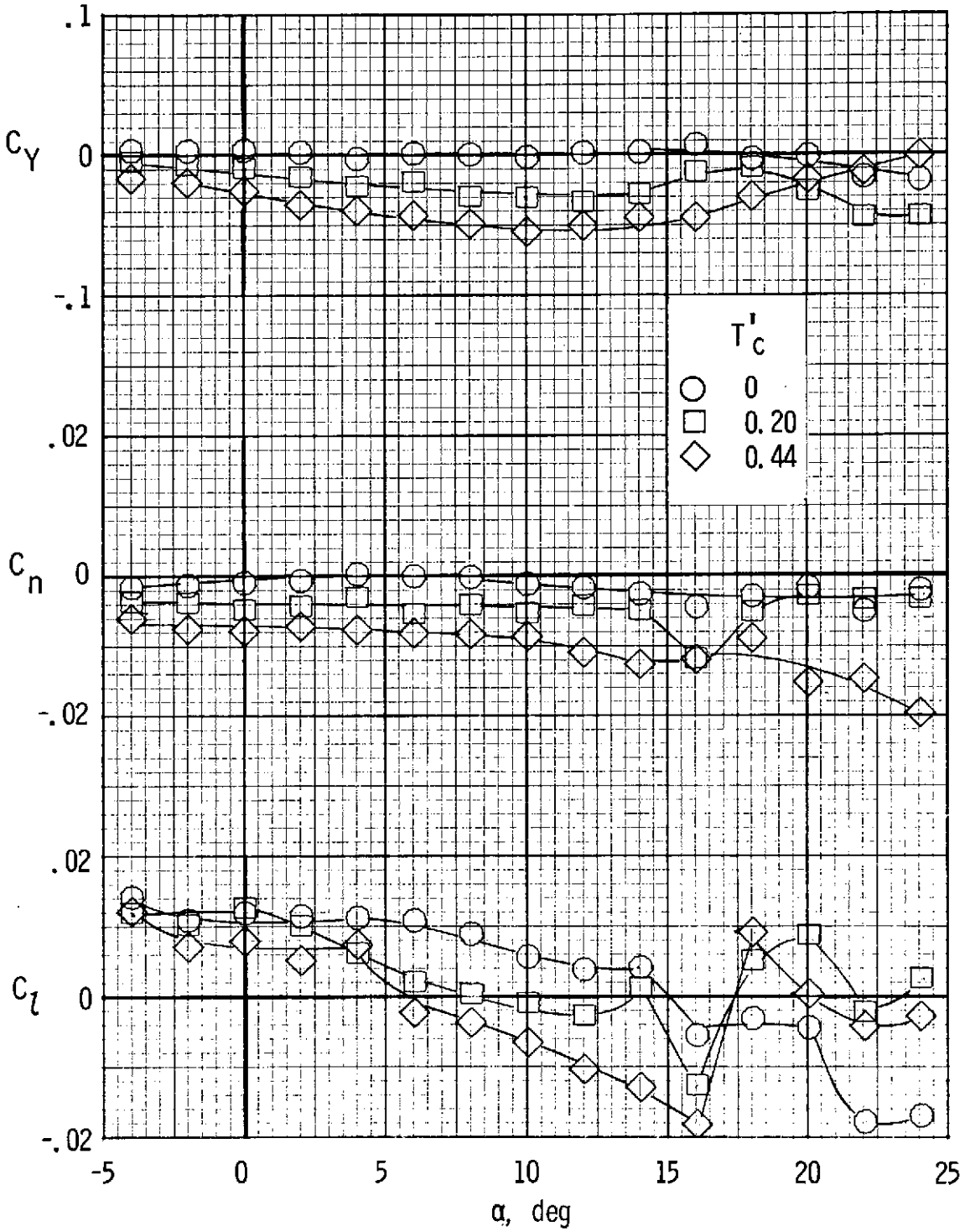

(a) 0.21b/2.

Figure 26.- Effect of power on lateral characteristics of the various auxiliary airfoil configurations. $\delta_f = 0^o$.

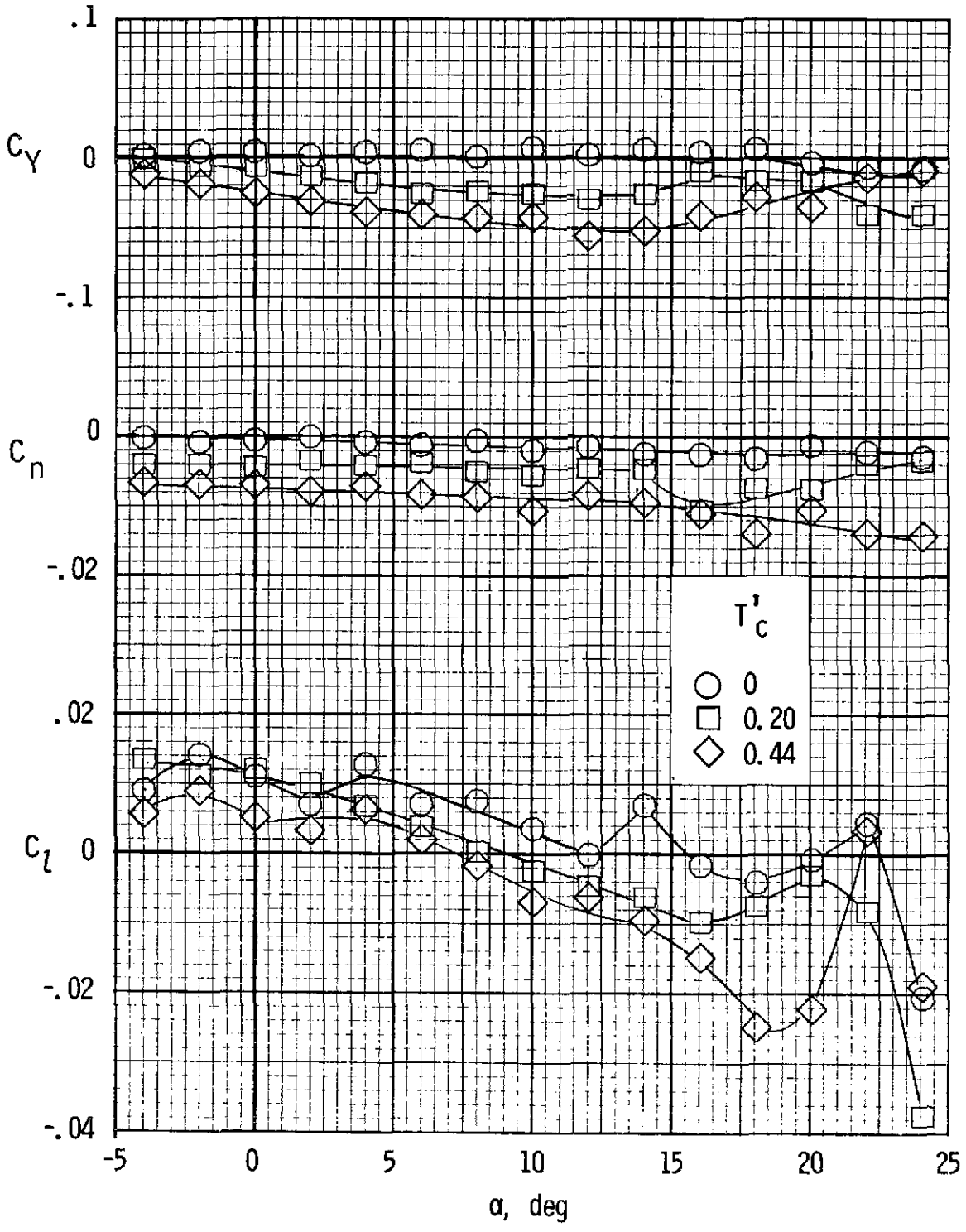

(b) 0.41b/2.

Figure 26.- Continued.

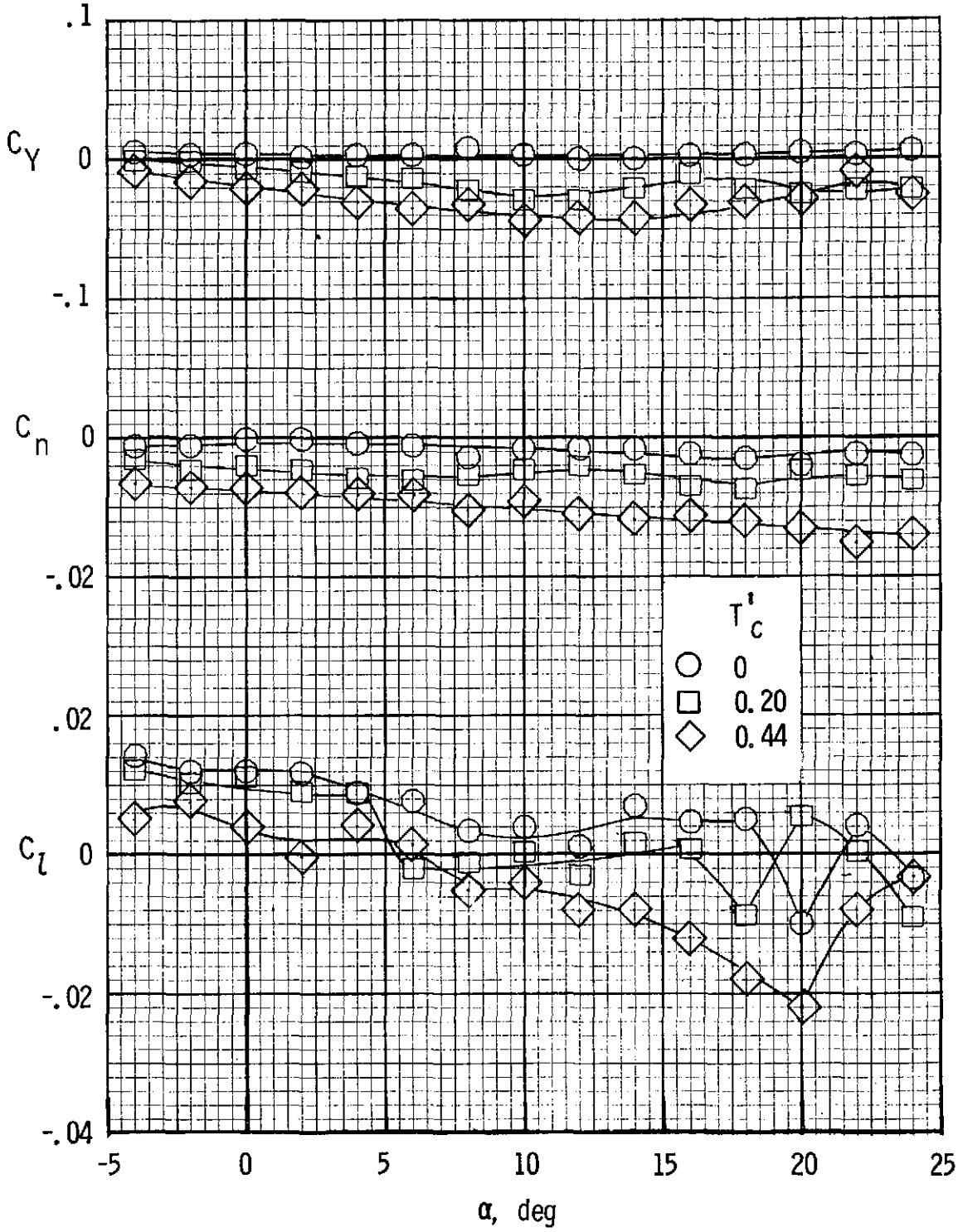

(c) 0.58b/2.

Figure 26.- Concluded.

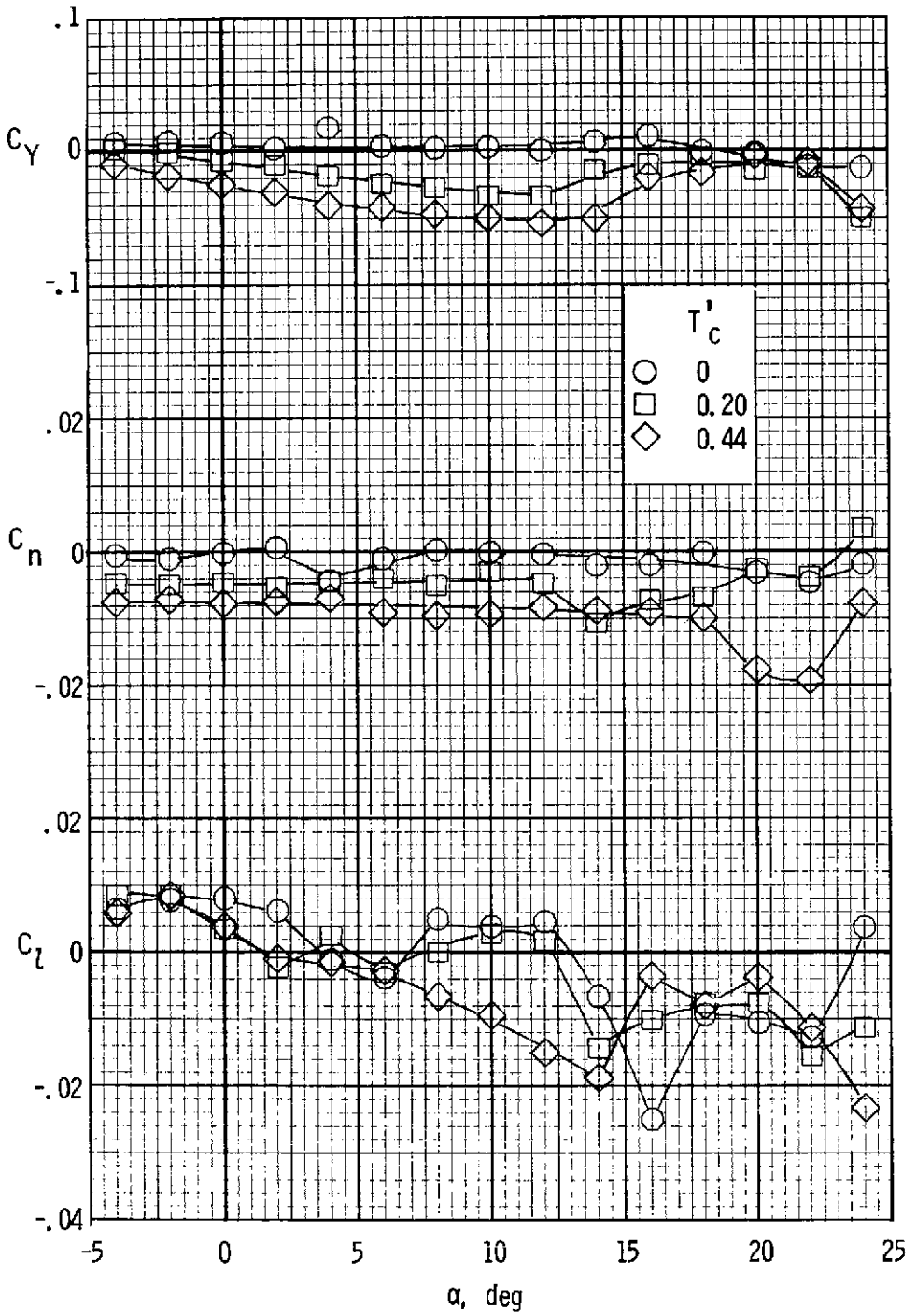

(a) 0.21b/2.

Figure 27.- Effect of power on the lateral characteristics of the various auxiliary airfoil configurations. $\delta_f = 27^o$.

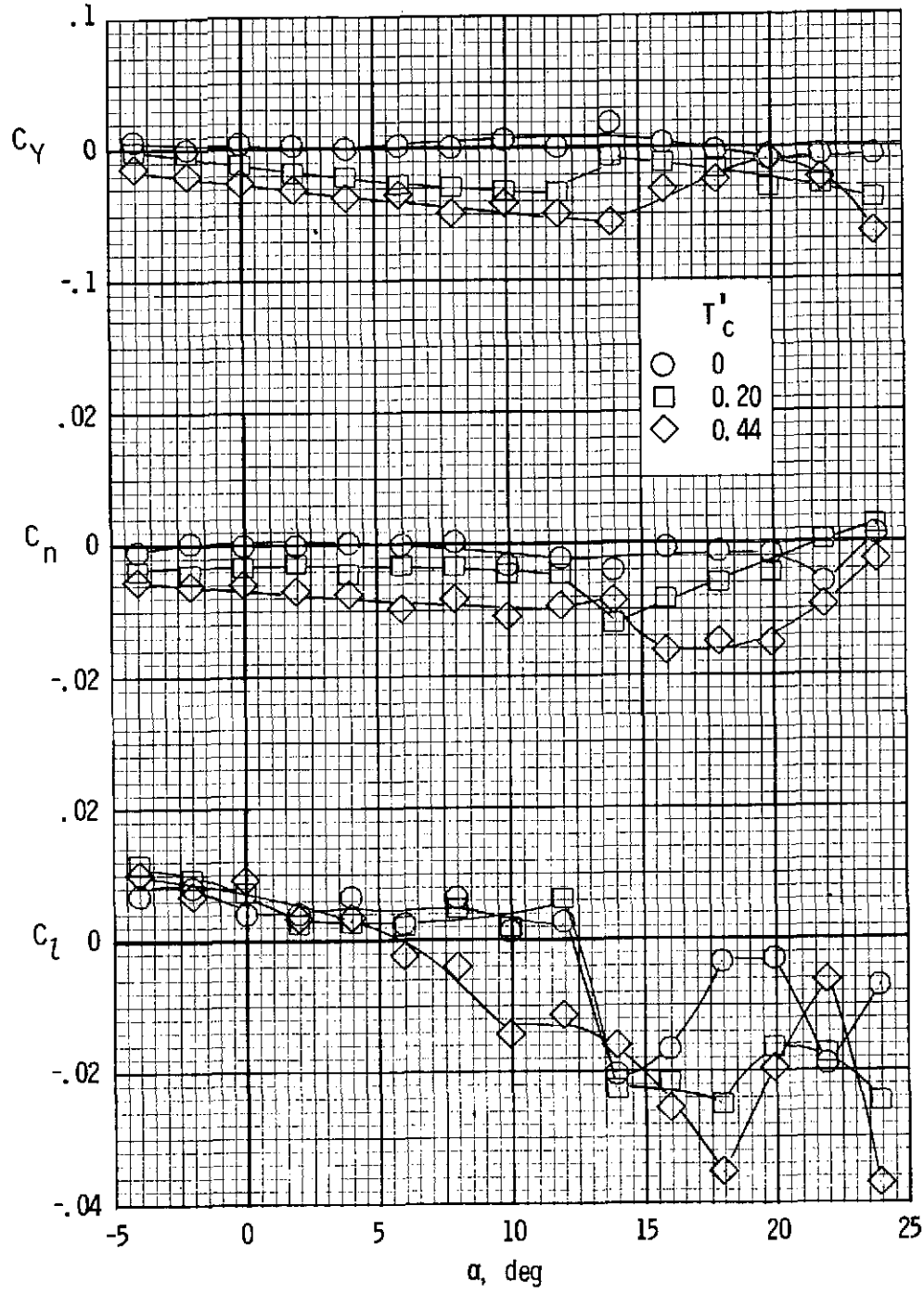

(b) 0.41b/2.

Figure 27.- Continued.

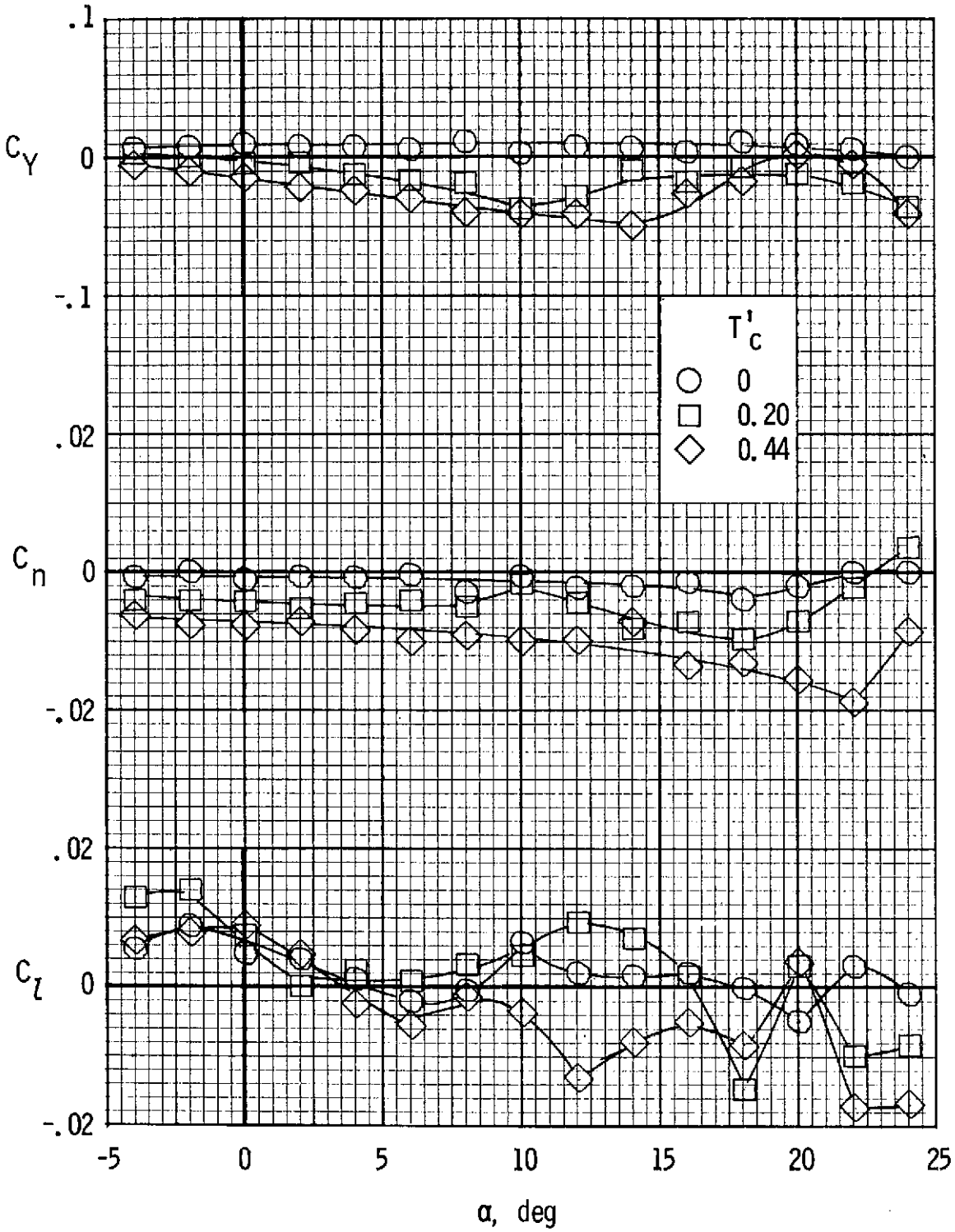

(c) 0.58b/2.

Figure 27.- Concluded.

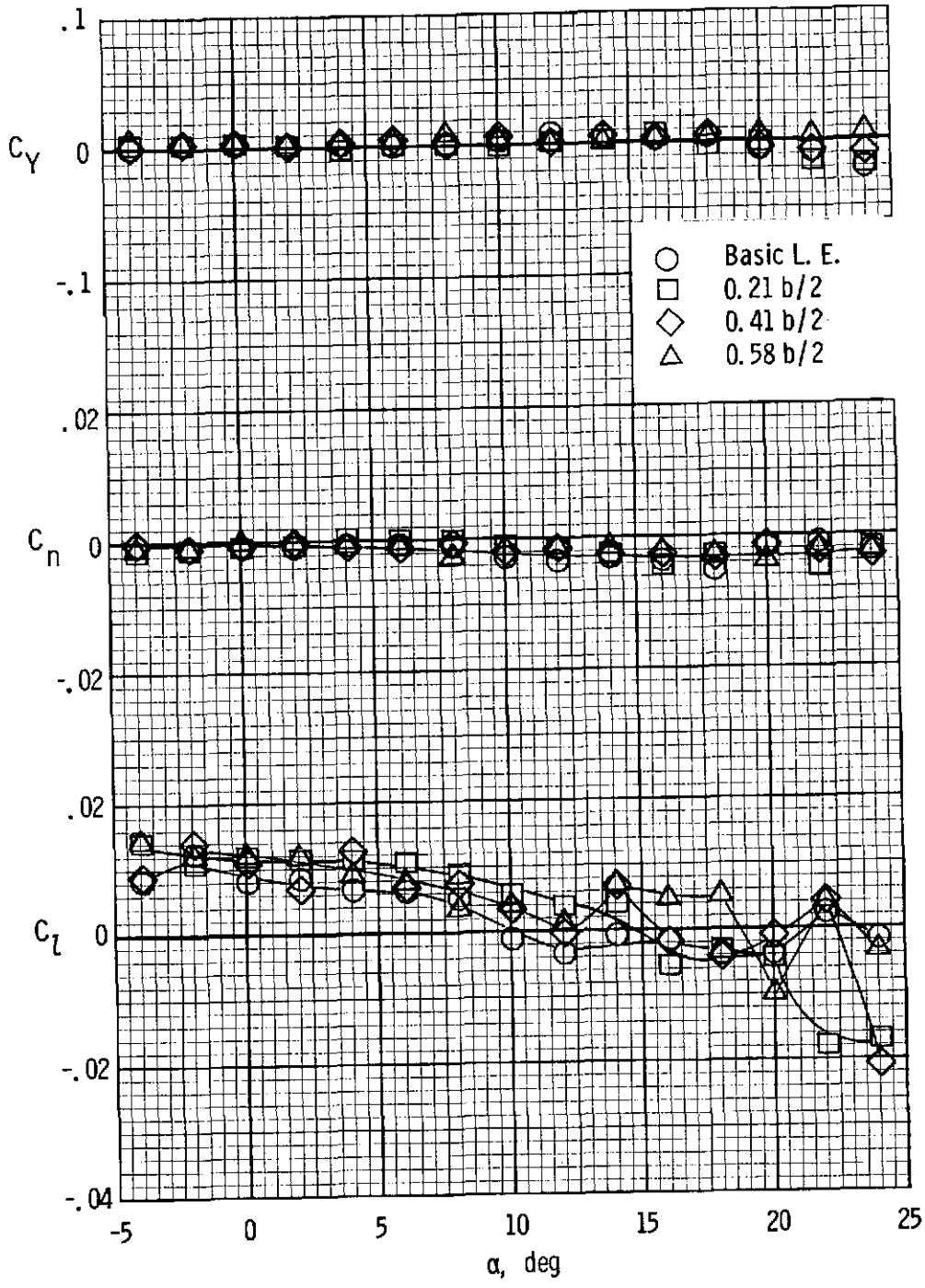

(a) $T_c' = 0$.

Figure 28.- Lateral characteristics for the various auxiliary airfoil configurations. $\delta_f = 0^o$.

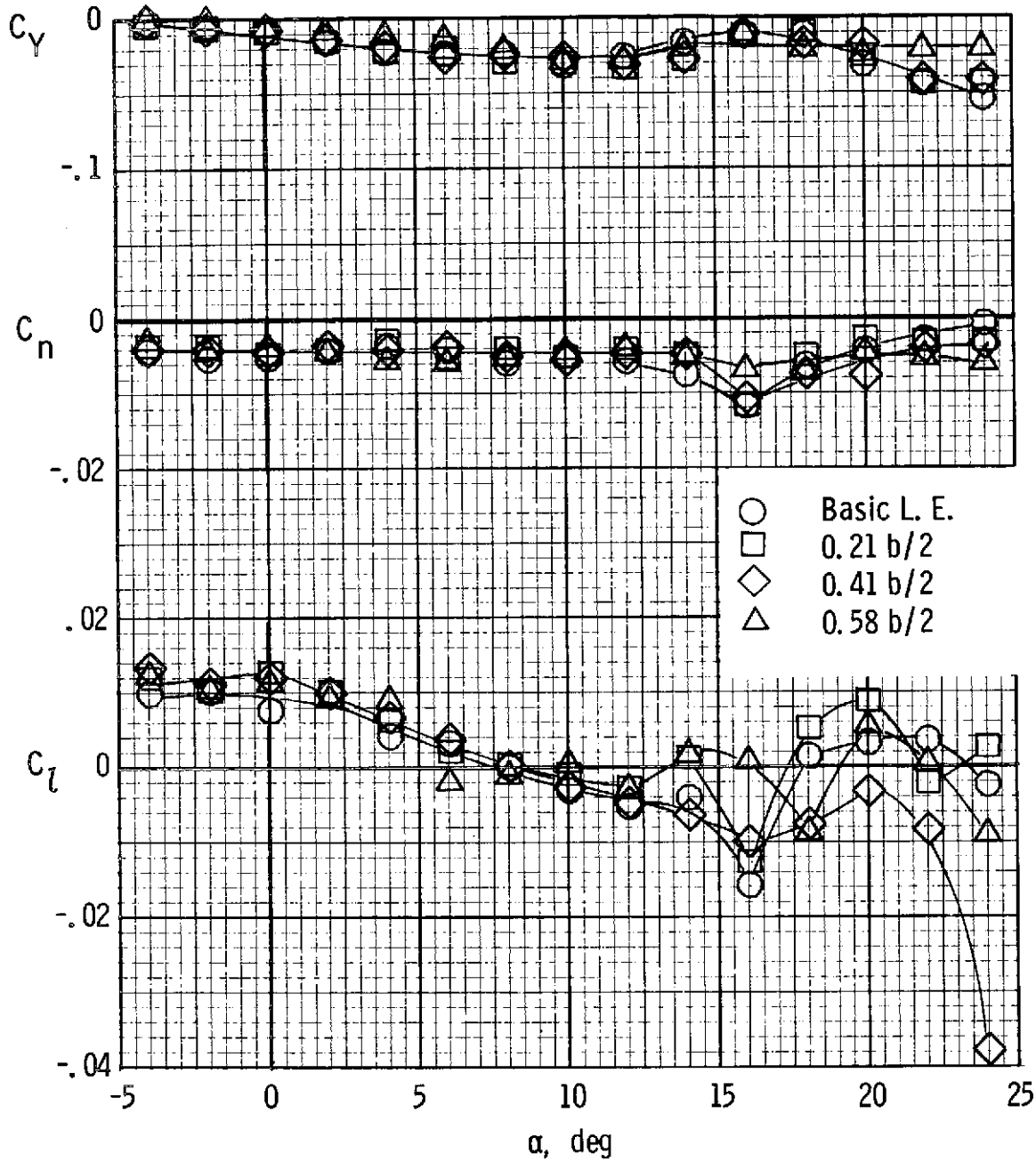

(b) $T_c' = 0.20$.

Figure 28.- Continued.

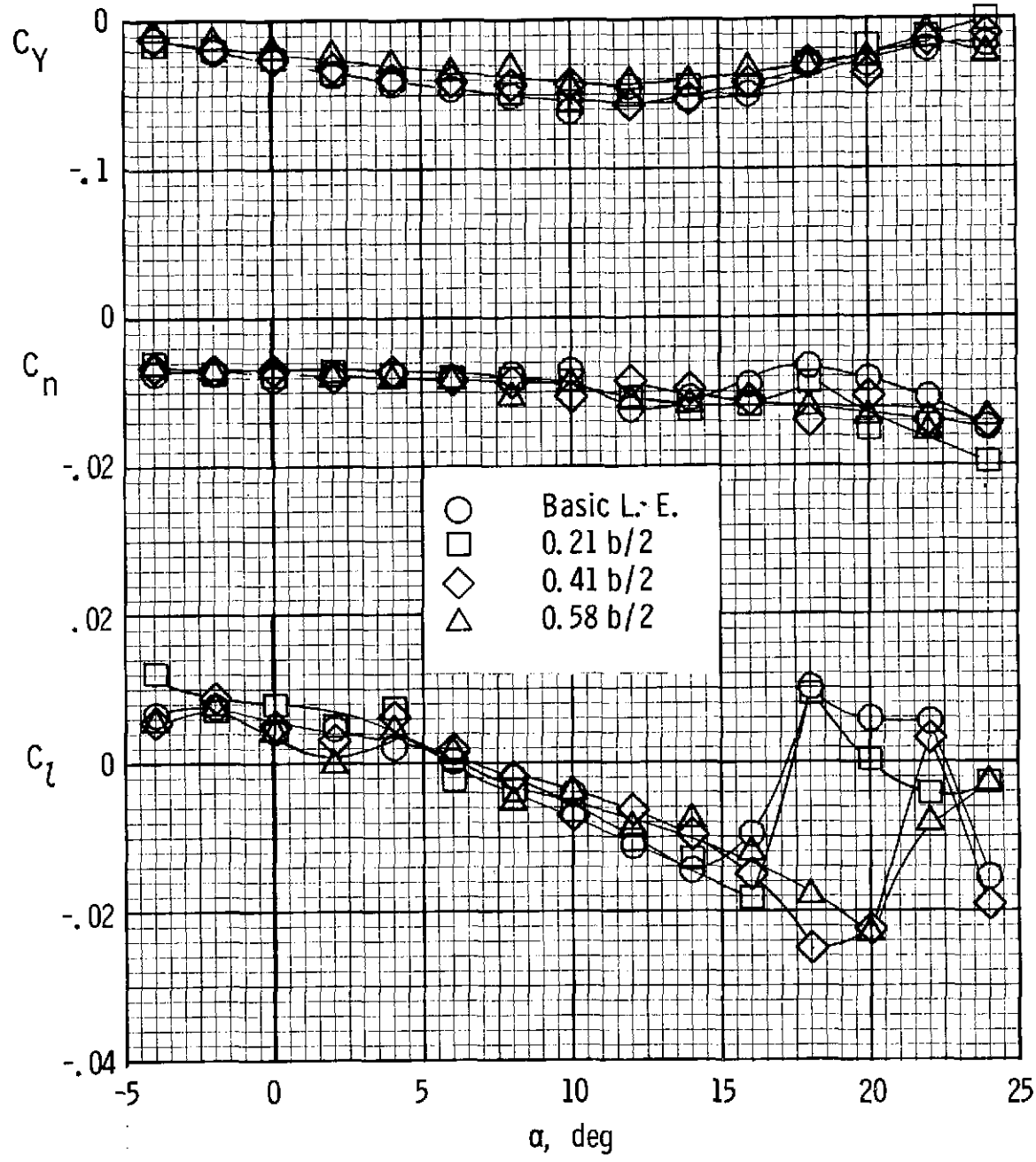

(c) $T_c' = 0.44$.

Figure 28.- Concluded.

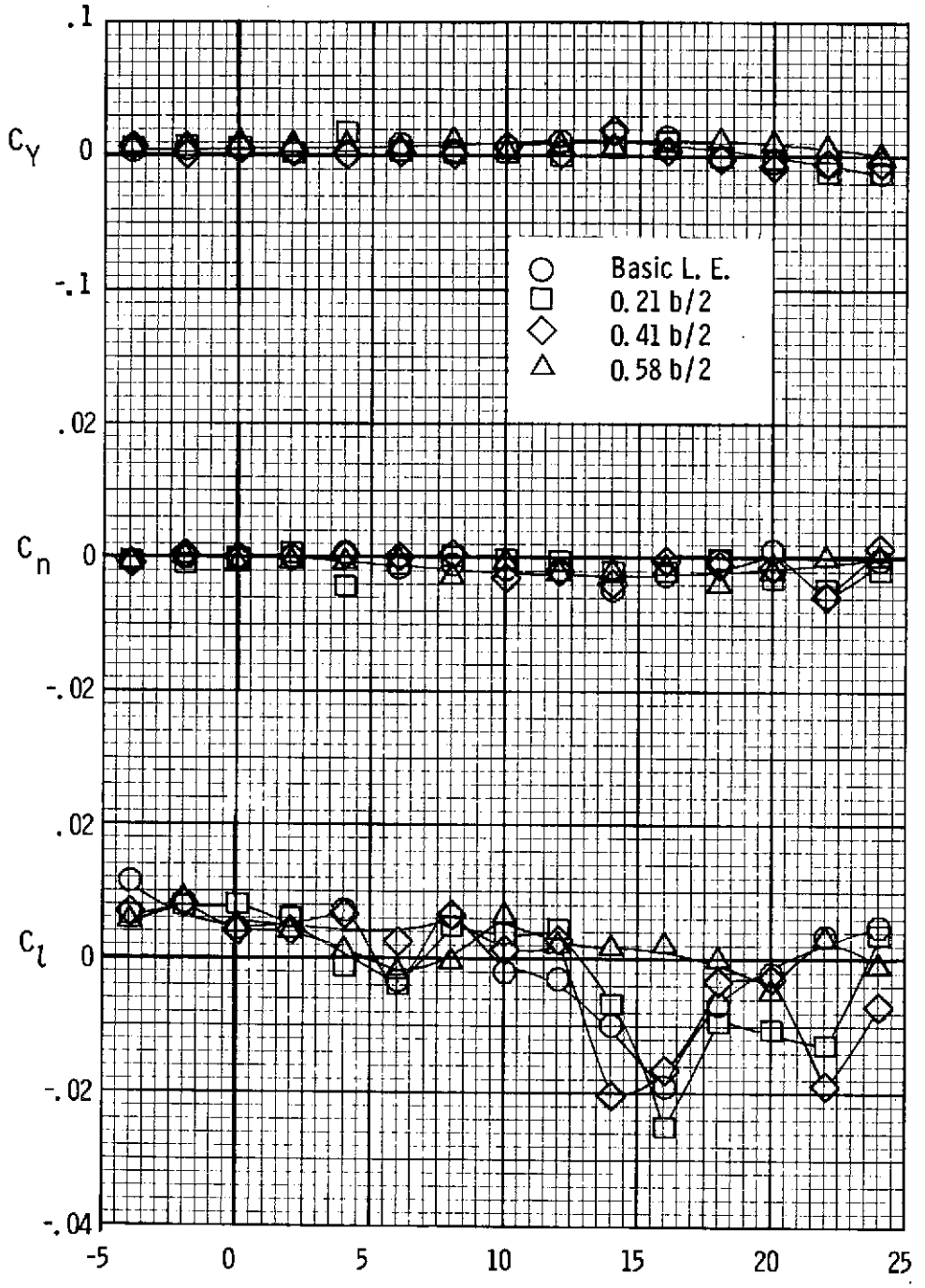

(a) $T_c' = 0.$

Figure 29.- Lateral characteristics for the various auxiliary airfoil configurations. $\delta_f = 27^o$.

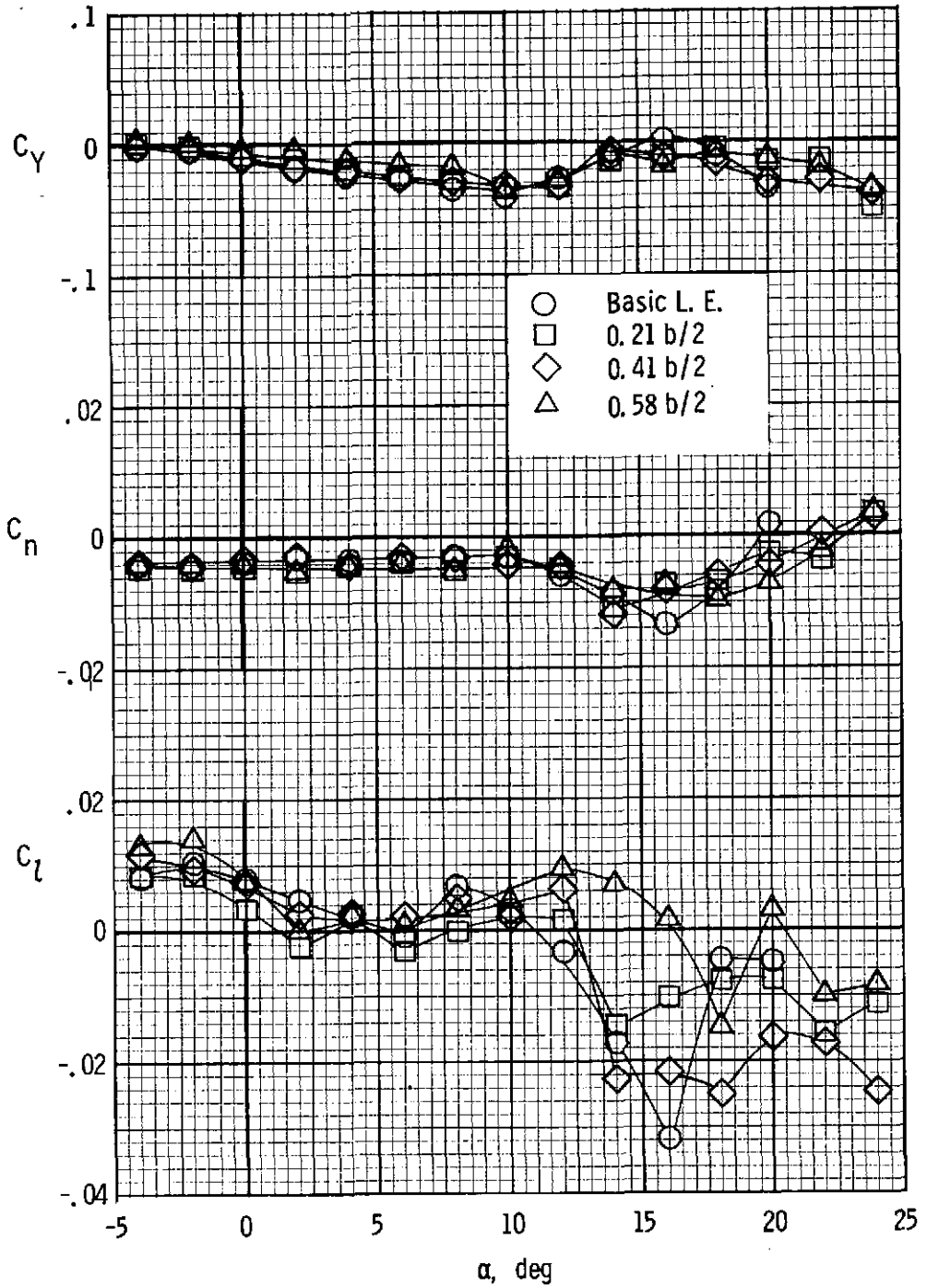

(b) $T_c' = 0.20$.

Figure 29.- Continued.

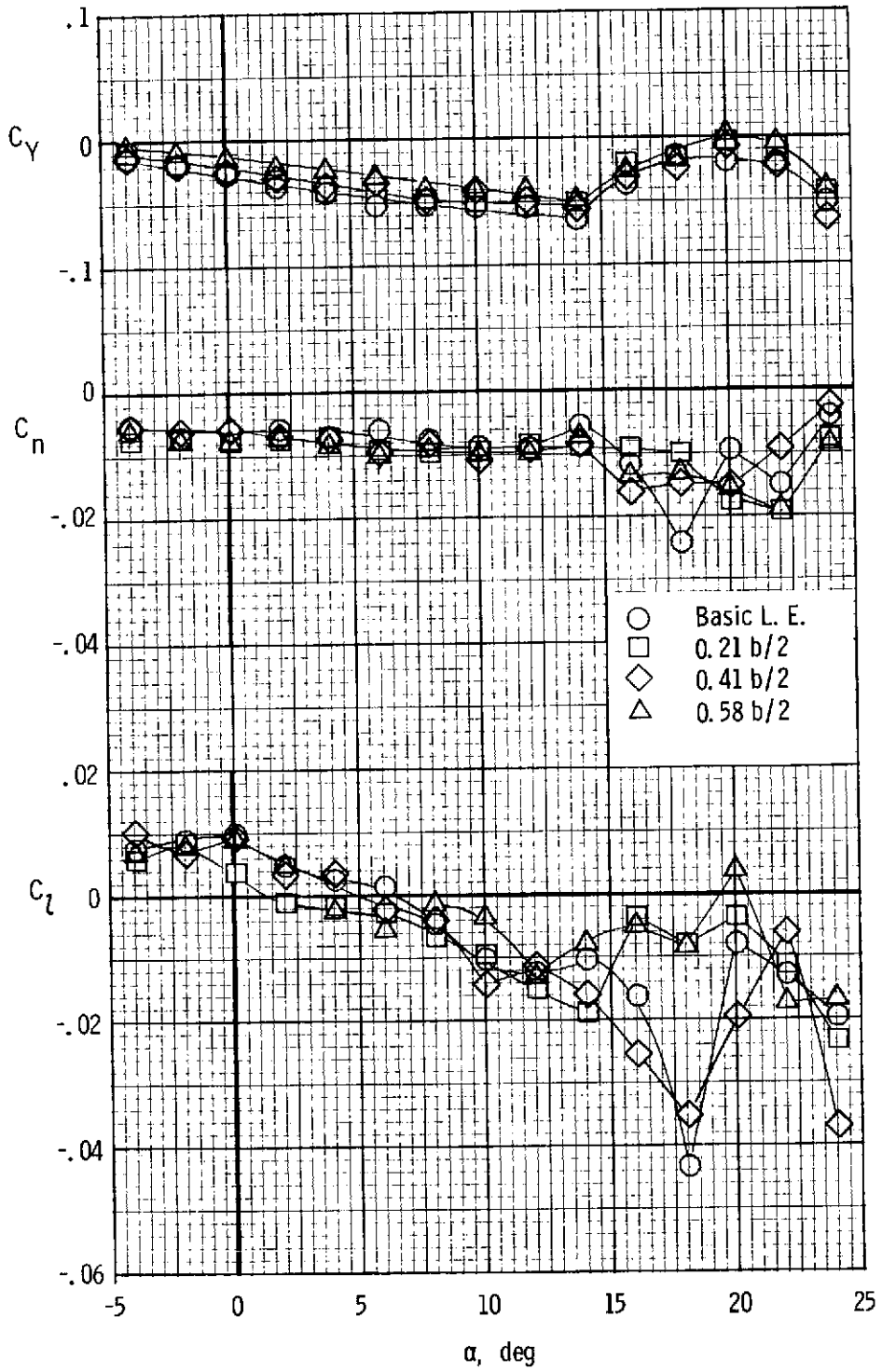

(c) $T_C' = 0.44$.

Figure 29.- Concluded.

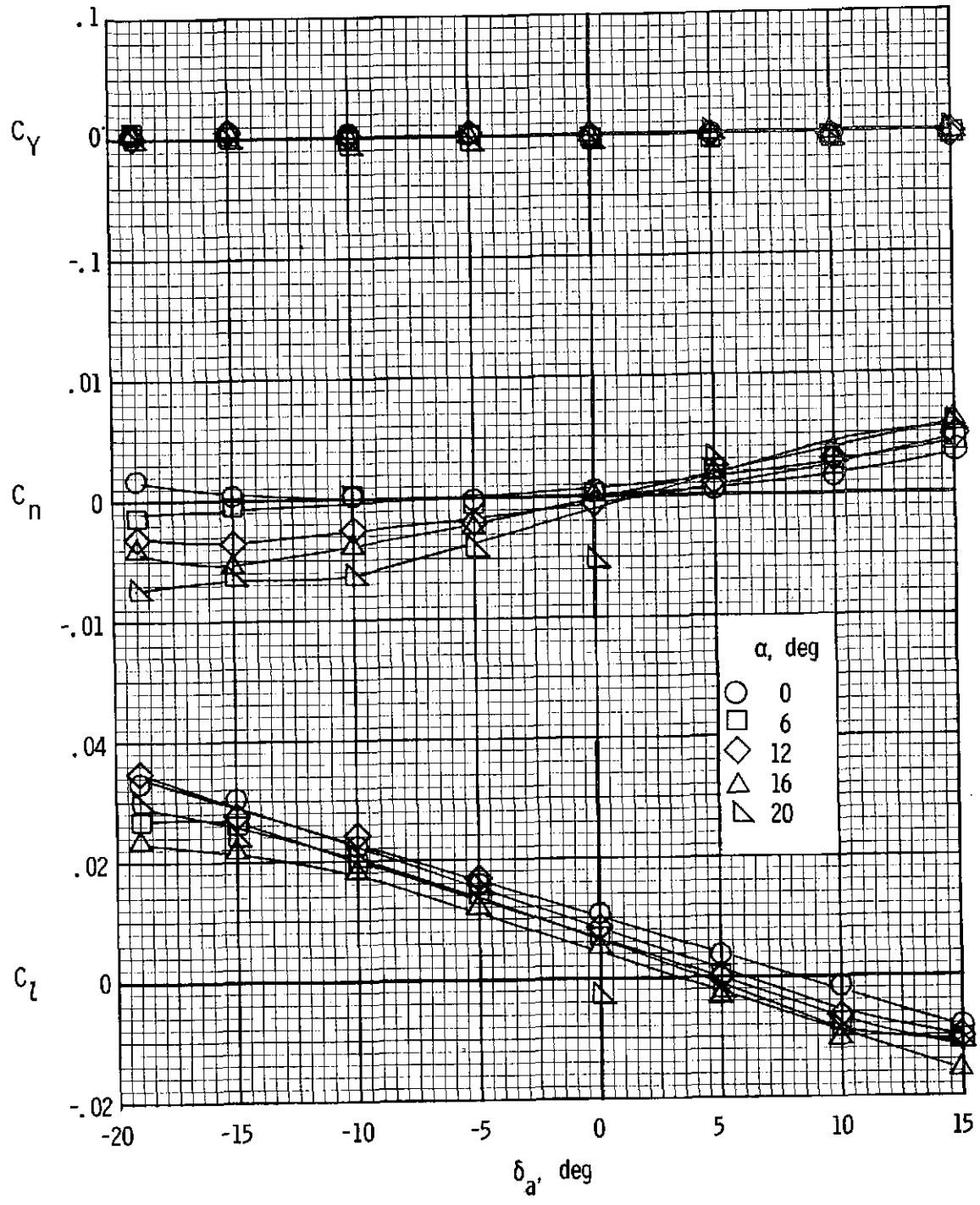

Figure 30.- Variation of the lateral characteristics with aileron deflection of the basic leading-edge configuration with propellers removed. $\delta_f = 0^o$.

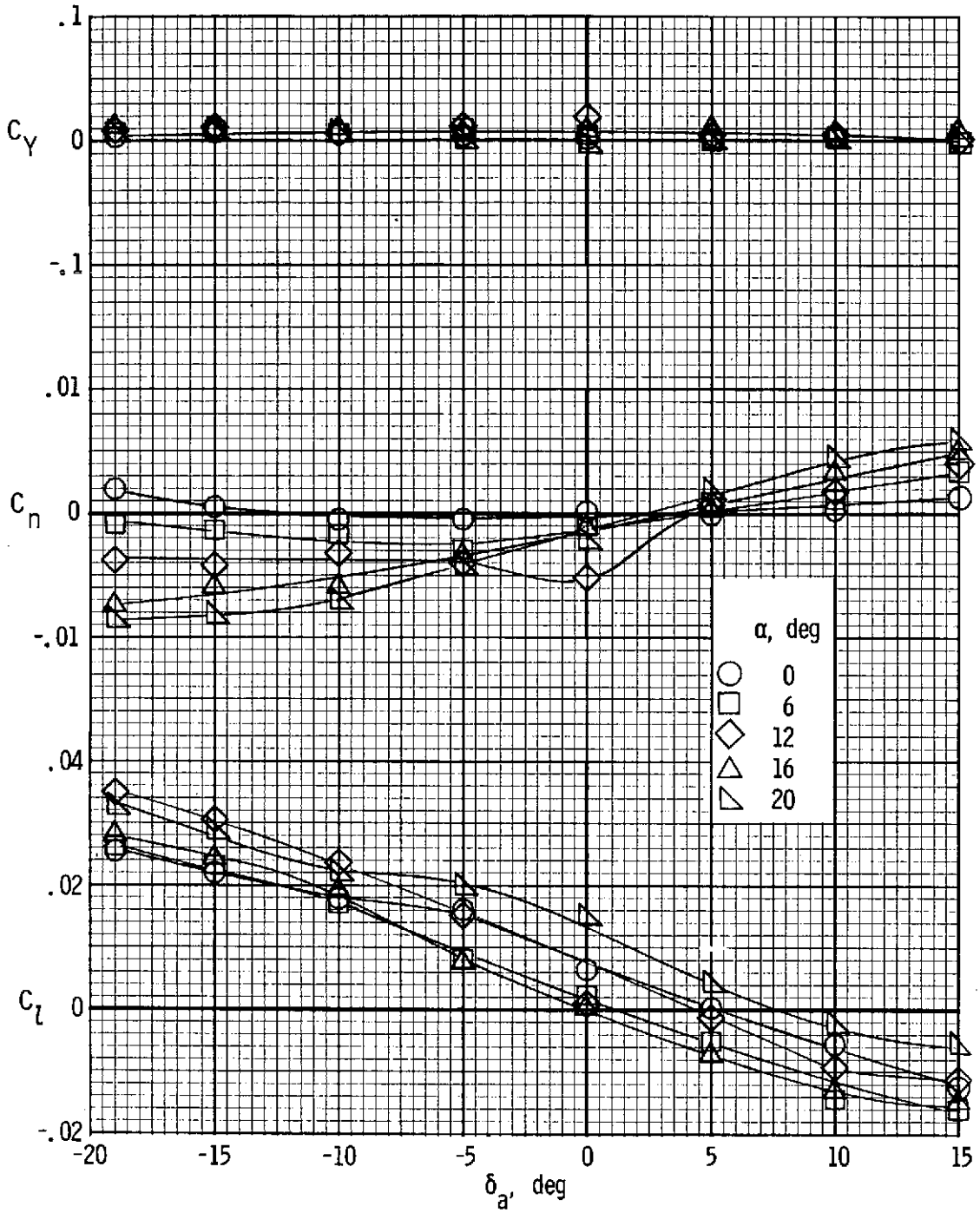

(a) $\delta_f = 0^o$.

Figure 31.- Variation of the lateral characteristics with aileron deflection of the 0.41b/2 leading-edge slot configuration with propellers removed.

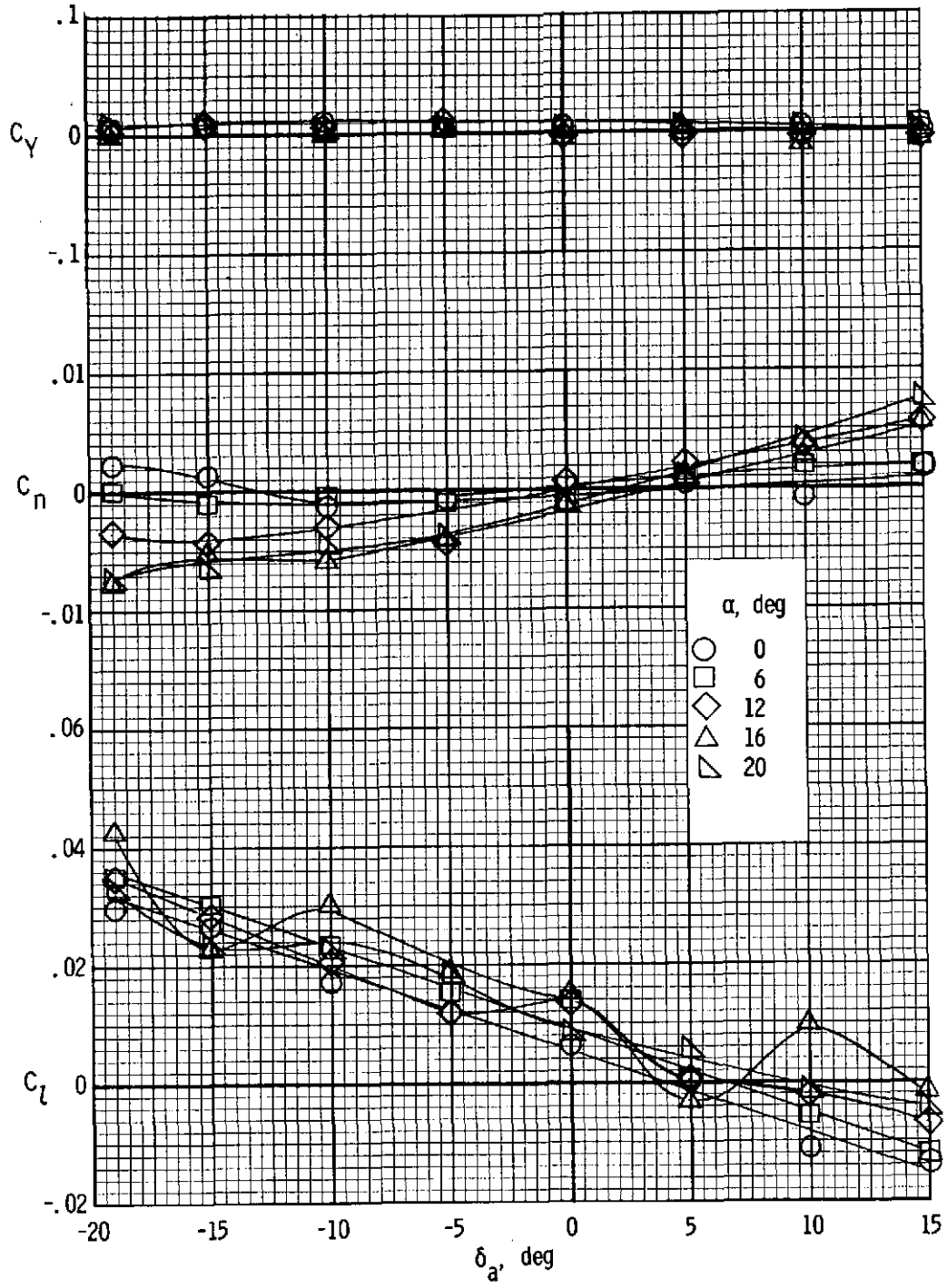

(b) $\delta_f = 27^o$.

Figure 31.- Concluded.

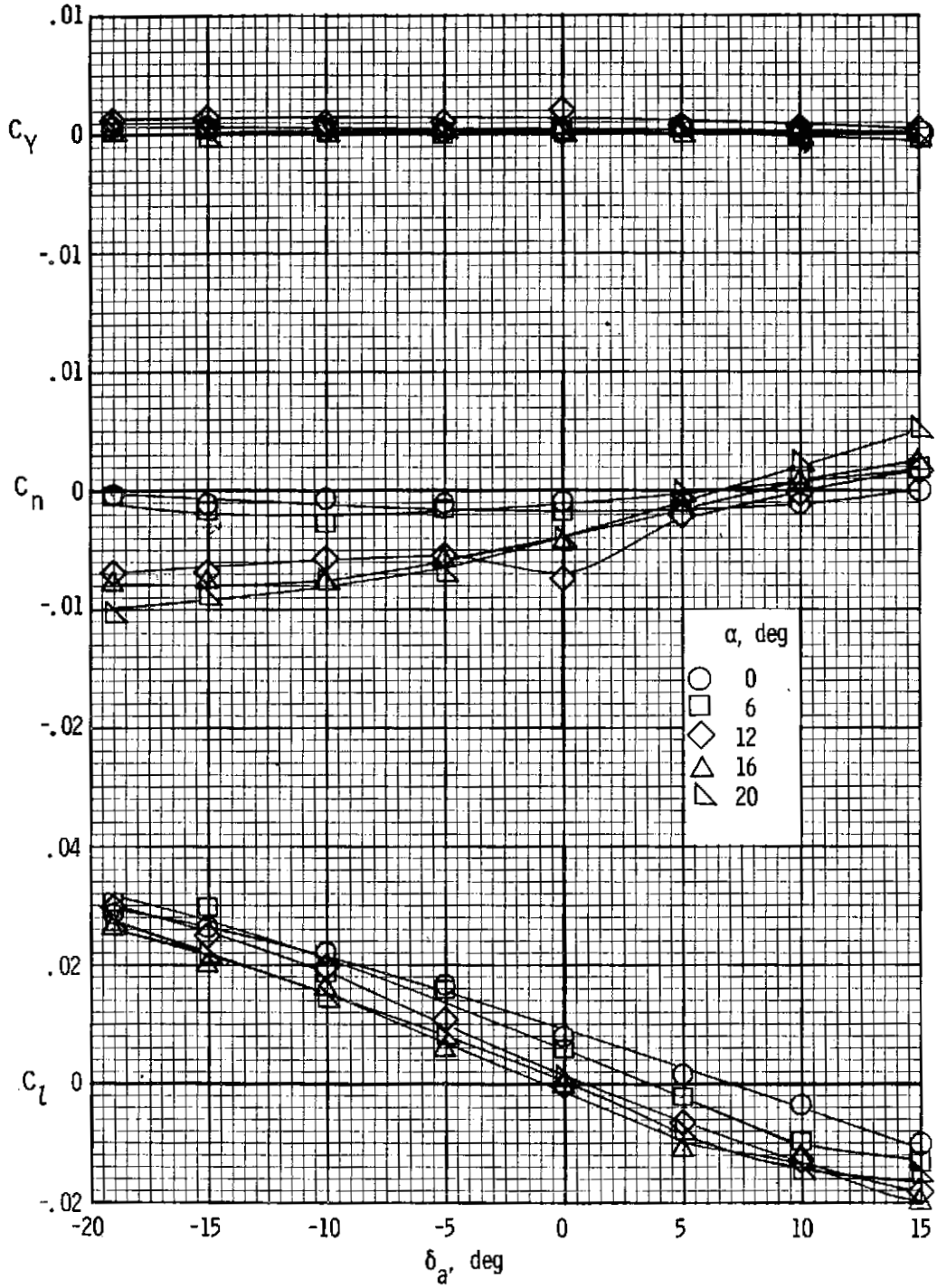

(a) $T_c' = 0$.

Figure 32.- Variation of the lateral characteristics with aileron deflection of the 0.41b/2 leading-edge slot configuration with power. $\delta_f = 0^o$.

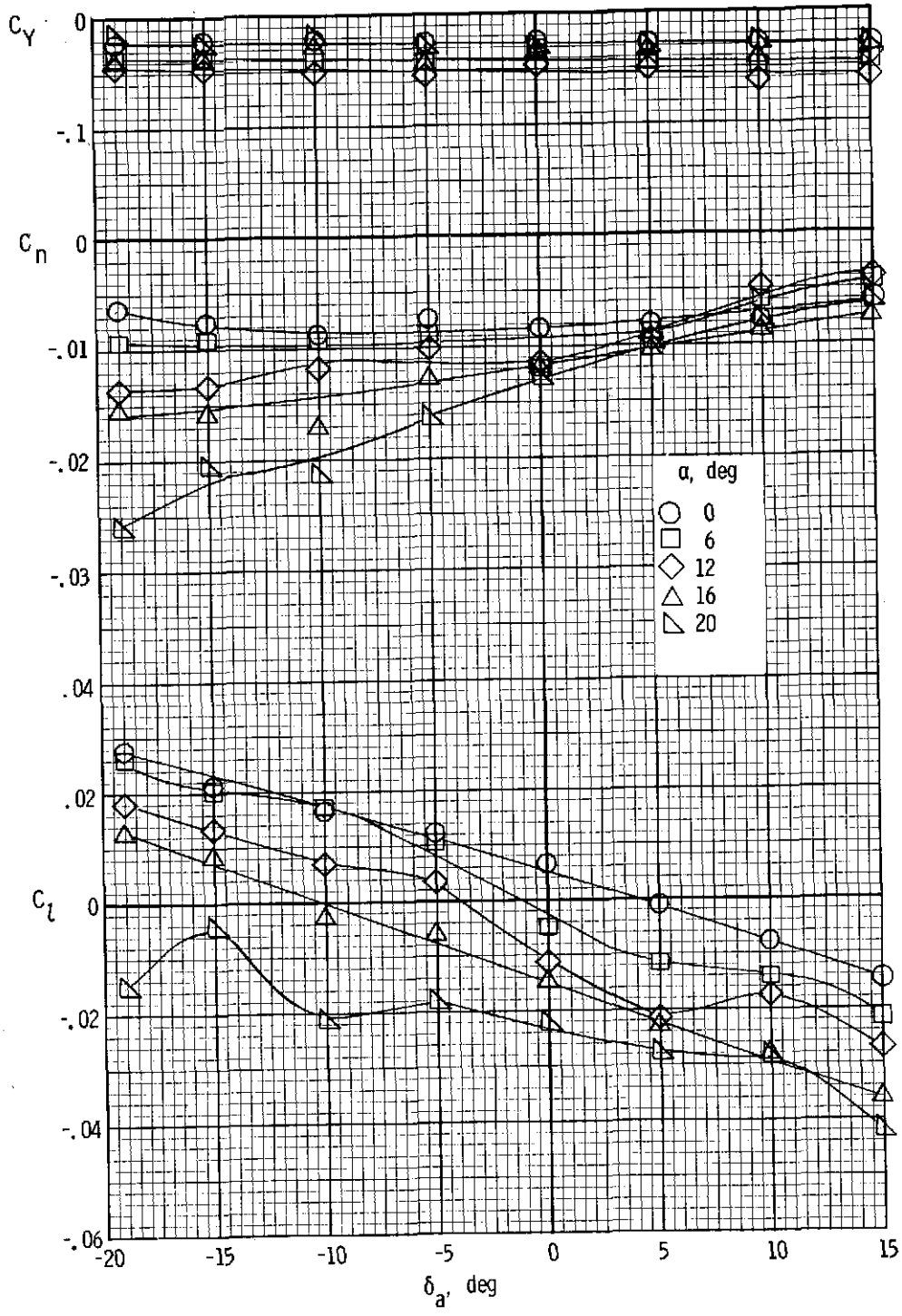

(b) $T_c' = 0.20$.

Figure 32.- Continued.

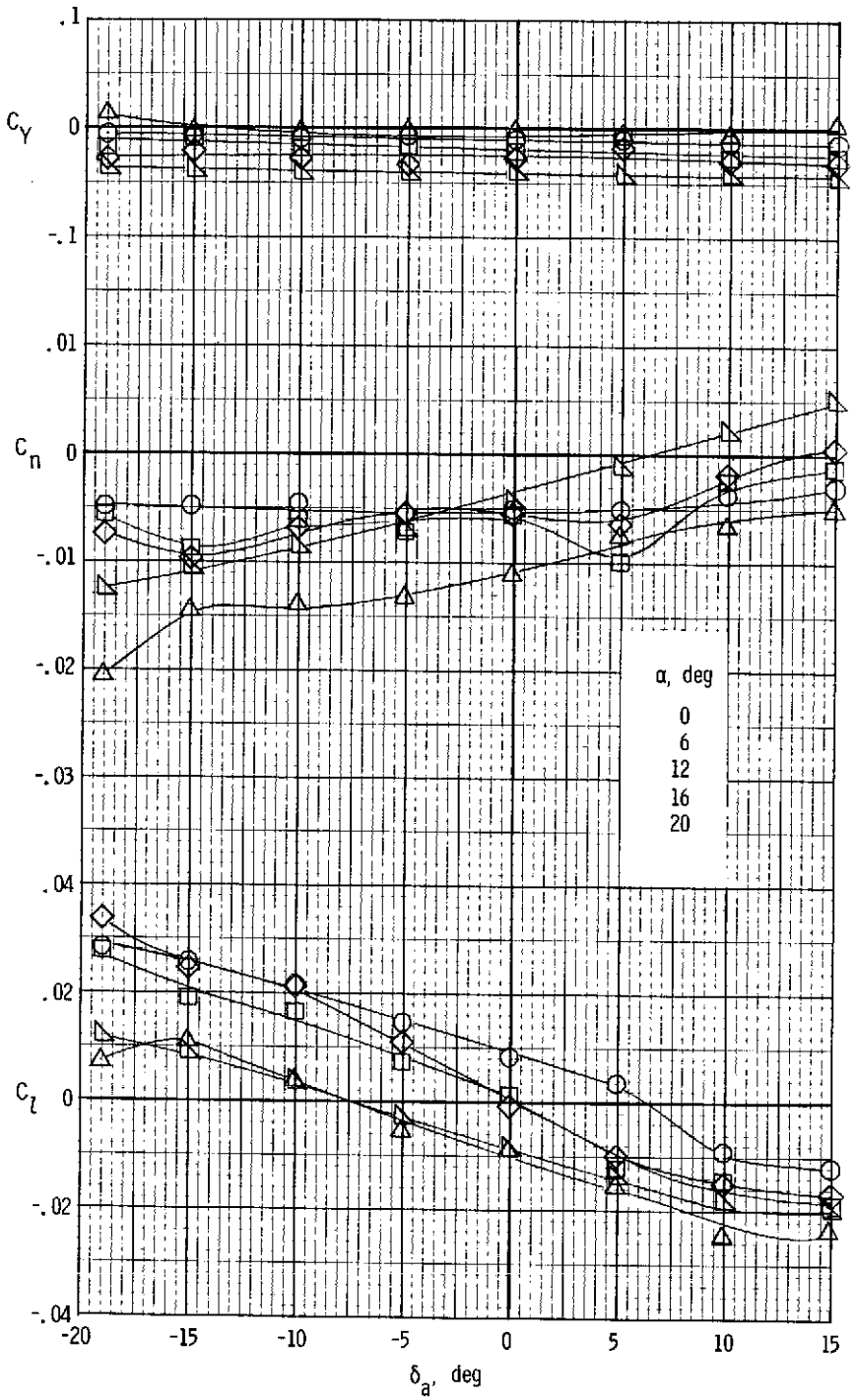

(c) $T_c' = 0.44$.

Figure 32.- Concluded.

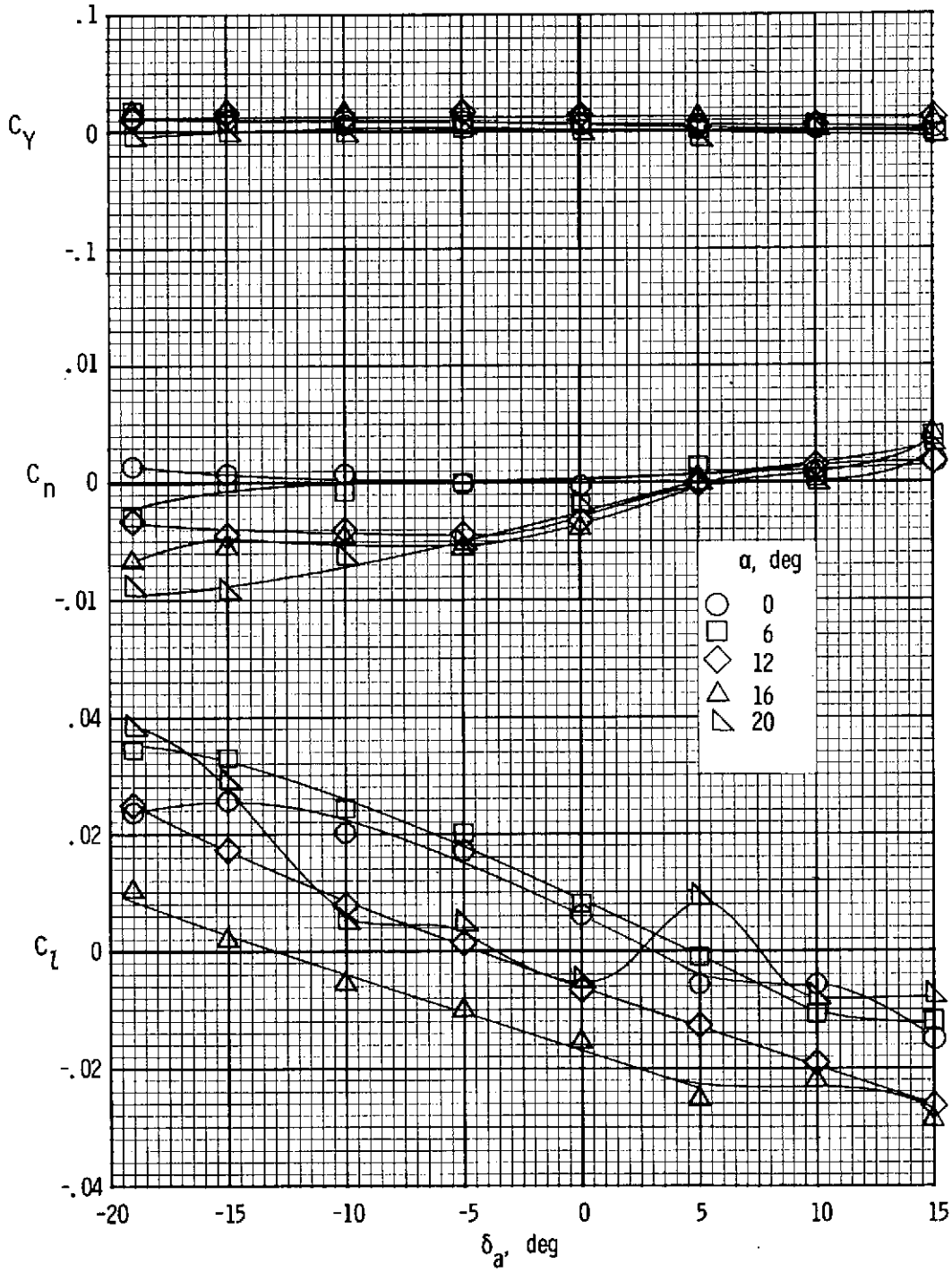

(a) $T_C' = 0$.

Figure 33.- Variation of the lateral characteristics with aileron deflection of the 0.41b/2 leading-edge slot configuration with power. $\delta_f = 27^o$.

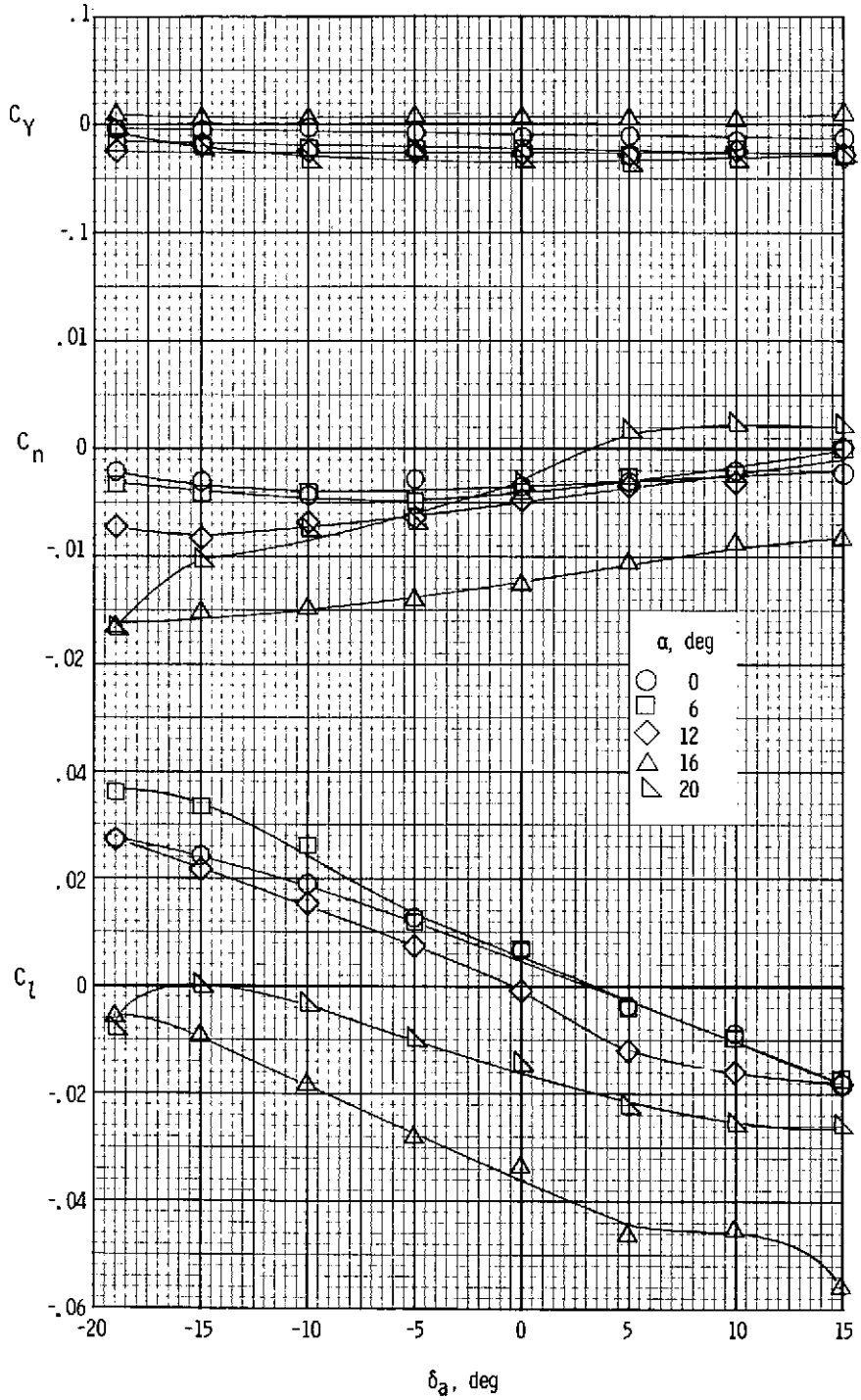

(b) $T_c' = 0.20$.

Figure 33.- Continued.

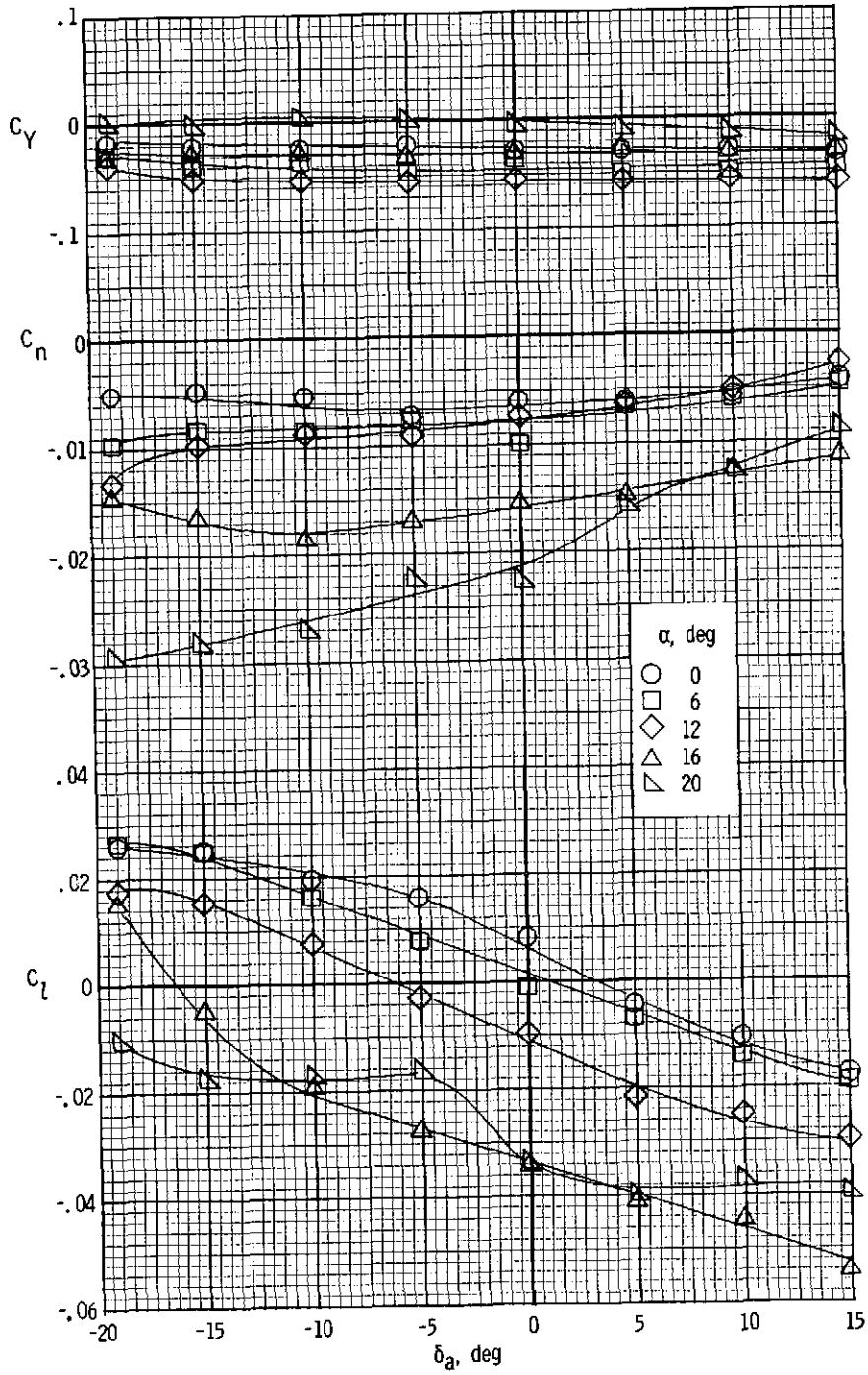

(c) $T_c' = 0.44$.

Figure 33.- Concluded.

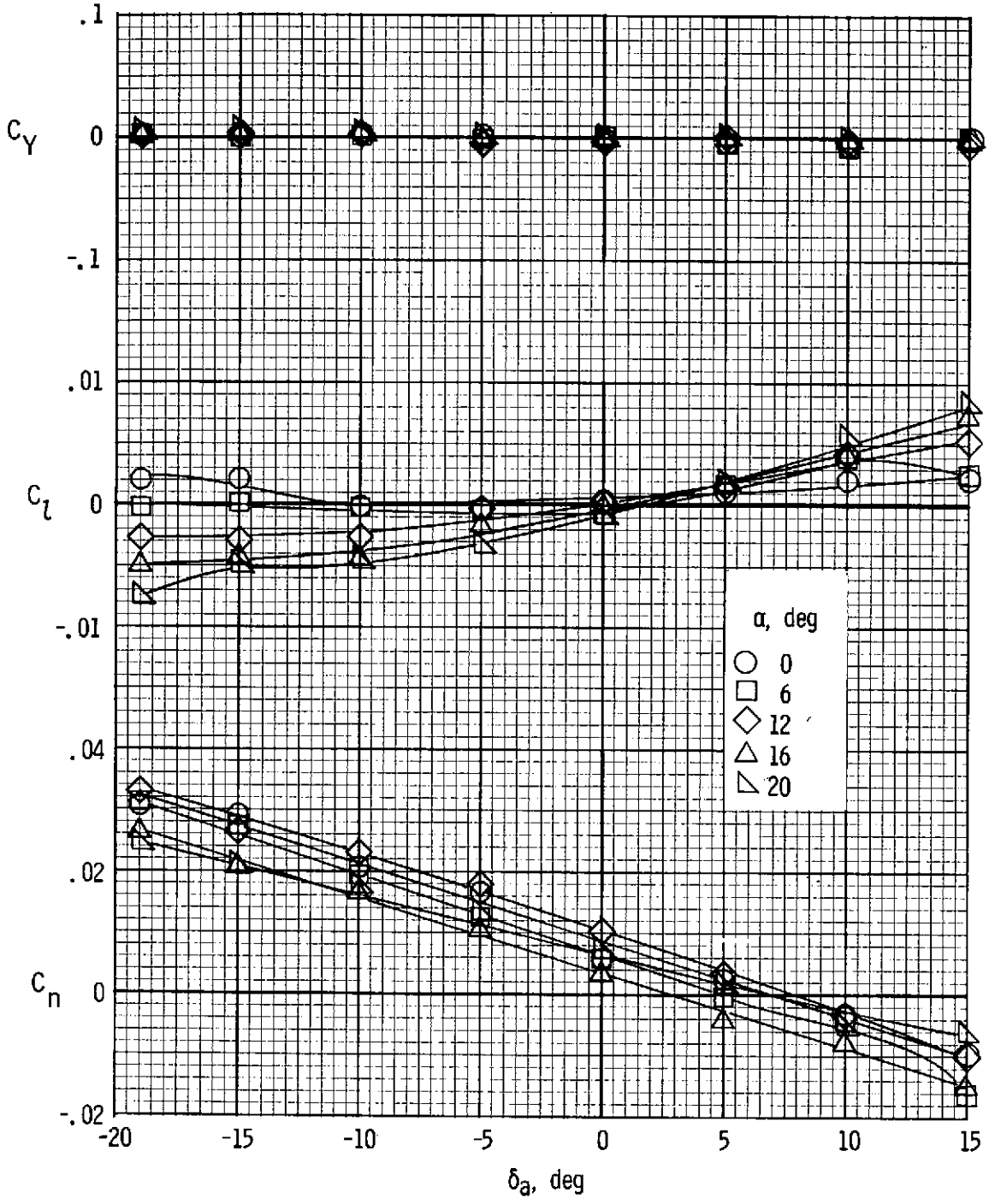

(a) 0.21b/2.

Figure 34.- Variation of the lateral characteristics with aileron deflection of the auxiliary airfoil configuration with propellers removed. $\delta_f = 0^o$.

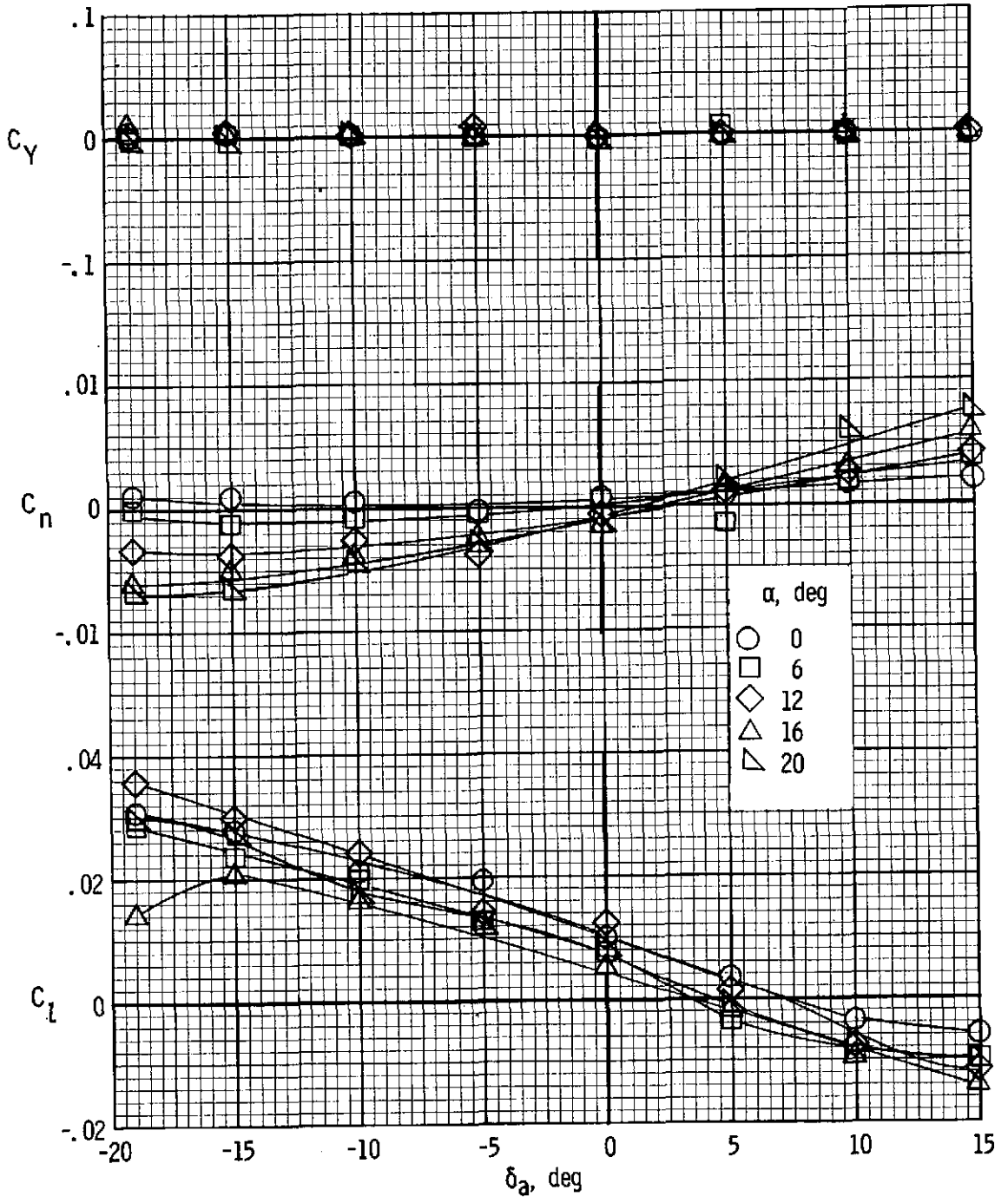

(b) 0.41b/2.

Figure 34.- Continued.

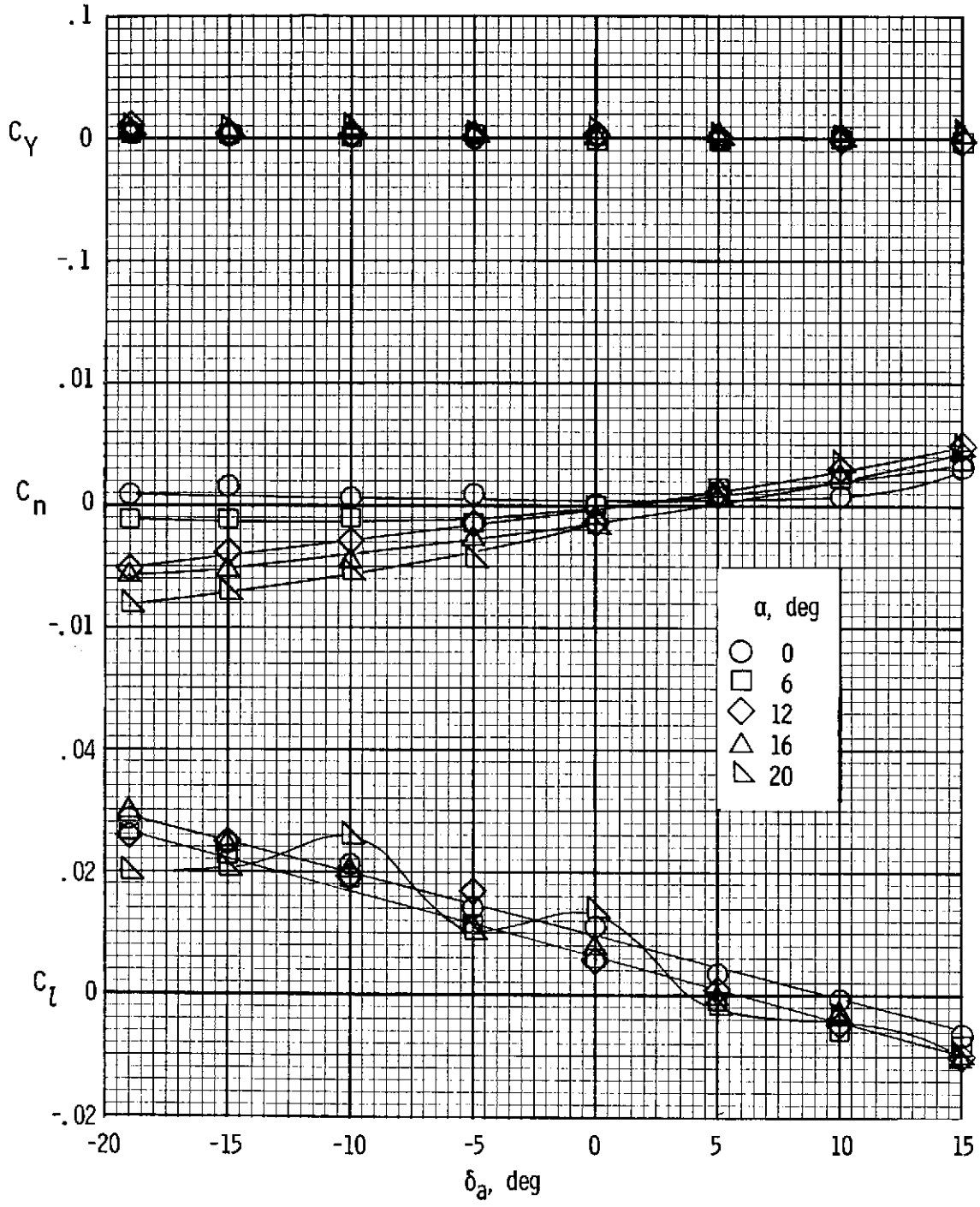

(c) 0.58b/2.

Figure 34.- Concluded.

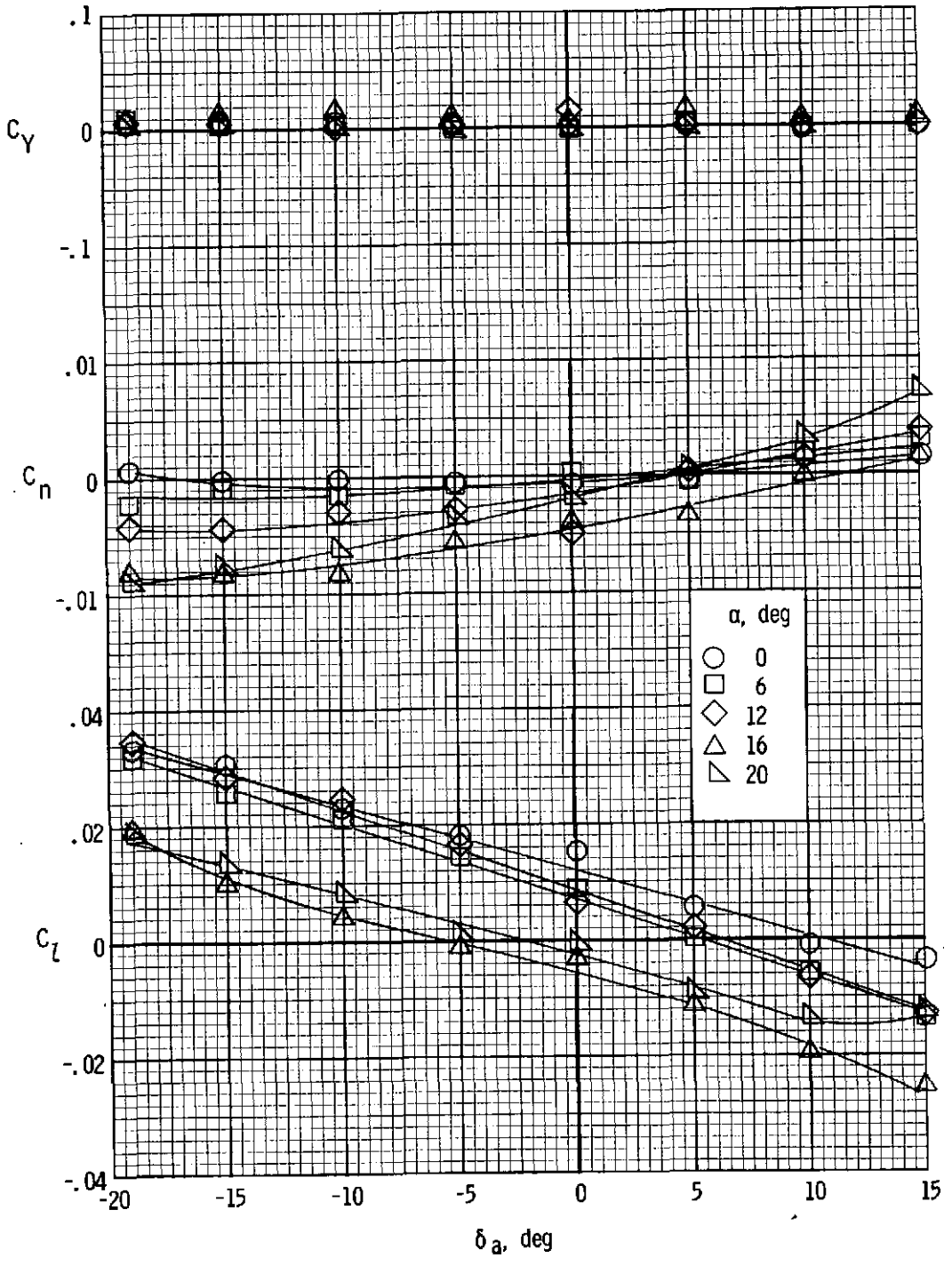

(a) $T_C' = 0$.

Figure 35.- Variation of the lateral characteristics with aileron deflection of the 0.21b/2 auxiliary airfoil configuration with power. $\delta_f = 0^o$.

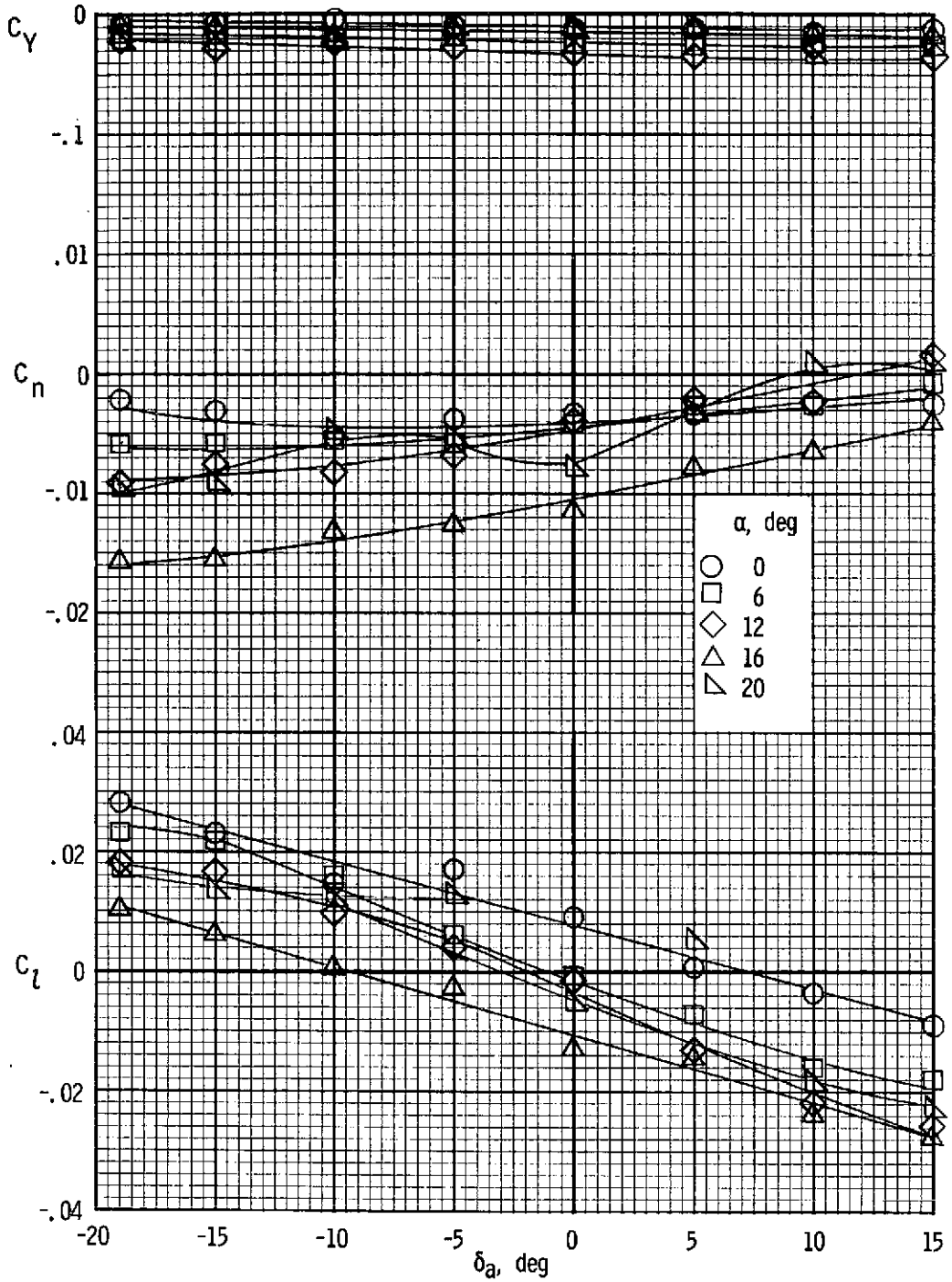

(b) $T_c' = 0.20$.

Figure 35.- Continued.

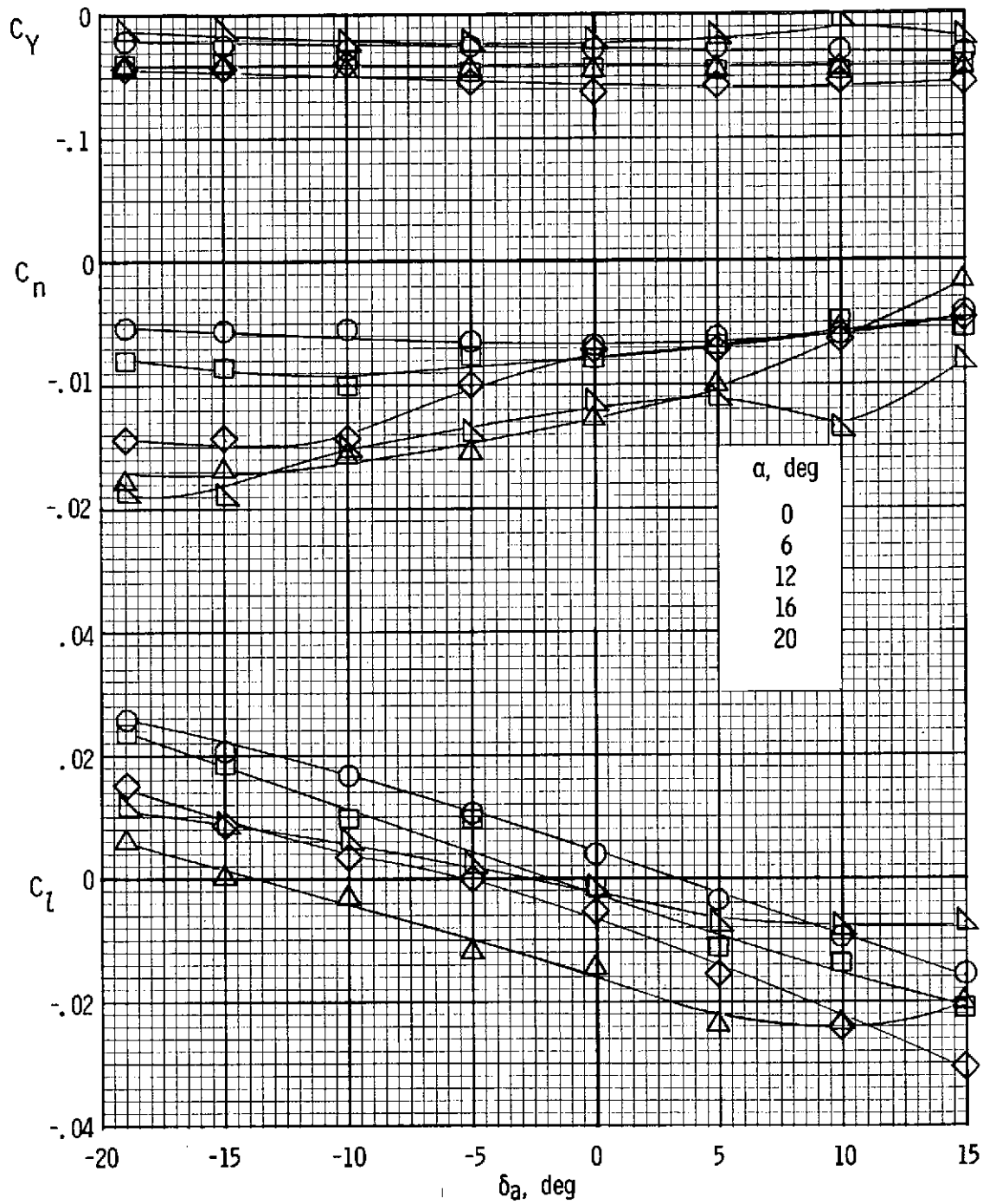

(c) $T_c' = 0.44$.

Figure 35.- Concluded.

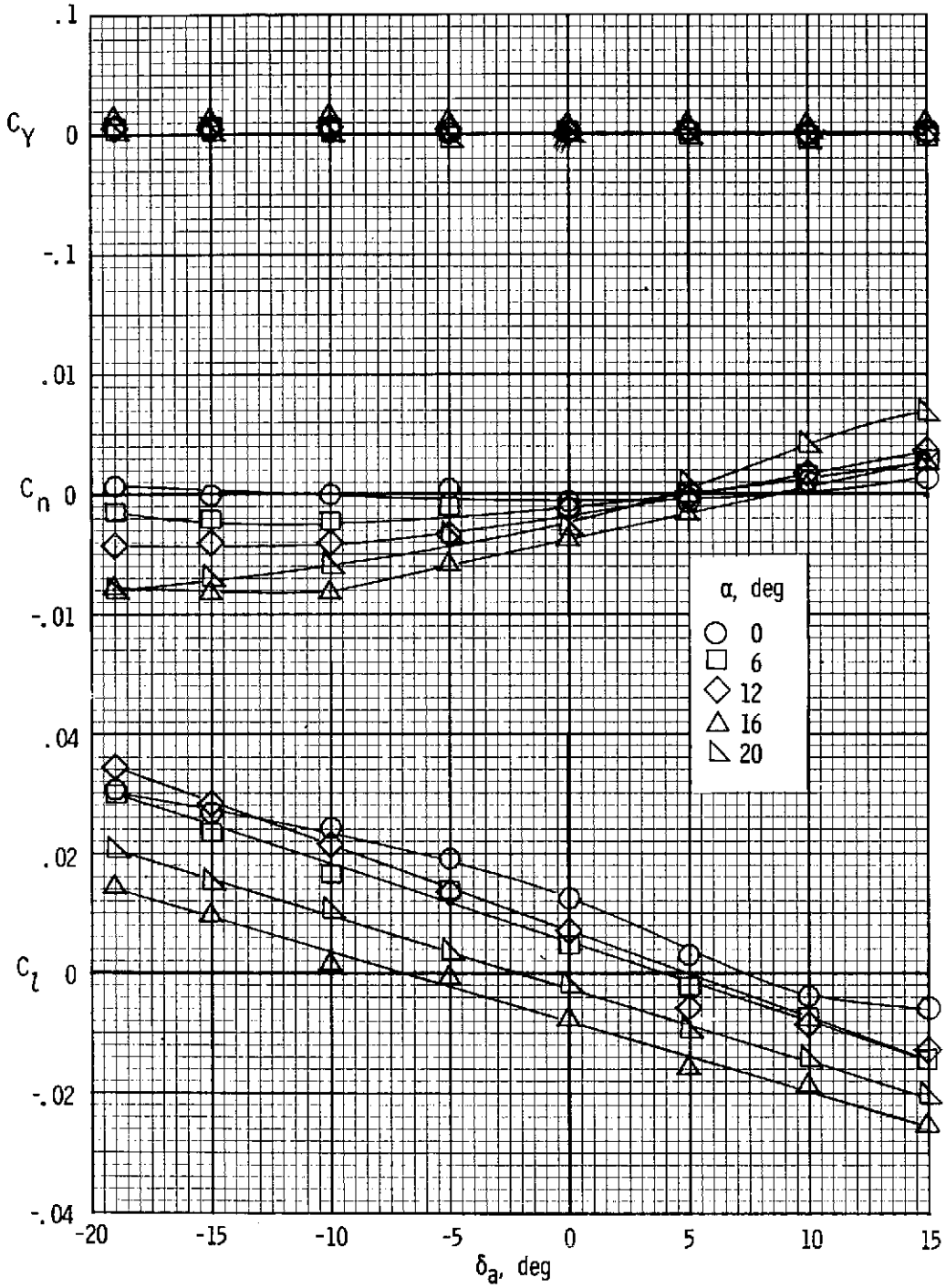

(a) $T_C' = 0$.

Figure 36.- Variation of the lateral characteristics with aileron deflection of the 0.41b/2 auxiliary airfoil configuration with power. $\delta_f = 0^o$.

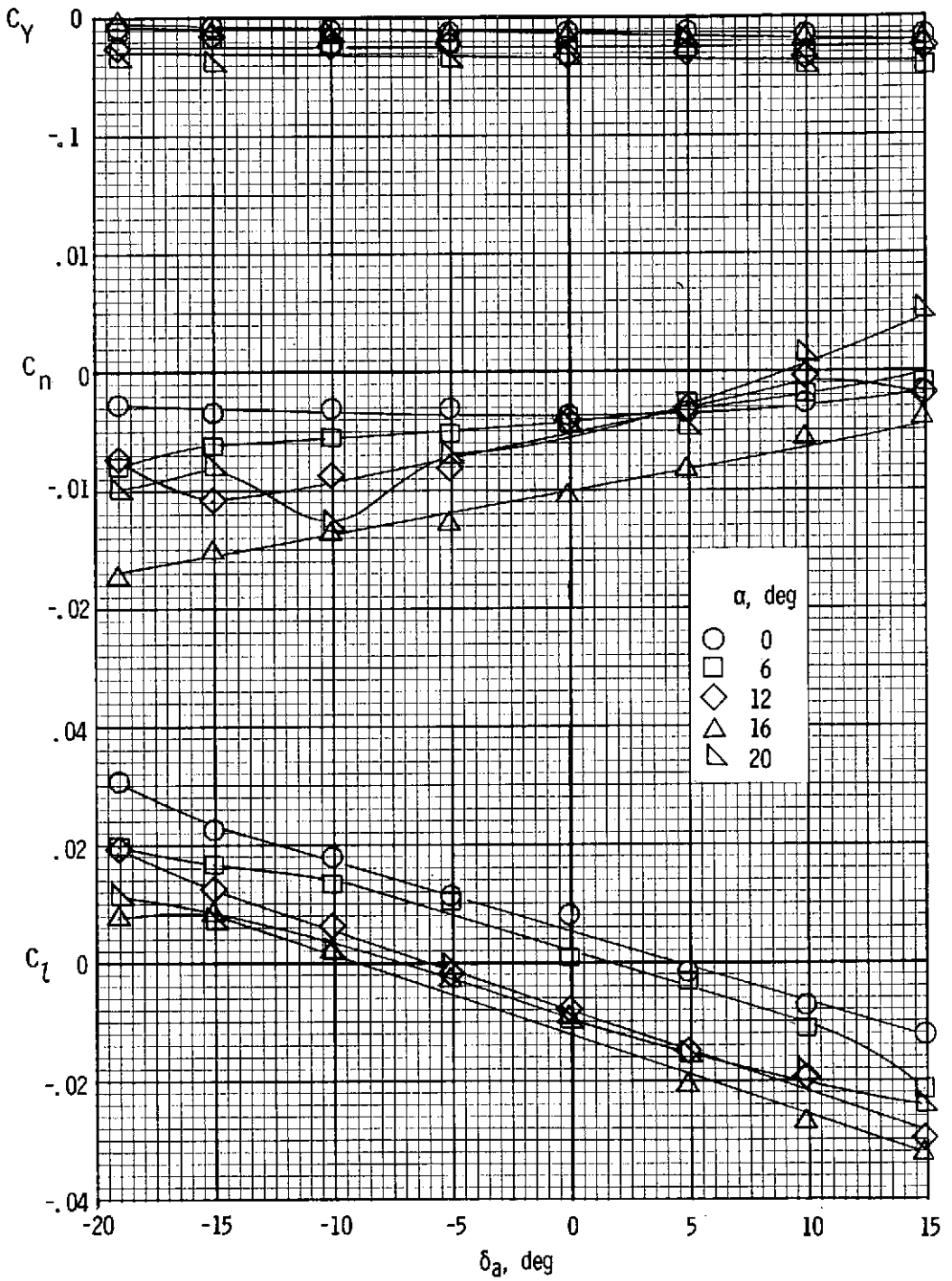

(b) $T_c' = 0.20$.

Figure 36.- Continued.

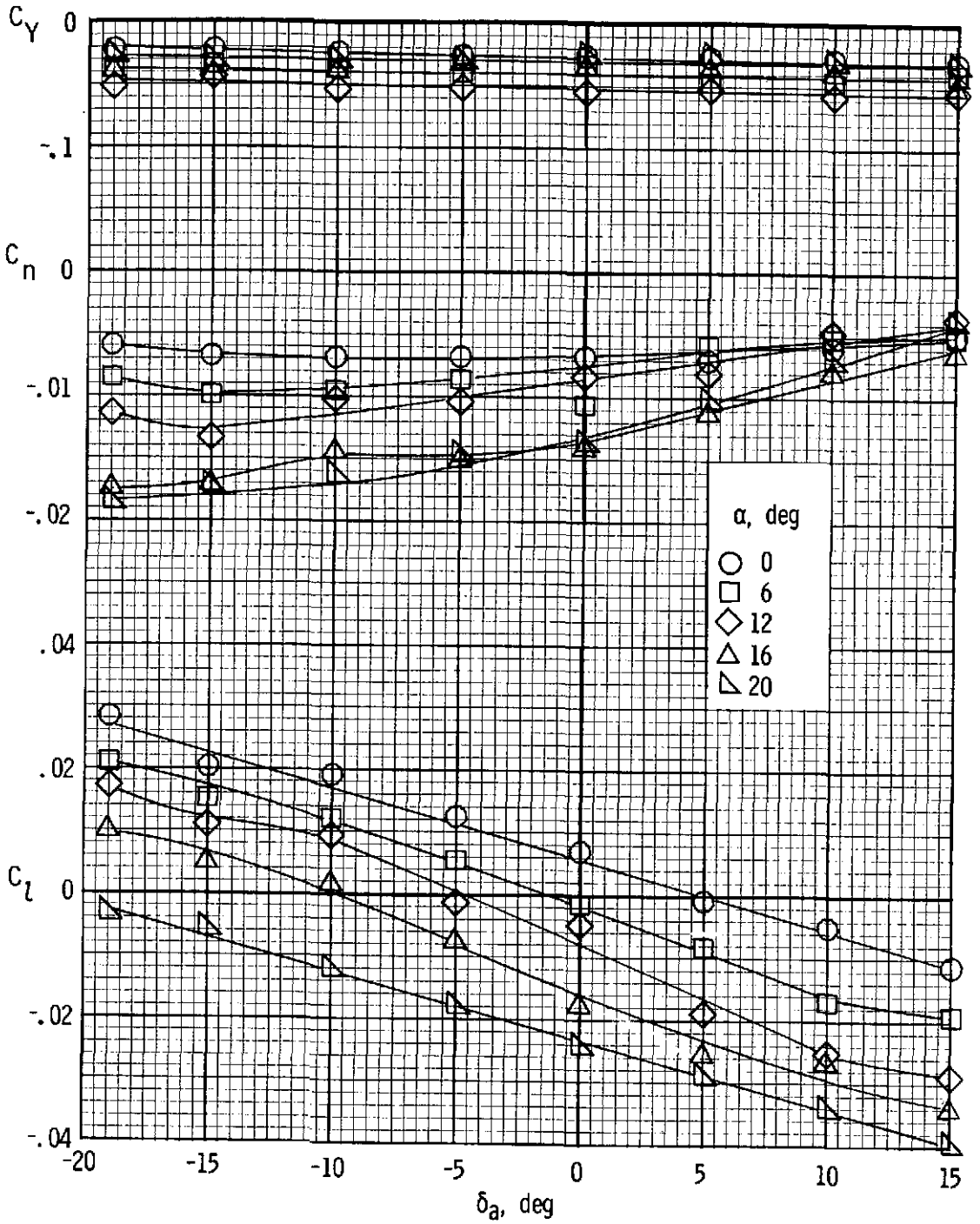

(c) $T_c' = 0.44$.

Figure 36.- Concluded.

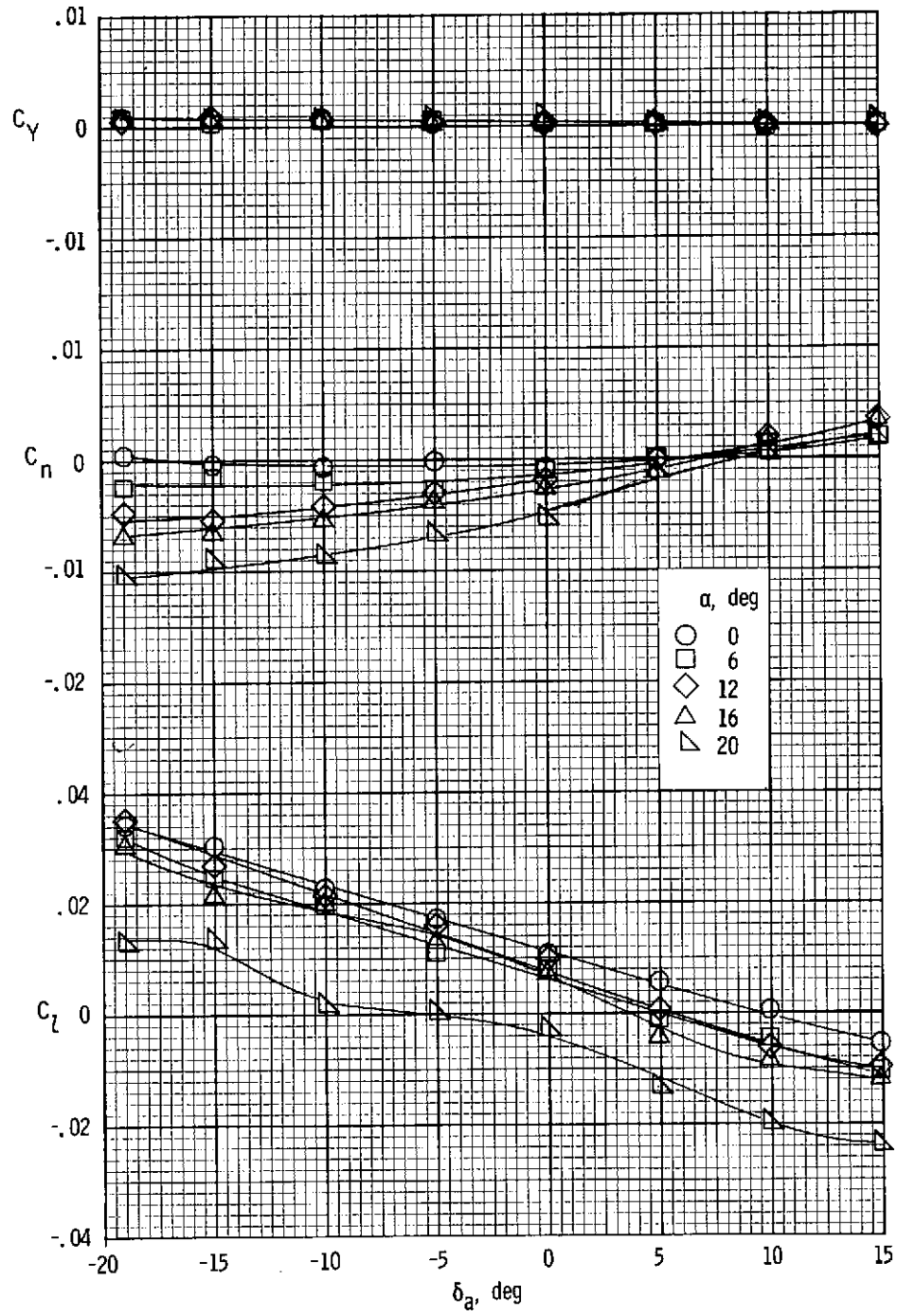

(a) $T_c' = 0$.

Figure 37.- Variation of the lateral characteristics with aileron deflection of the 0.58b/2 auxiliary airfoil configuration with power. $\delta_f = 0^o$.

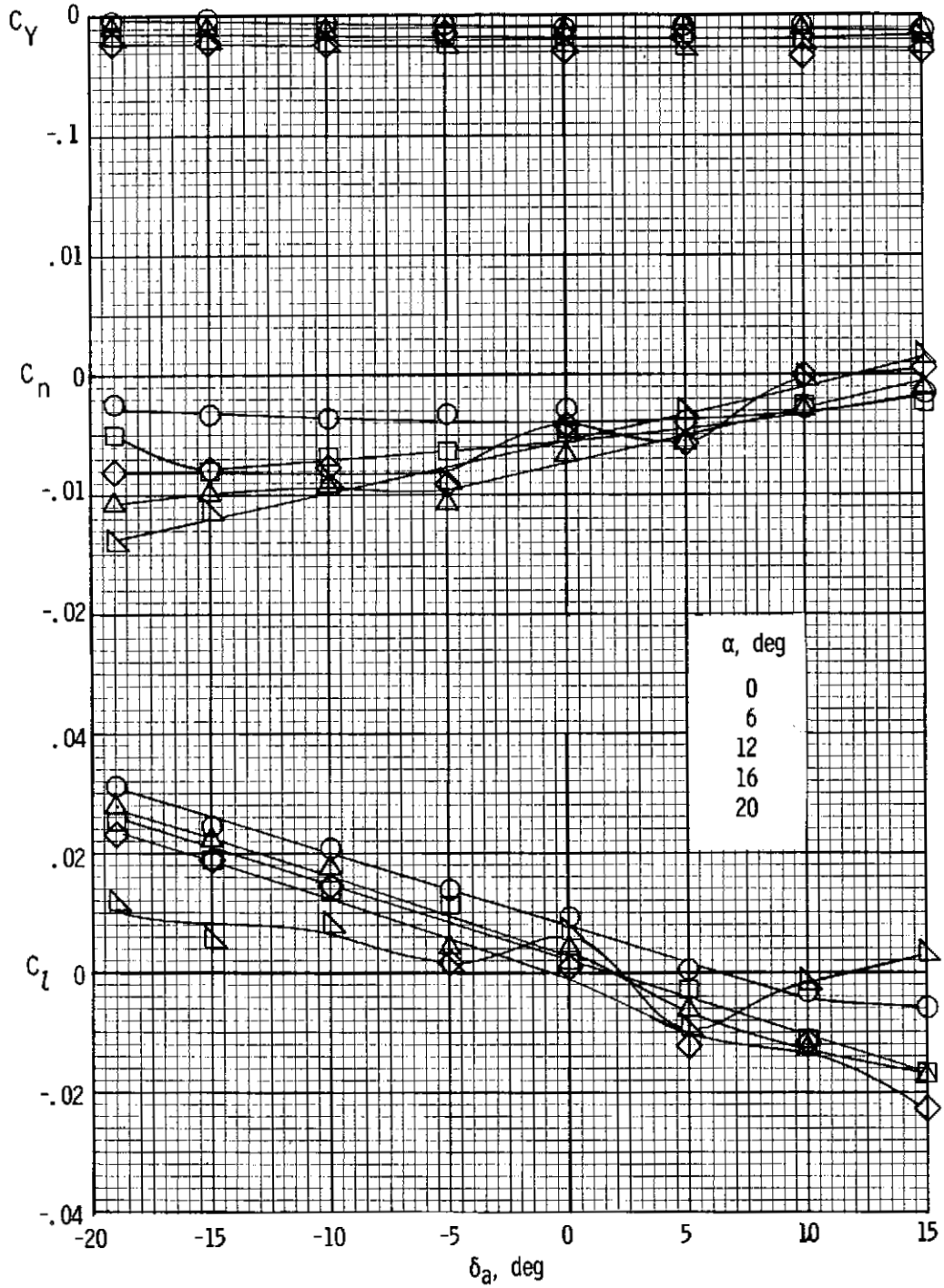

(b) $T_c' = 0.20$.

Figure 37.- Continued.

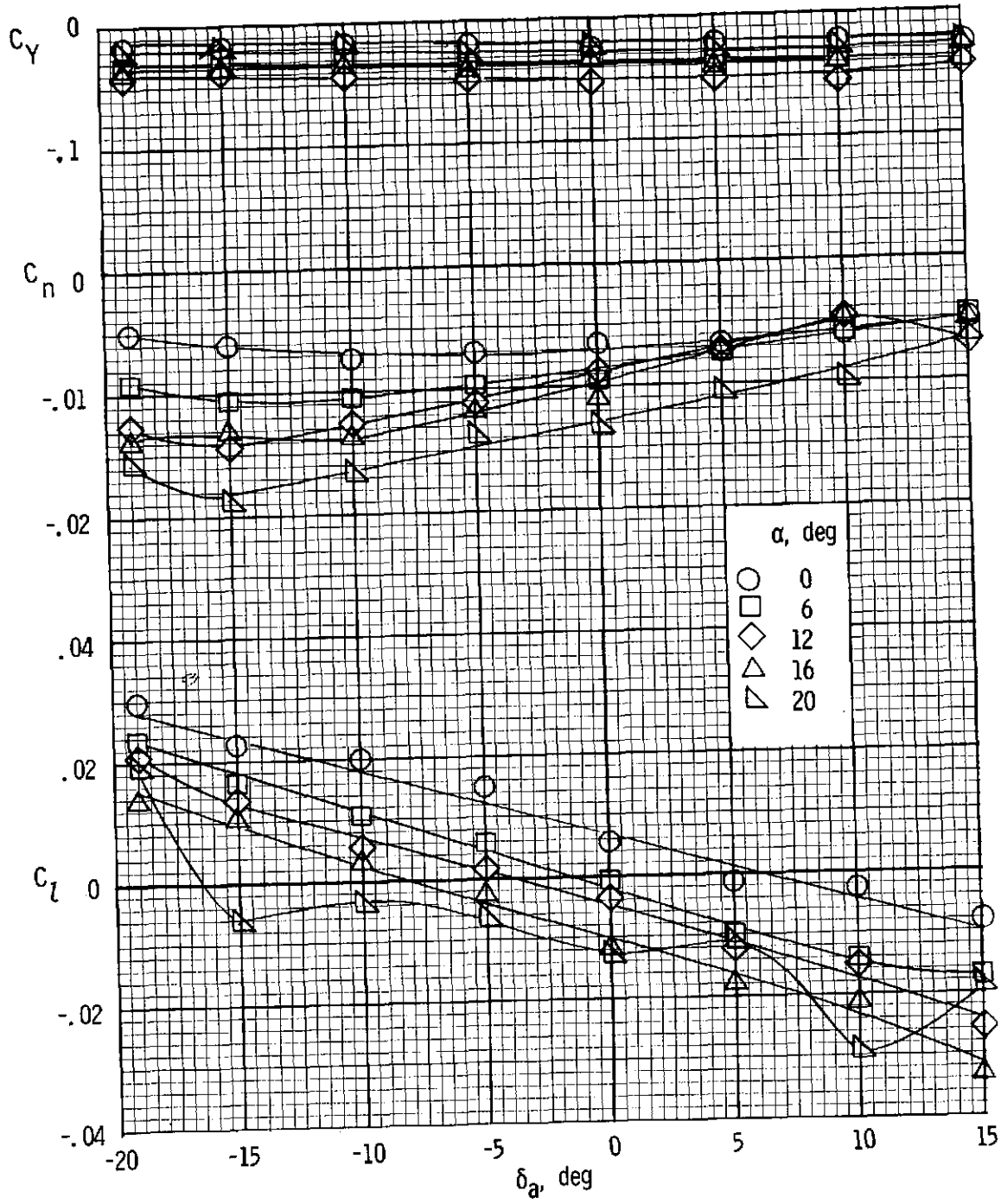

(c) $T_c' = 0.44$.

Figure 37.- Concluded.

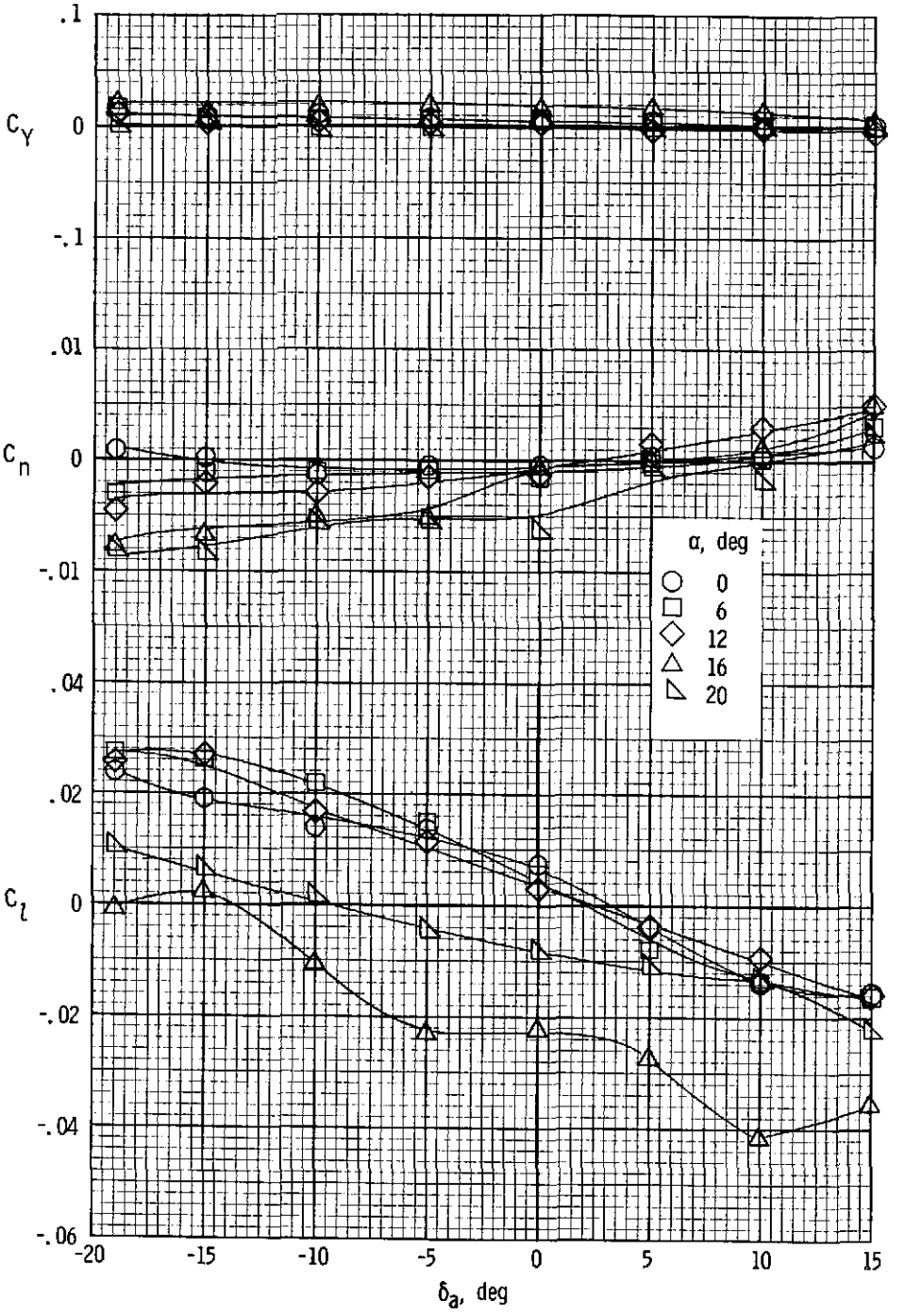

(a) $T_c' = 0$.

Figure 38.- Variation of the lateral characteristics with aileron deflection of the 0.21b/2 auxiliary airfoil configuration with power. $\delta_f = 27^o$.

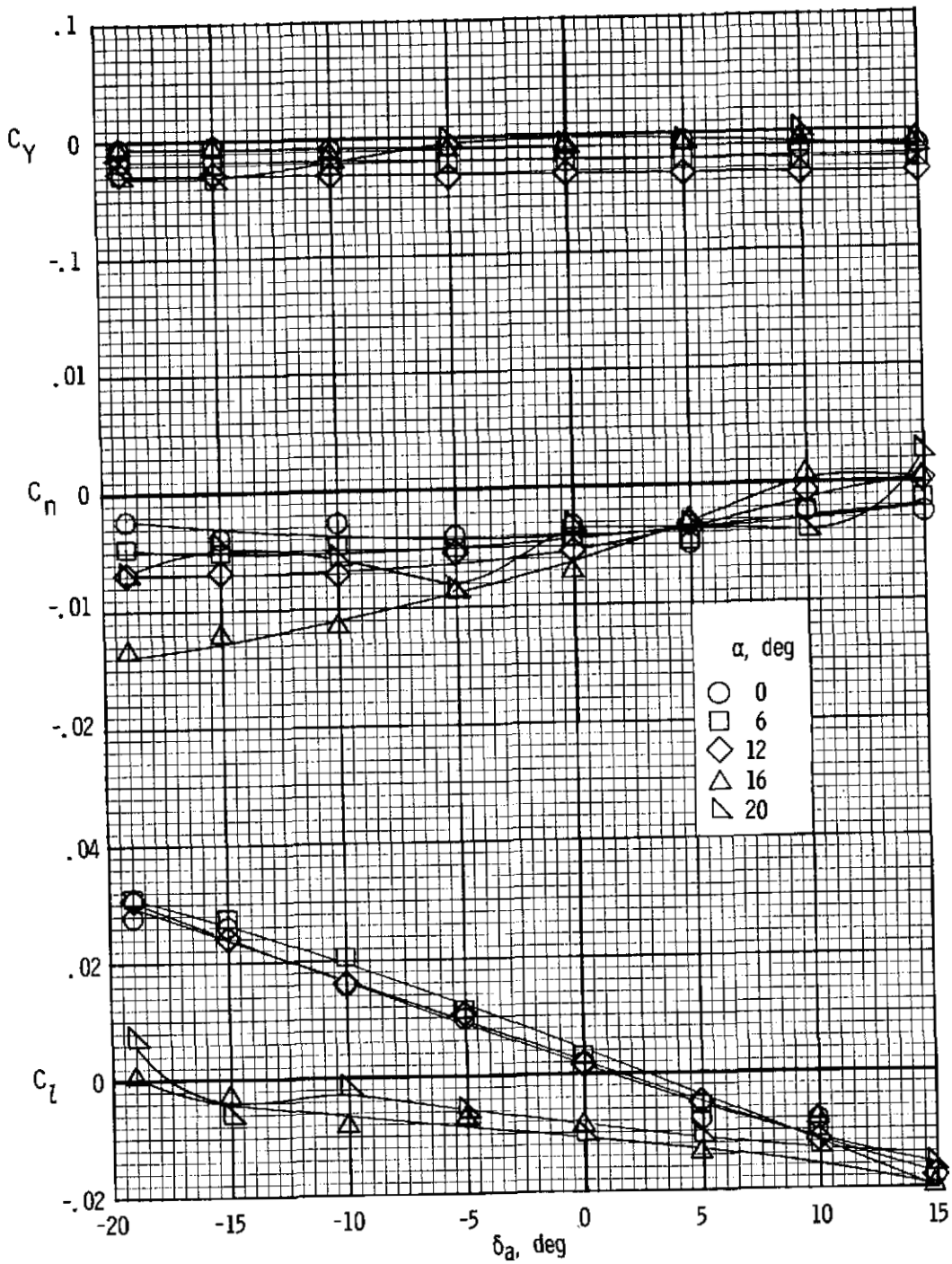

(b) $T_c' = 0.20$.

Figure 38.- Continued.

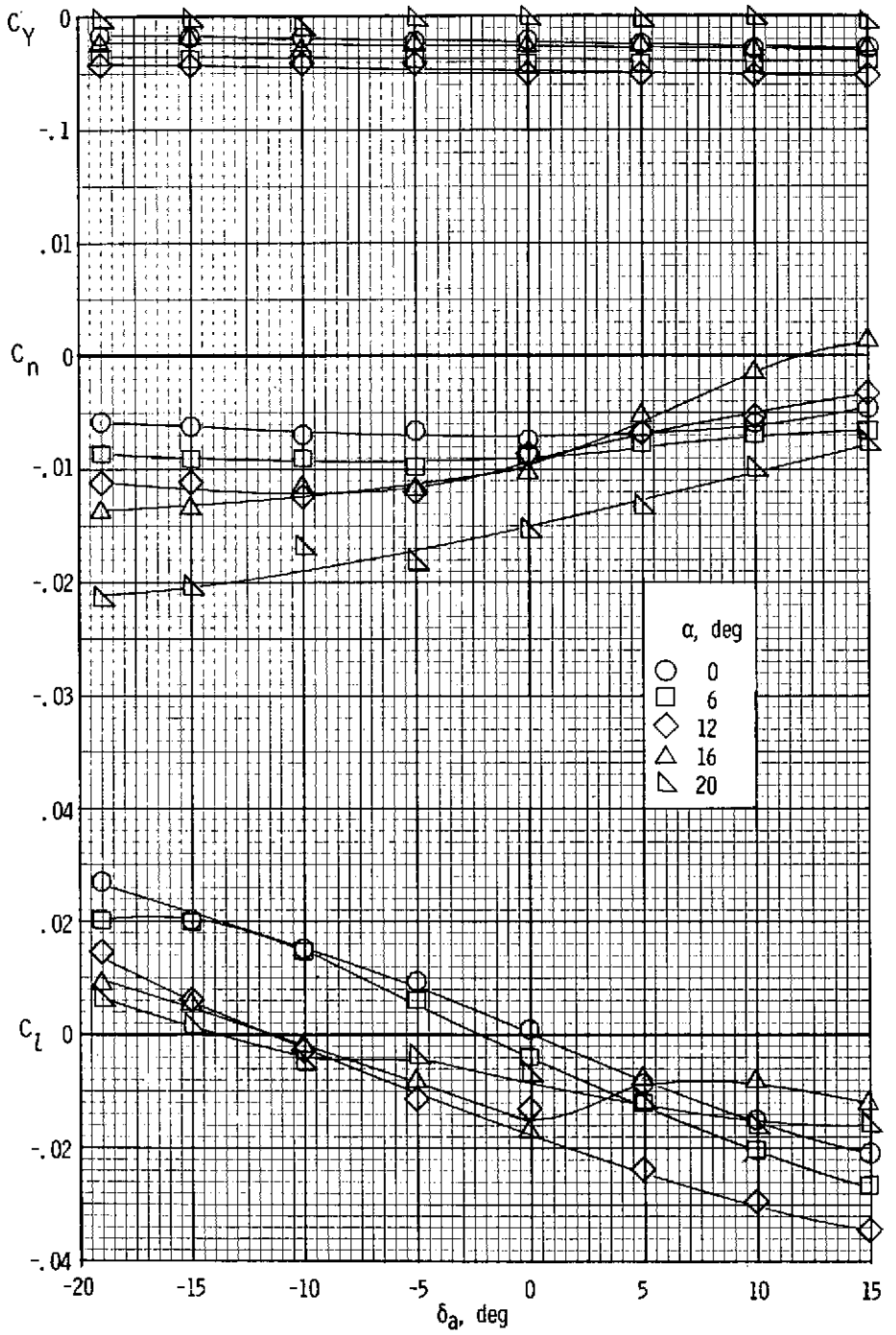

(c) $T_c' = 0.44$.

Figure 38.- Concluded.

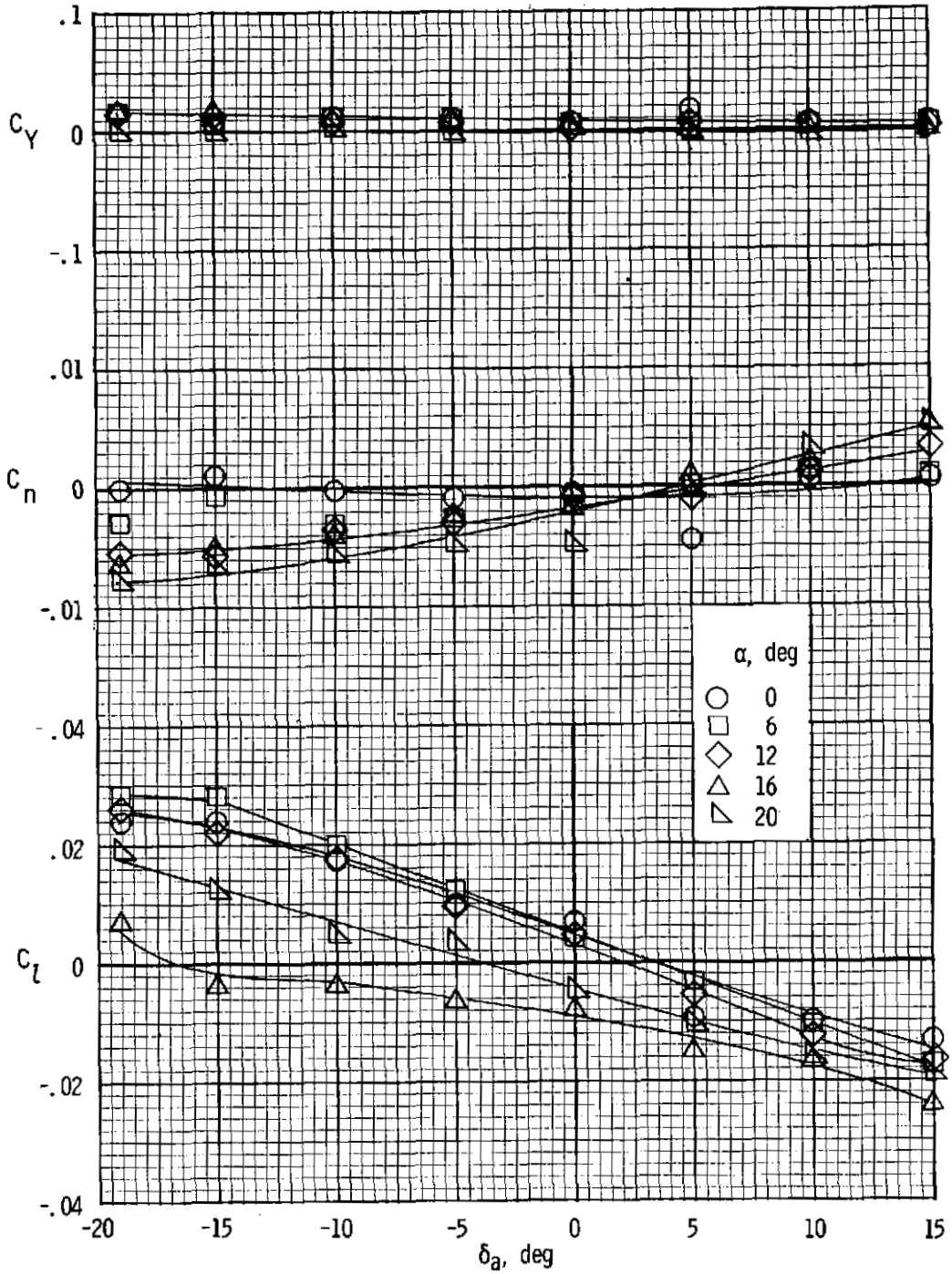

(a) $T_c' = 0$.

Figure 39.- Variation of the lateral characteristics with aileron deflection of the 0.41b/2 auxiliary airfoil configuration with power. $\delta_f = 27^o$.

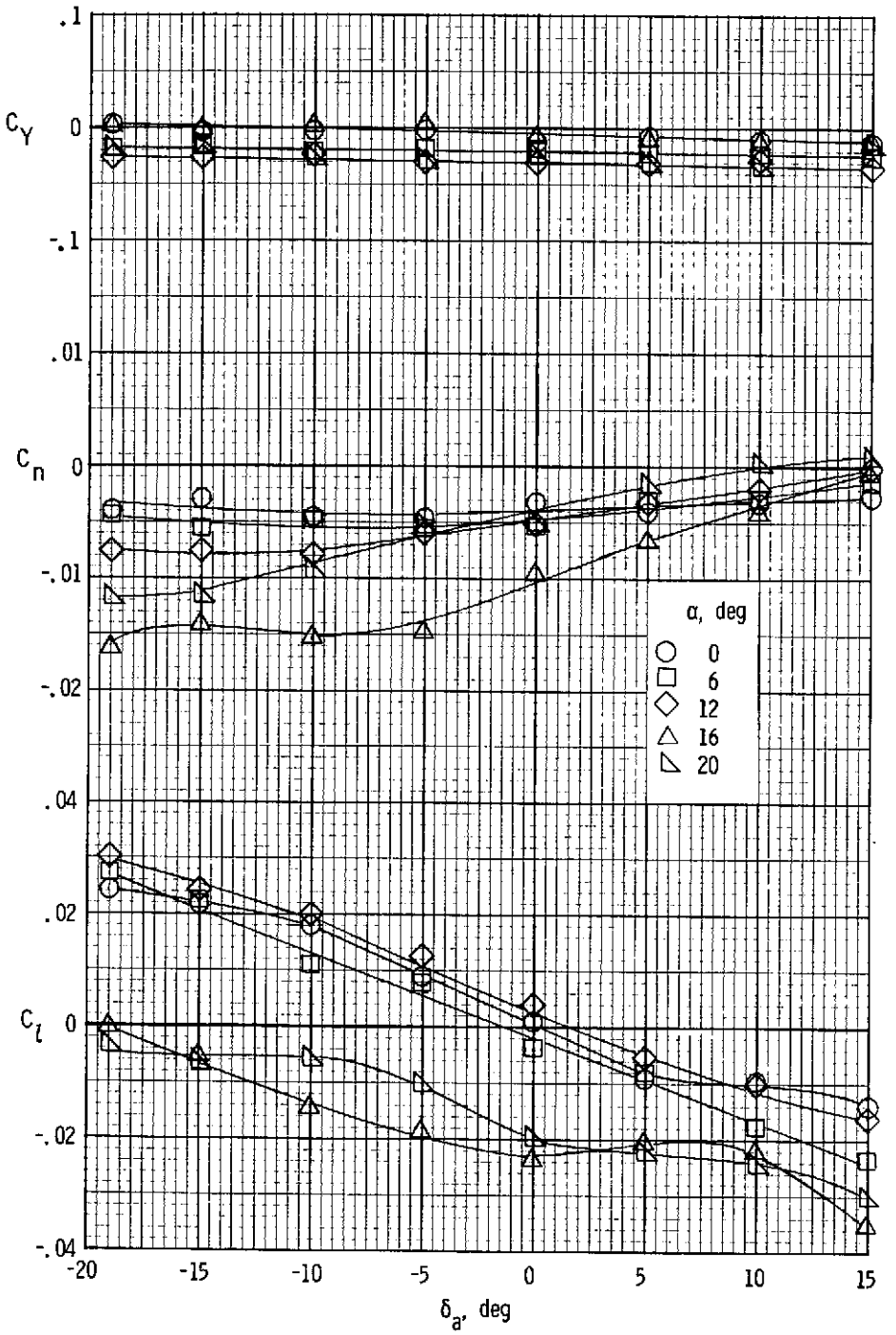

(b) $T_c' = 0.20$.

Figure 39.- Continued.

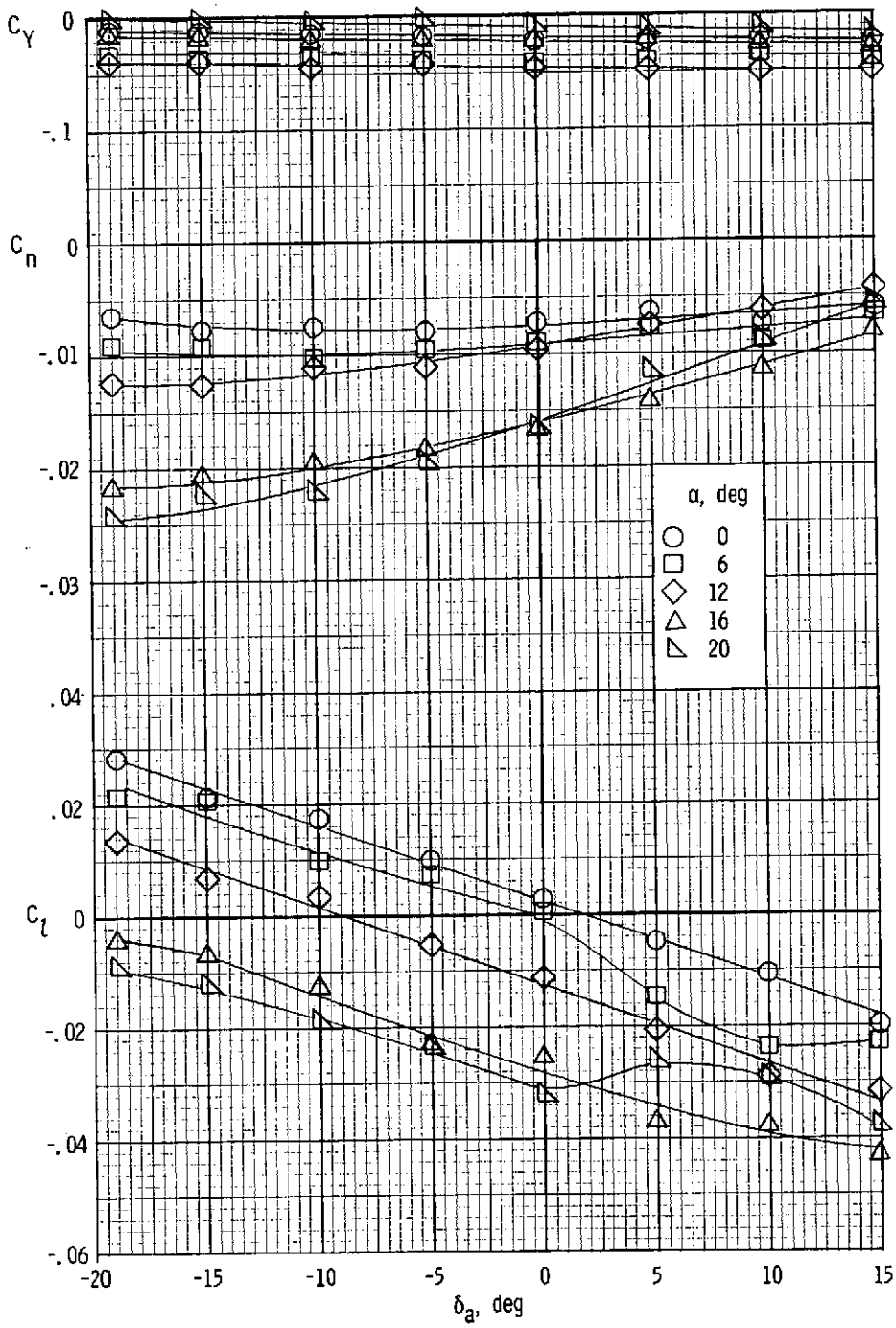

(c) $T_c' = 0.44$.

Figure 39.- Concluded.

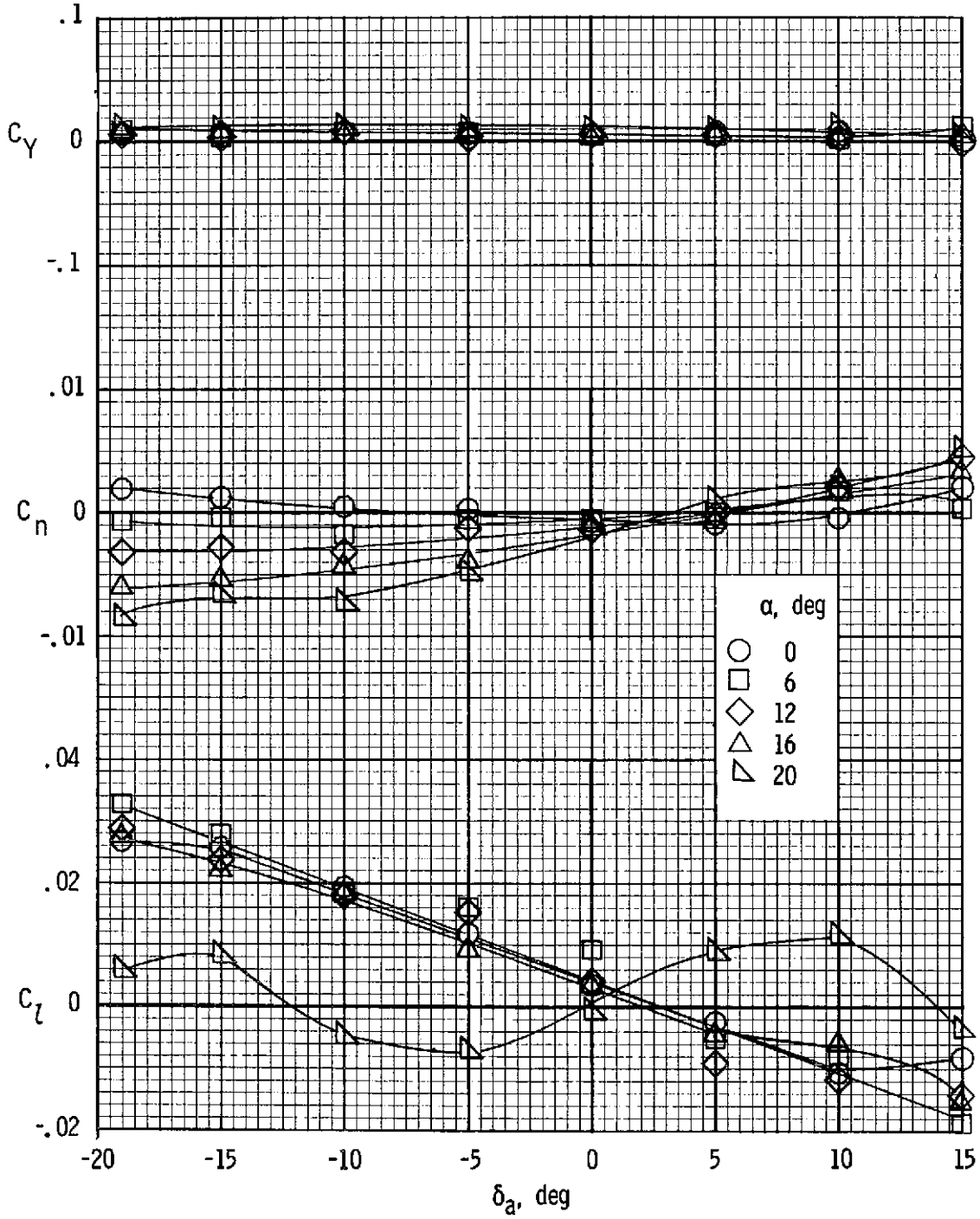

(a) $T_c' = 0$.

Figure 40.- Variation of the lateral characteristics with aileron deflection of the 0.58b/2 auxiliary airfoil configuration with power. $\delta_f = 27^o$.

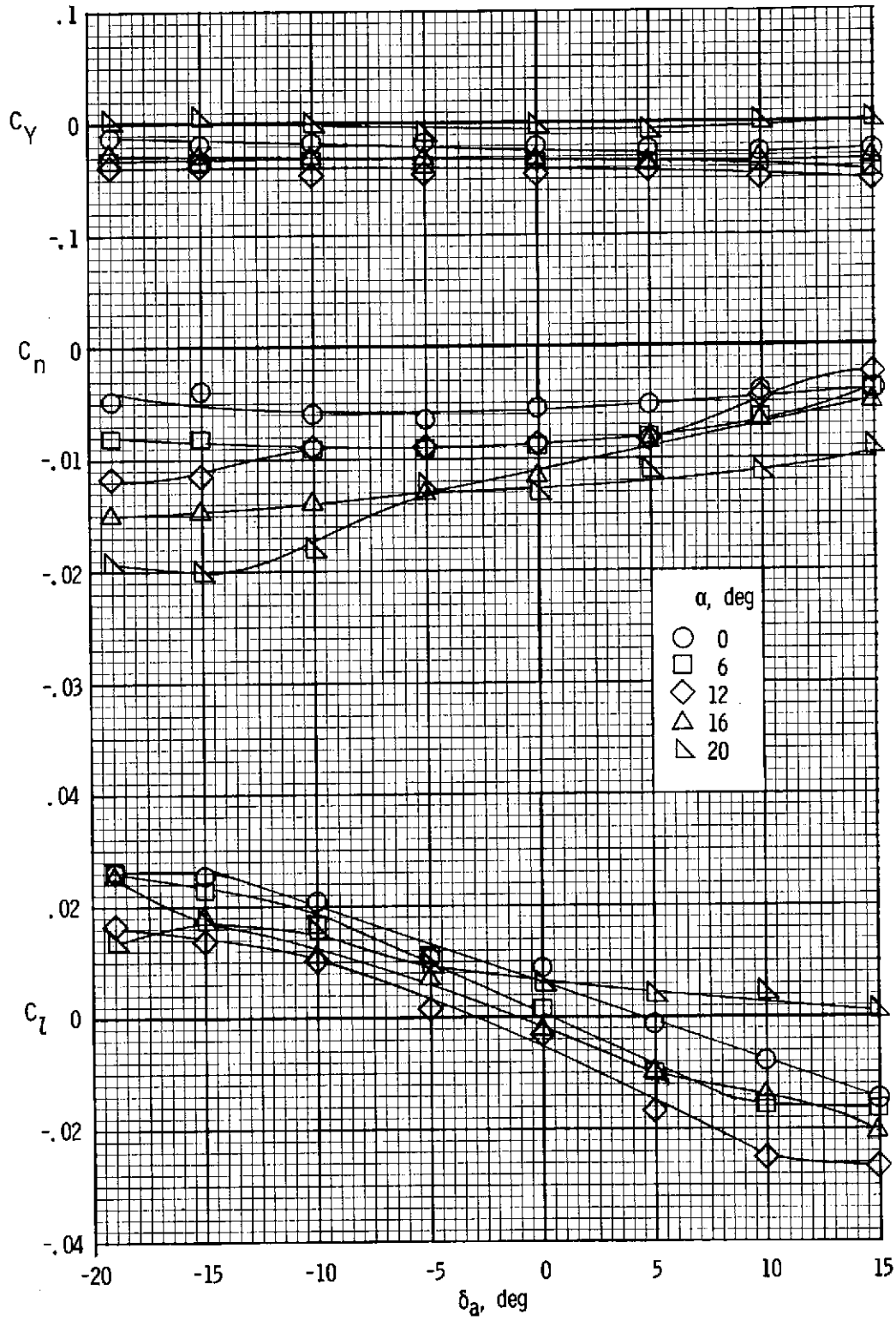

(b) $T_c' = 0.20$.

Figure 40.- Continued.

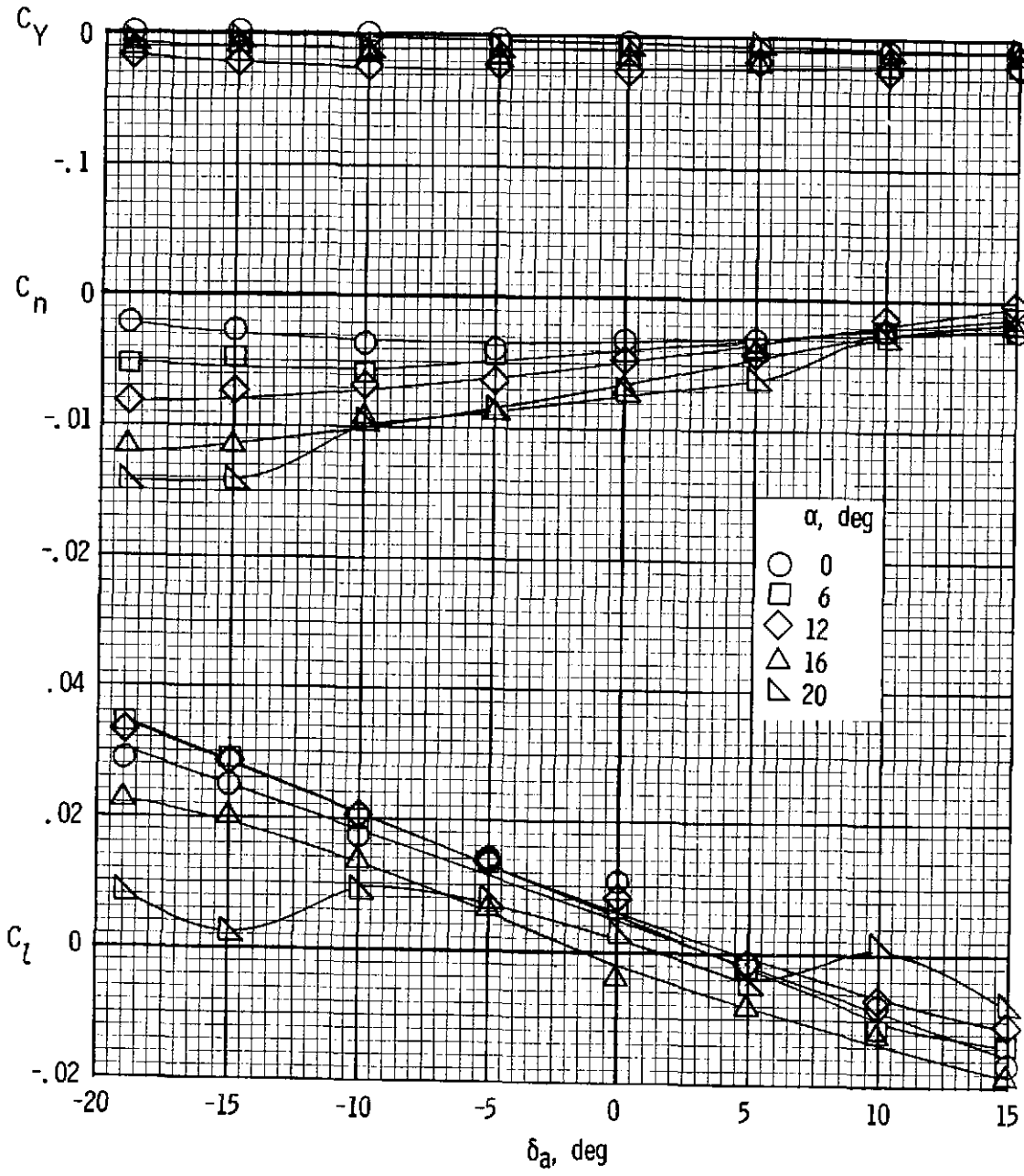

(c) $T_c' = 0.44$.

Figure 40.- Concluded.

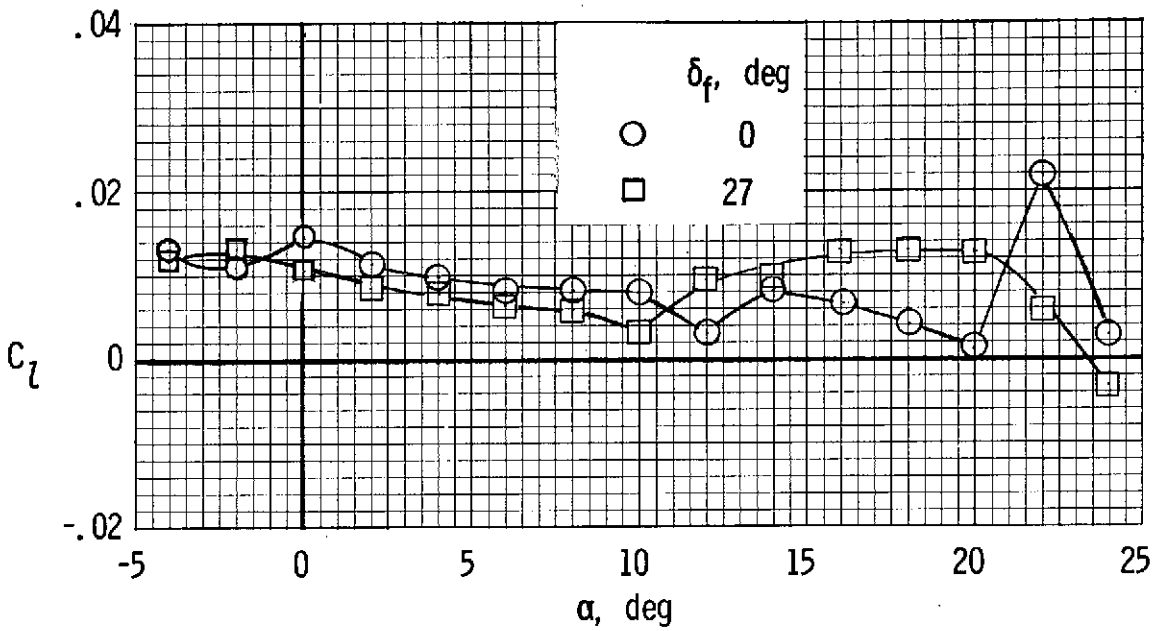

Figure 41.- Variation of rolling-moment coefficient with angle of attack for the basic leading-edge configuration with propellers removed.

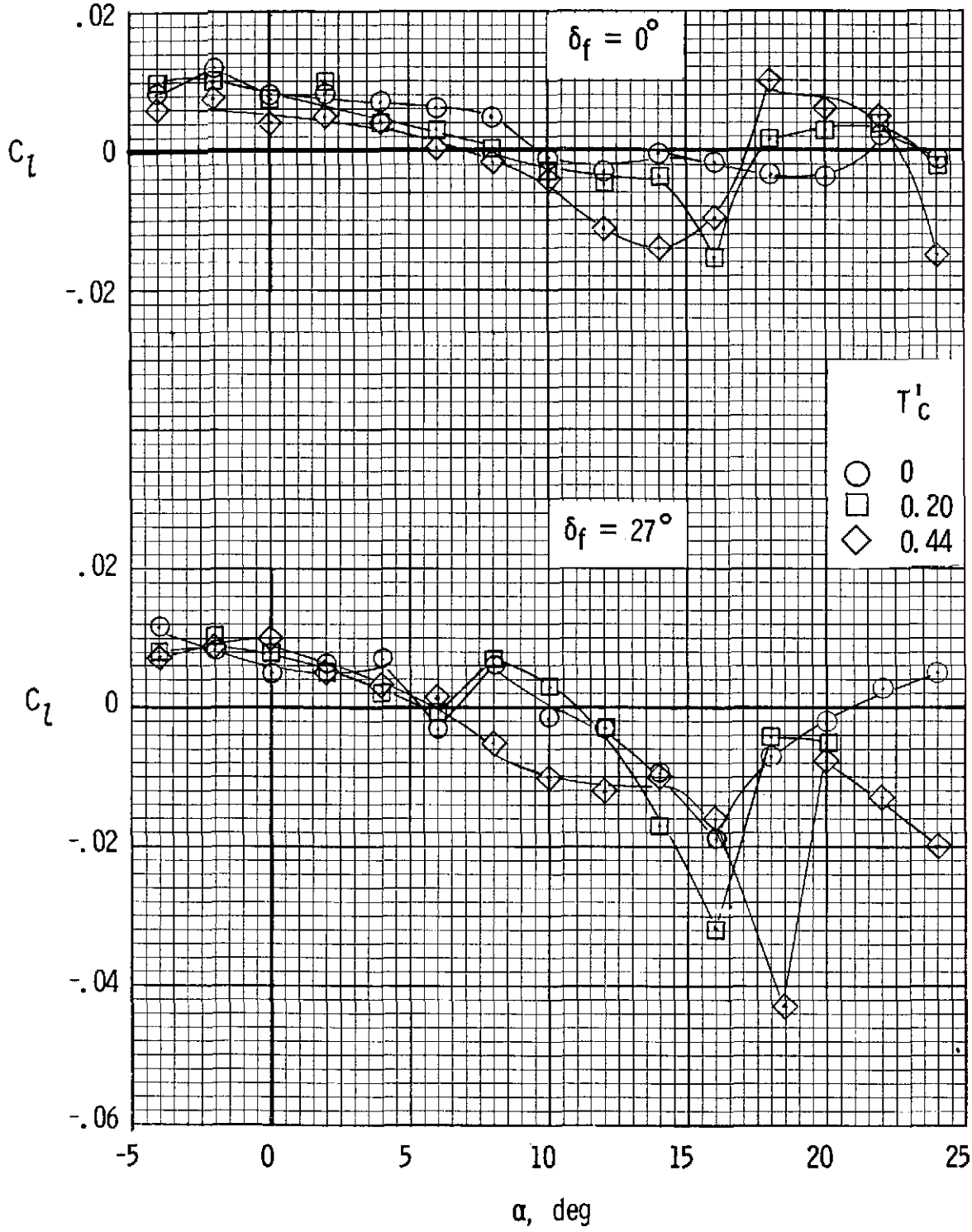

Figure 42.- Variation of rolling-moment coefficient with angle of attack for the basic leading edge at several power and flap conditions.

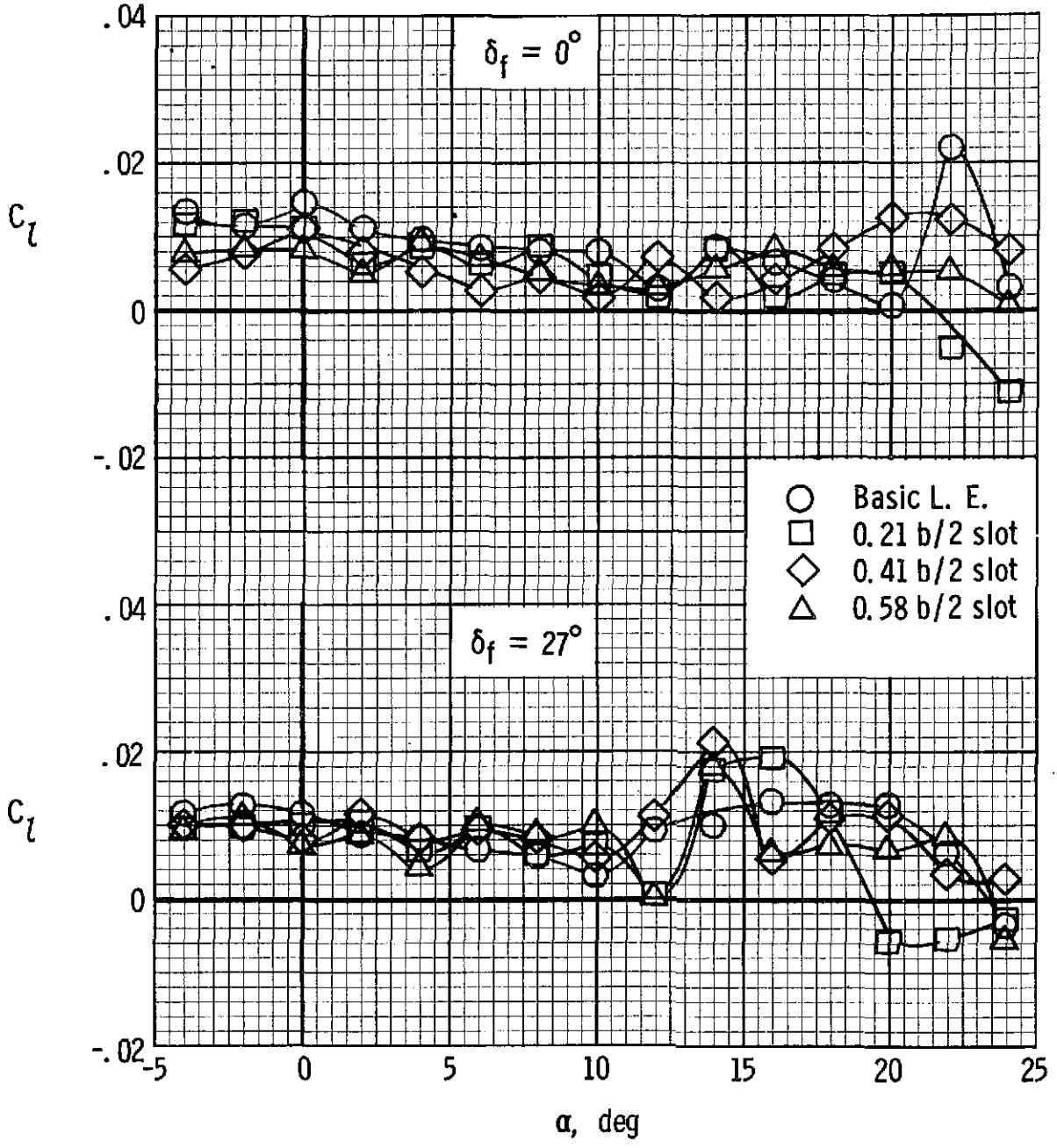

Figure 43.- Variation of rolling-moment coefficient with angle of attack for various leading-edge slots and flap deflections with propellers removed.

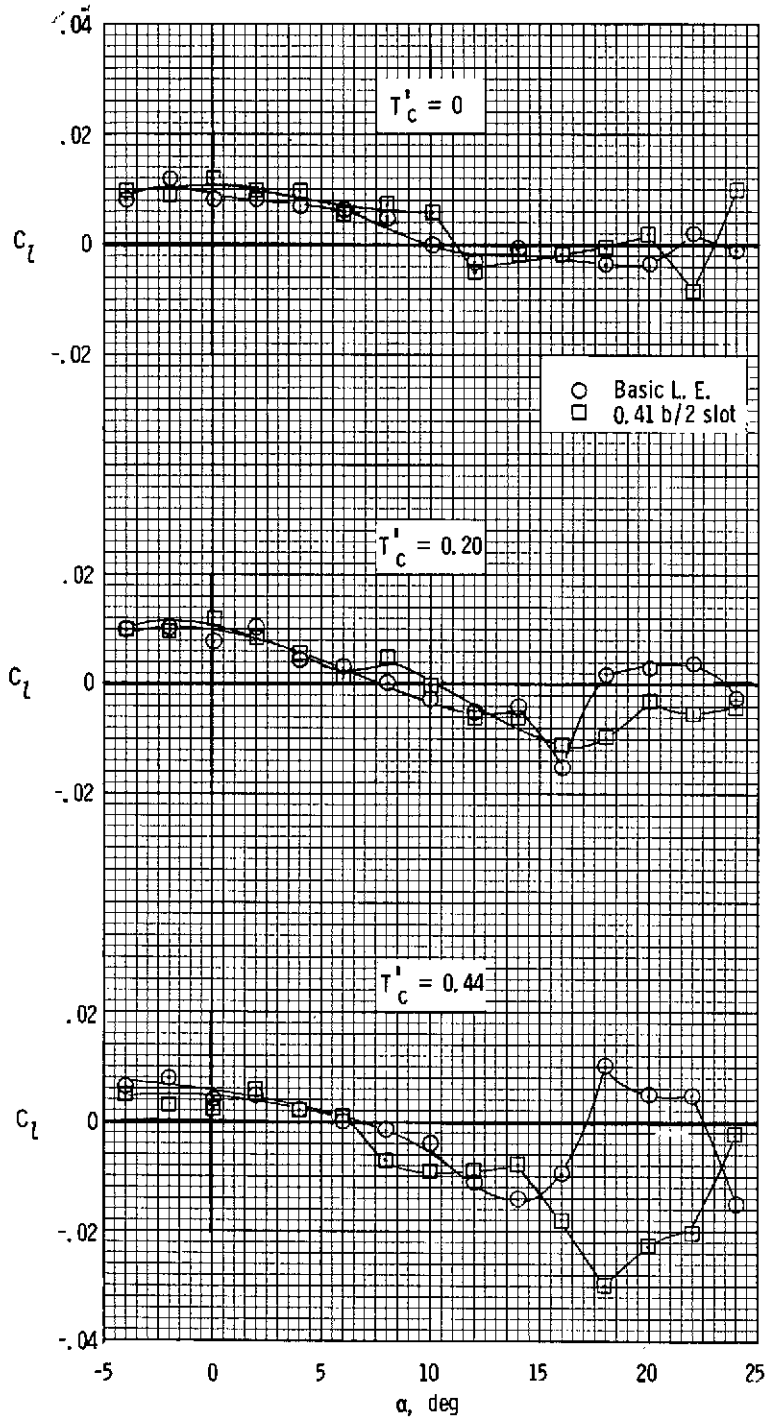

(a) $\delta_f = 0^o$.

Figure 44.- Comparison of rolling moments of basic leading edge with 0.41b/2 leading-edge slot at several power and flap conditions.

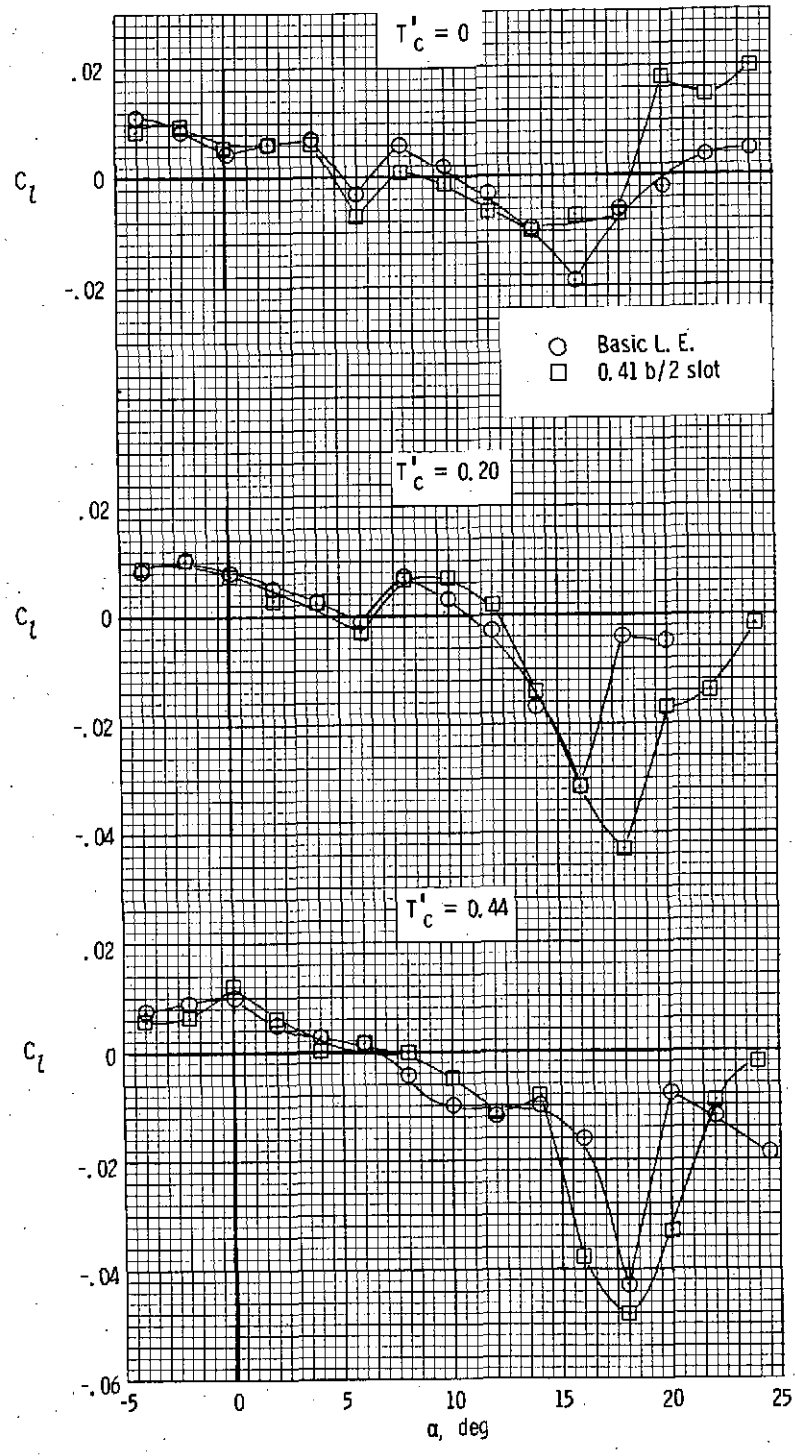

(b) $\delta_f = 27^o$.

Figure 44.- Concluded.

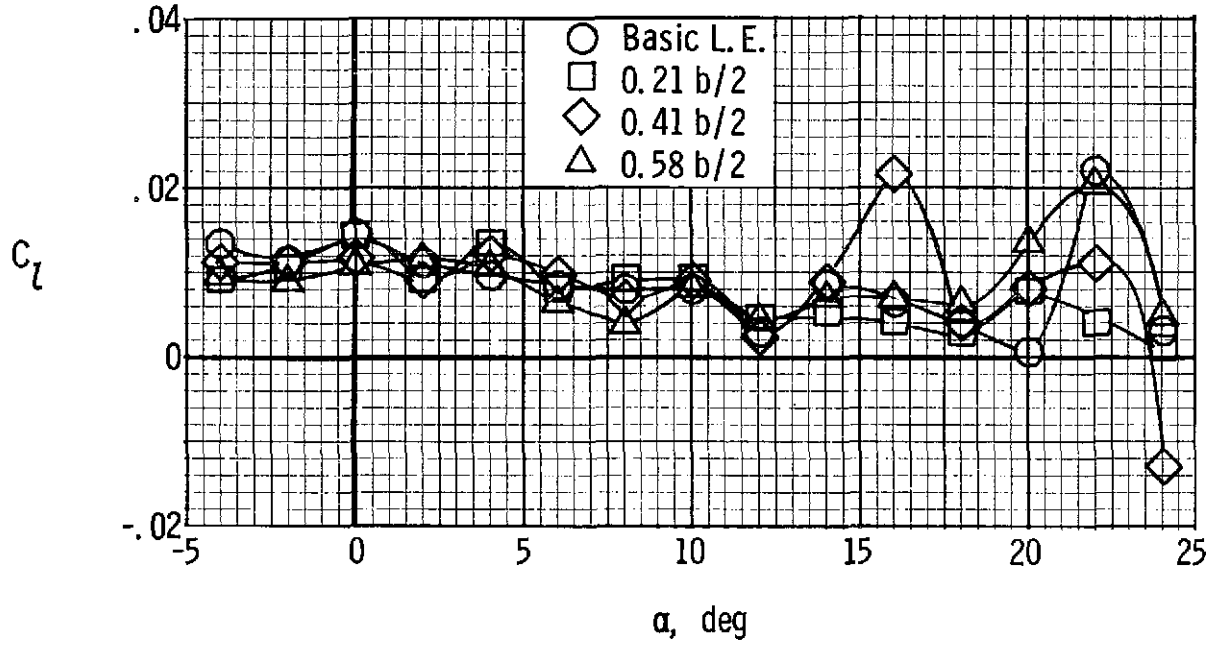

Figure 45.- Comparison of rolling-moment coefficients of basic leading edge with various auxiliary airfoils with the propeller removed. $\delta_f = 0^o$.

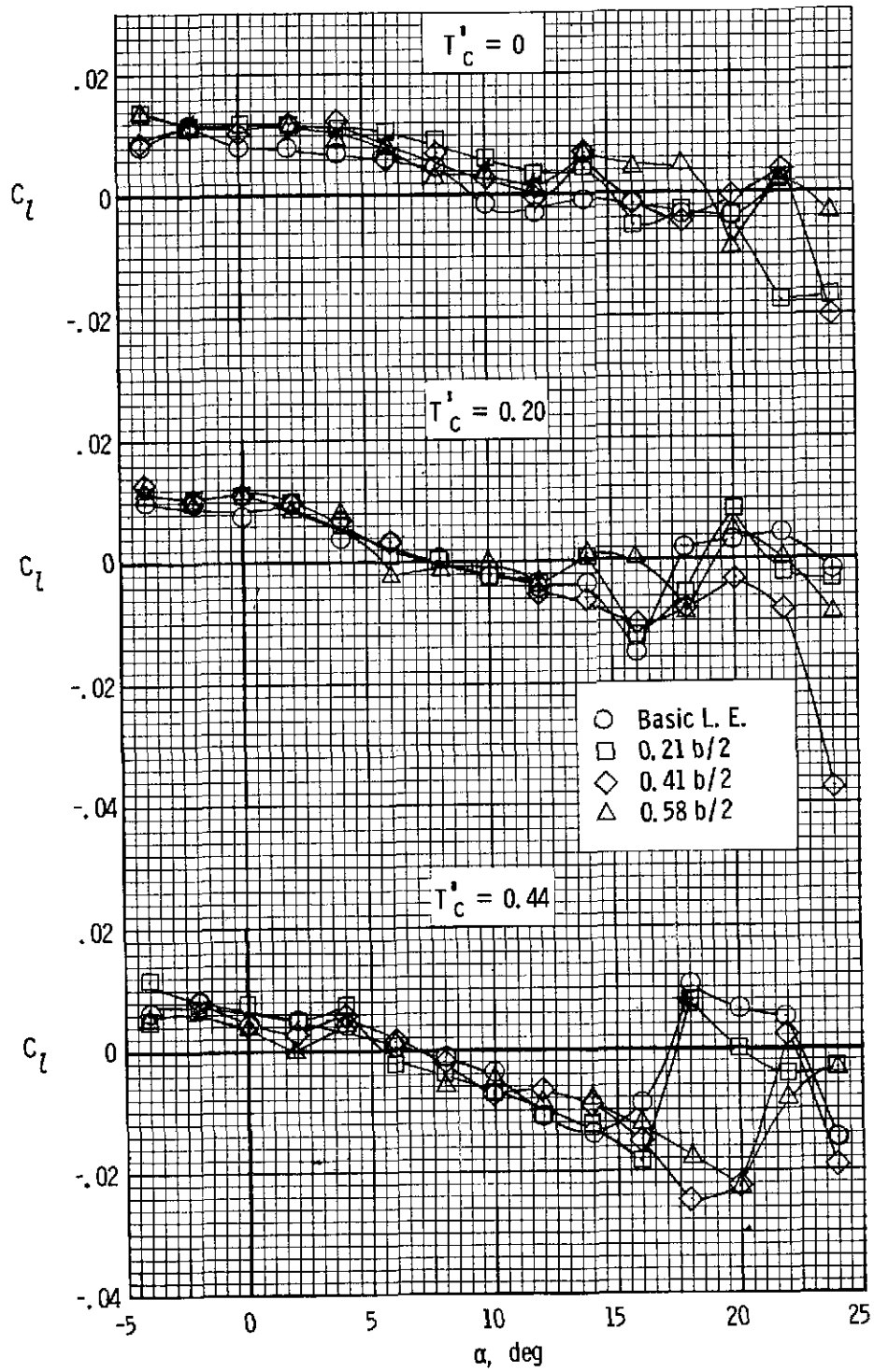

(a) $\delta_f = 0^o$.

Figure 46.- Comparison of rolling-moment coefficients of basic leading edge with various auxiliary airfoils for several power and flap conditions.

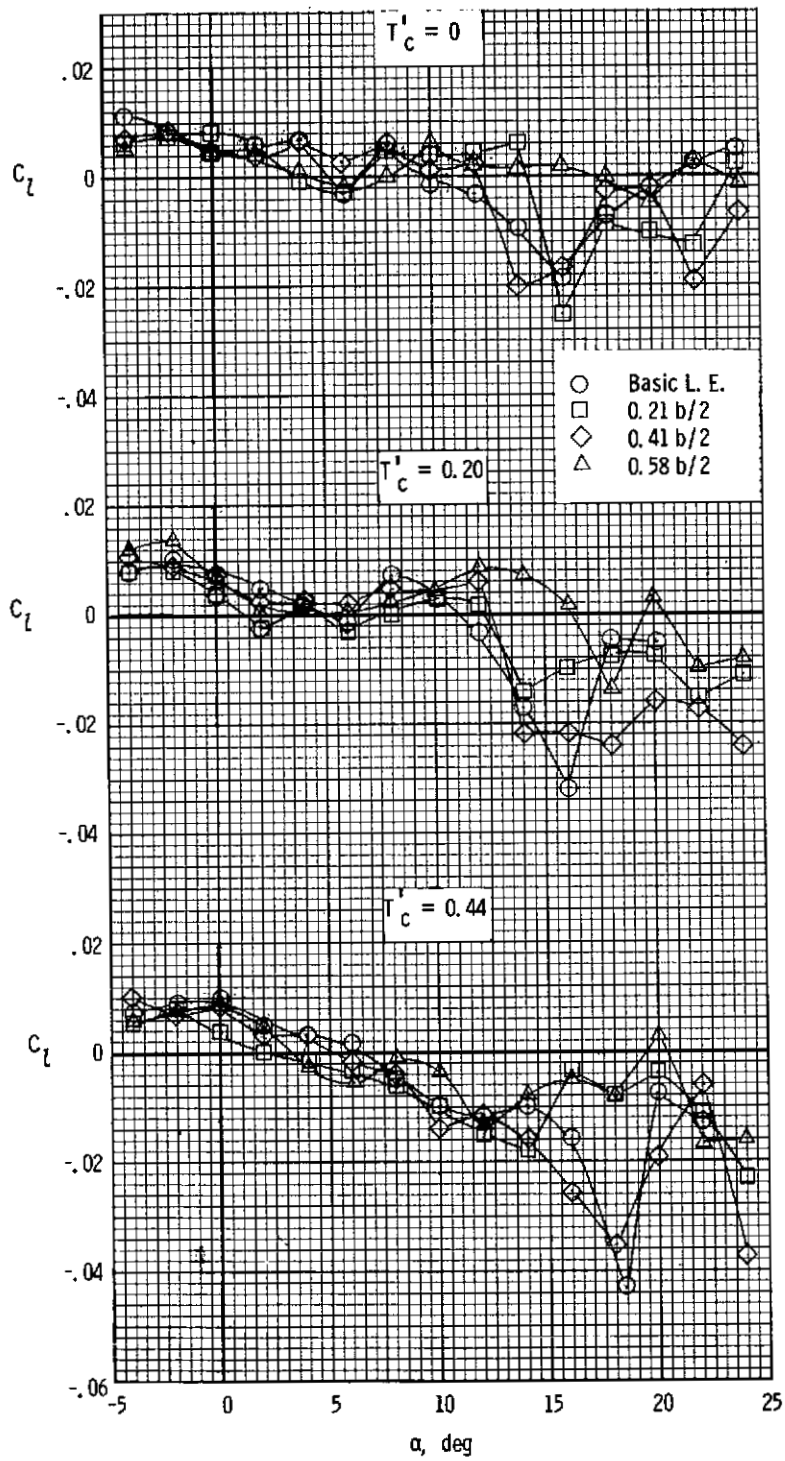

(b) $\delta_f = 27^o$.

Figure 46.- Concluded.

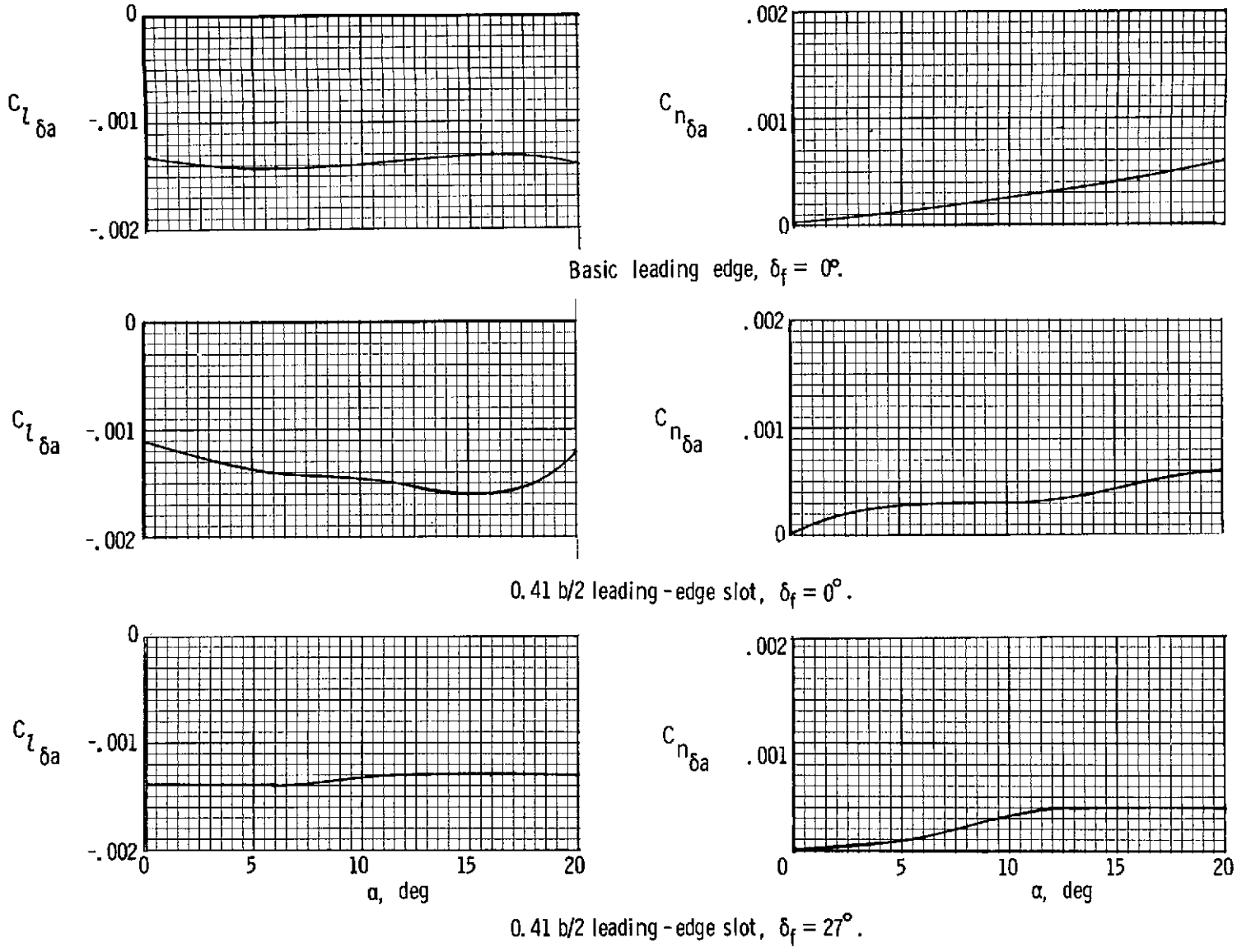

(a) Aileron effectiveness.

(b) Yawing moment due to aileron deflection.

Figure 47.- Aileron effectiveness and effect of aileron deflection on yawing moment with the propellers removed.

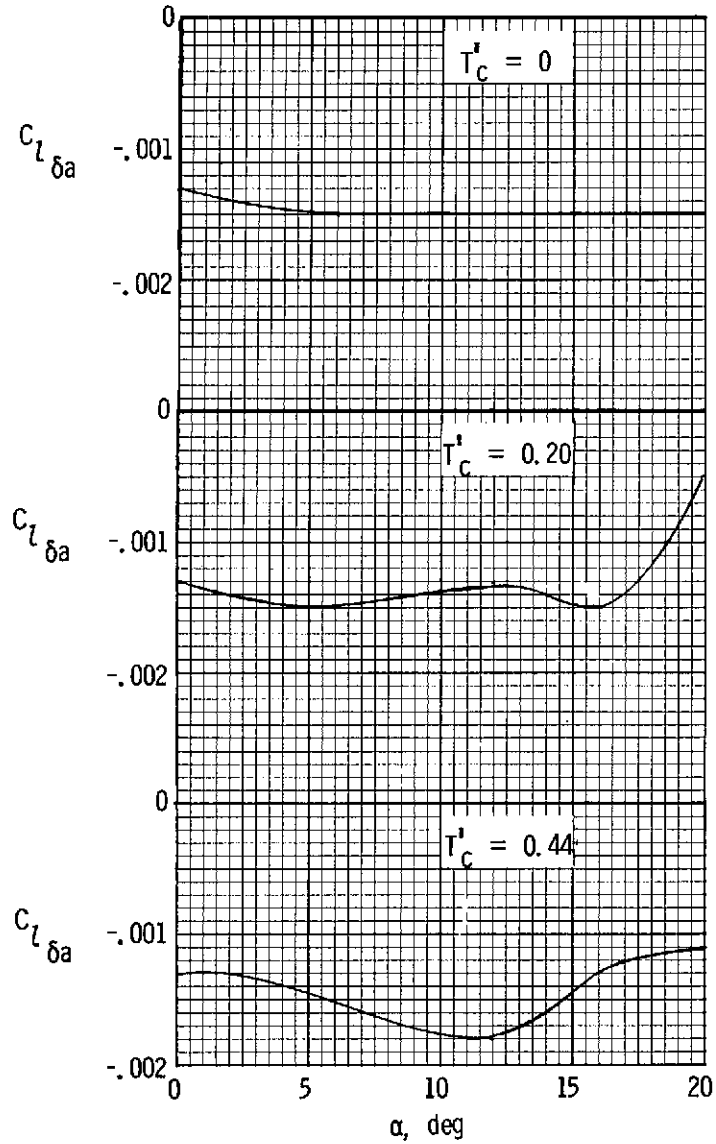

(a) $\delta_f = 0^o$.

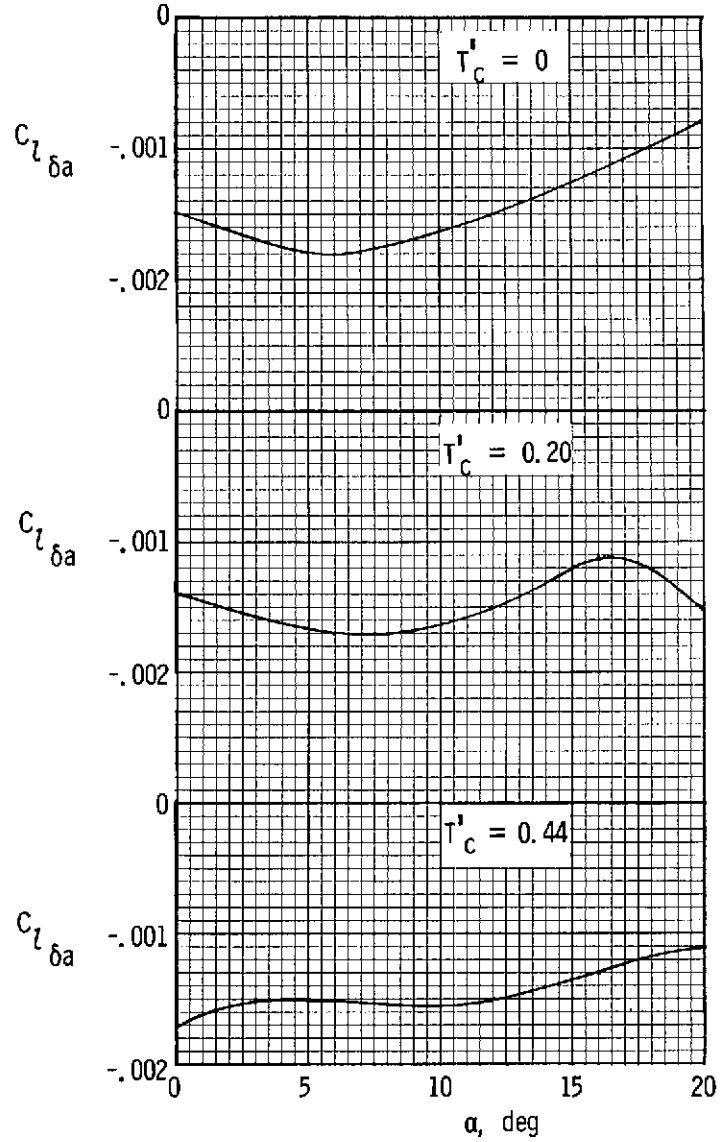

(b) $\delta_f = 27^o$.

Figure 48.- Aileron effectiveness with 0.41b/2 leading-edge slot at several power and flap settings.

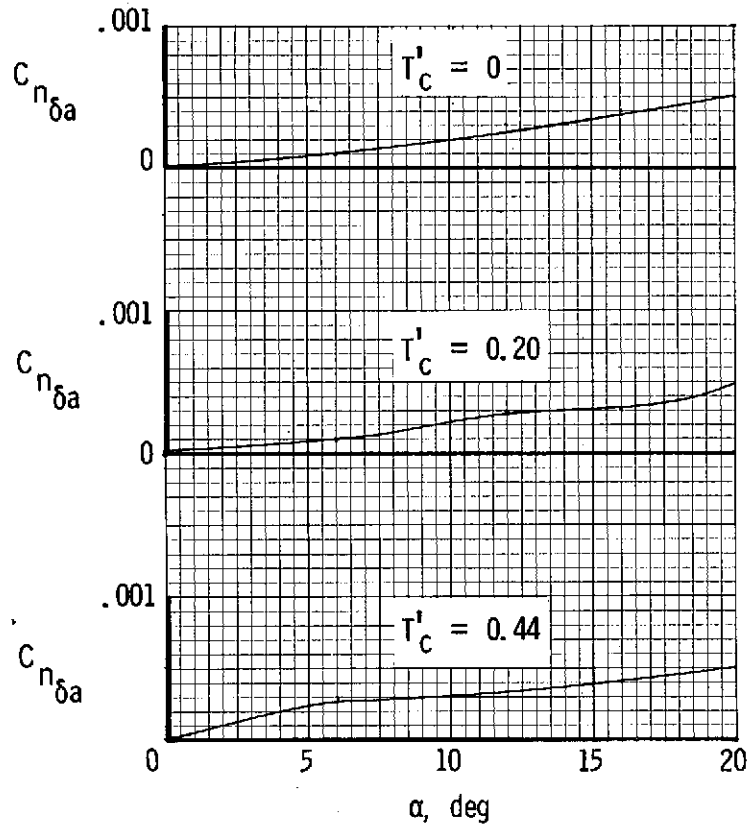

(a) $\delta_f = 0^o$.

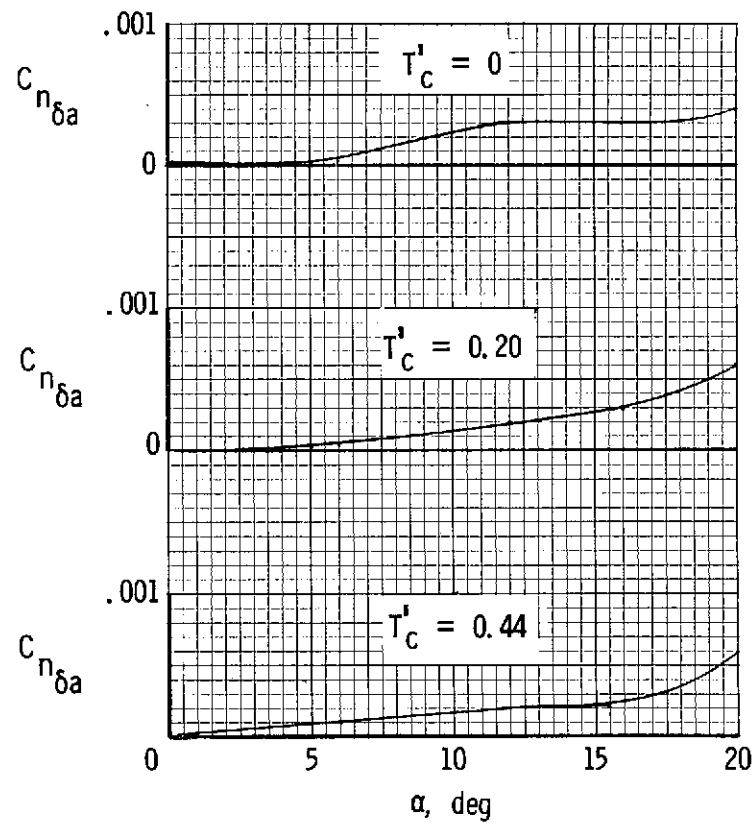

(b) $\delta_f = 27^o$.

Figure 49.- Effect of aileron deflection on yawing-moment coefficient with 0.41b/2 leading-edge slot.

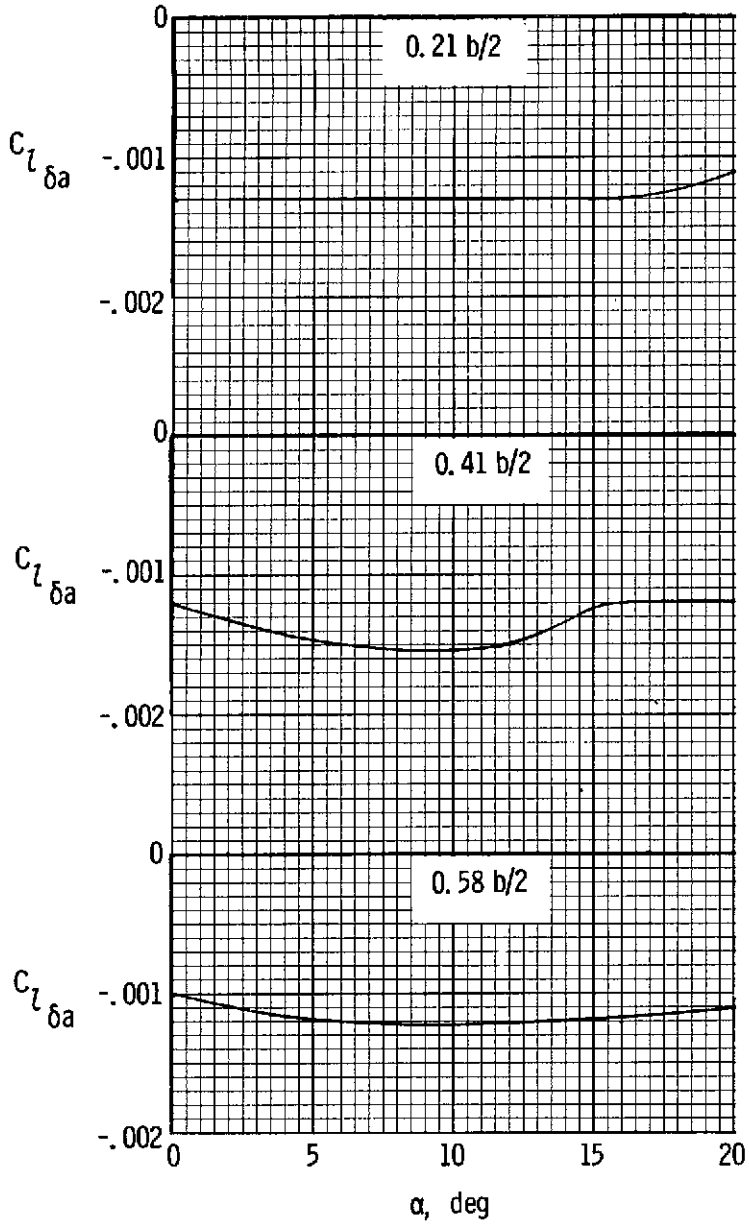

(a) Aileron effectiveness.

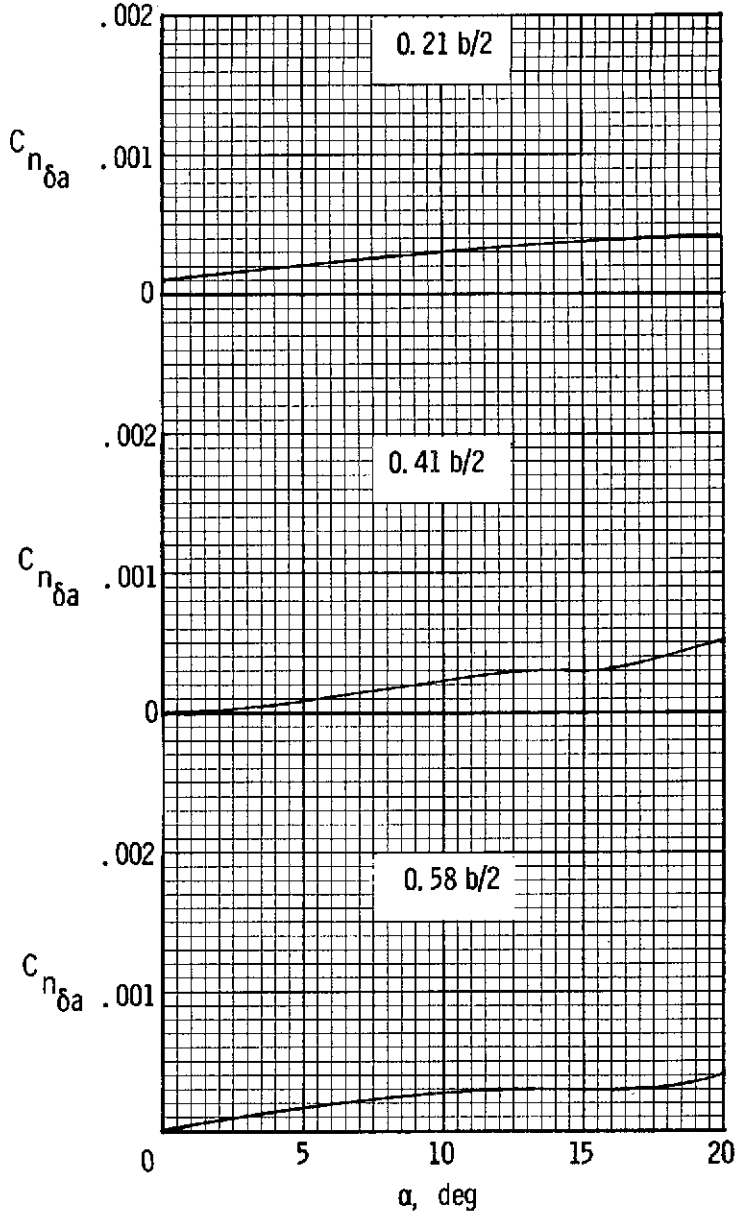

(b) Yawing moment due to aileron deflection.

Figure 50.- Aileron effectiveness and yawing-moment coefficient for various spanwise sections of the auxiliary airfoil with propellers removed. $\delta_f = 0^o$.

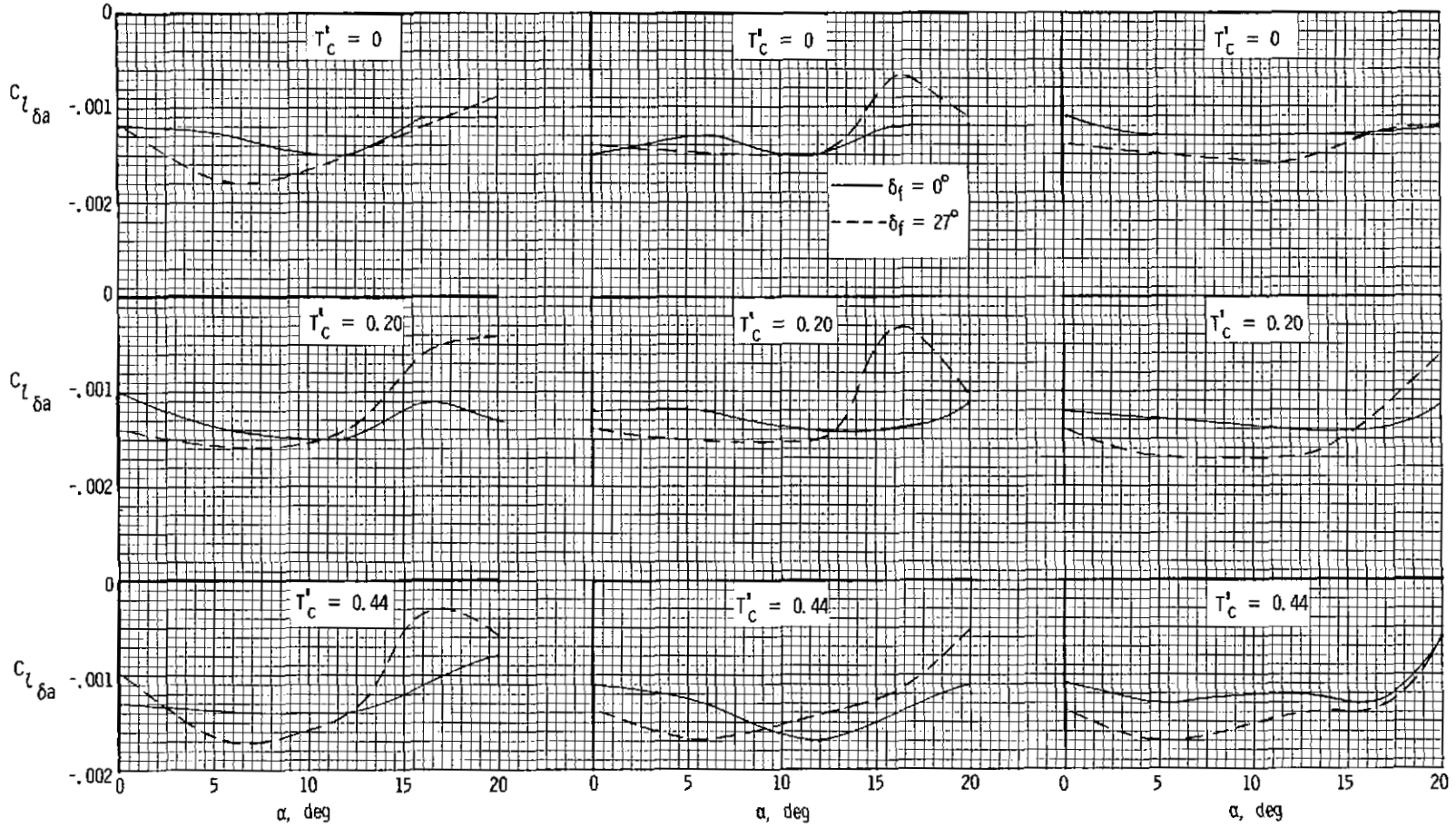

(a) 0.21b/2. (b) 0.41b/2. (c) 0.58b/2.

Figure 51.- Aileron effectiveness for various spanwise sections of the auxiliary airfoil with power.

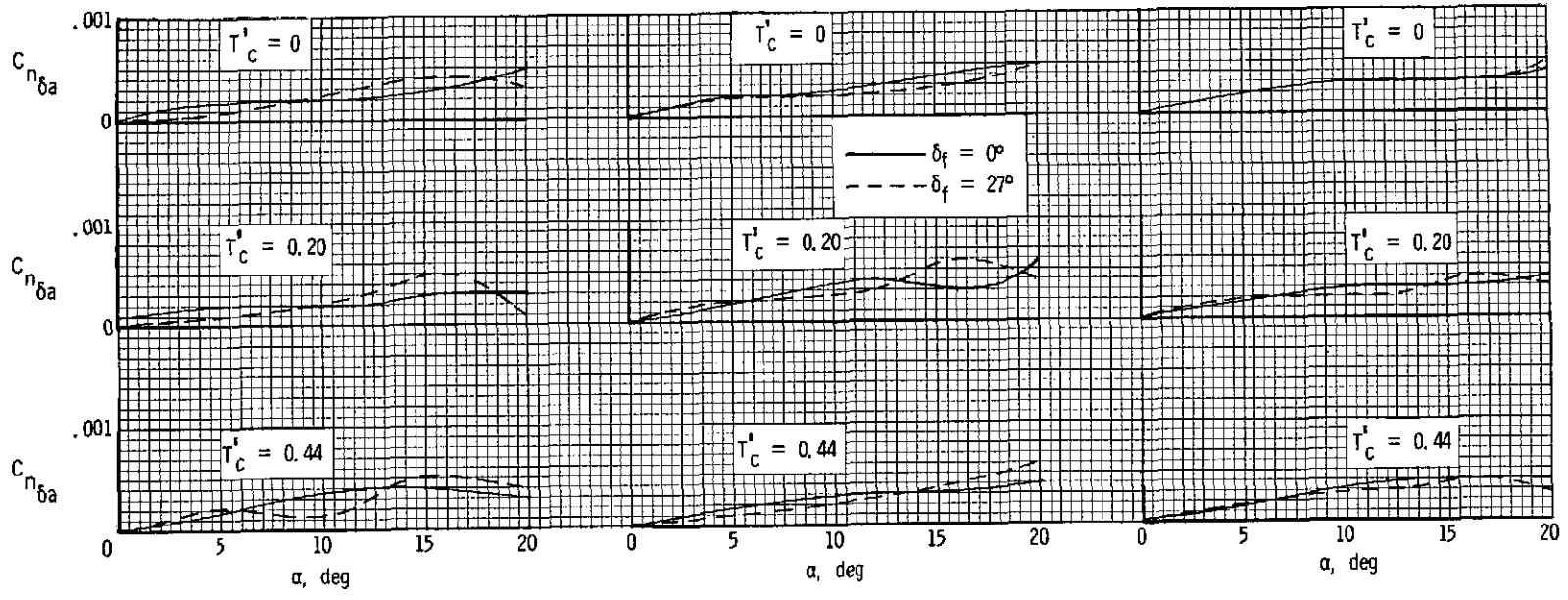

(a) 0.21b/2. (b) 0.41b/2. (c) 0.58b/2.

Figure 52.- Effect of aileron deflection on yawing-moment coefficient for various spanwise sections of the auxiliary airfoil with power.

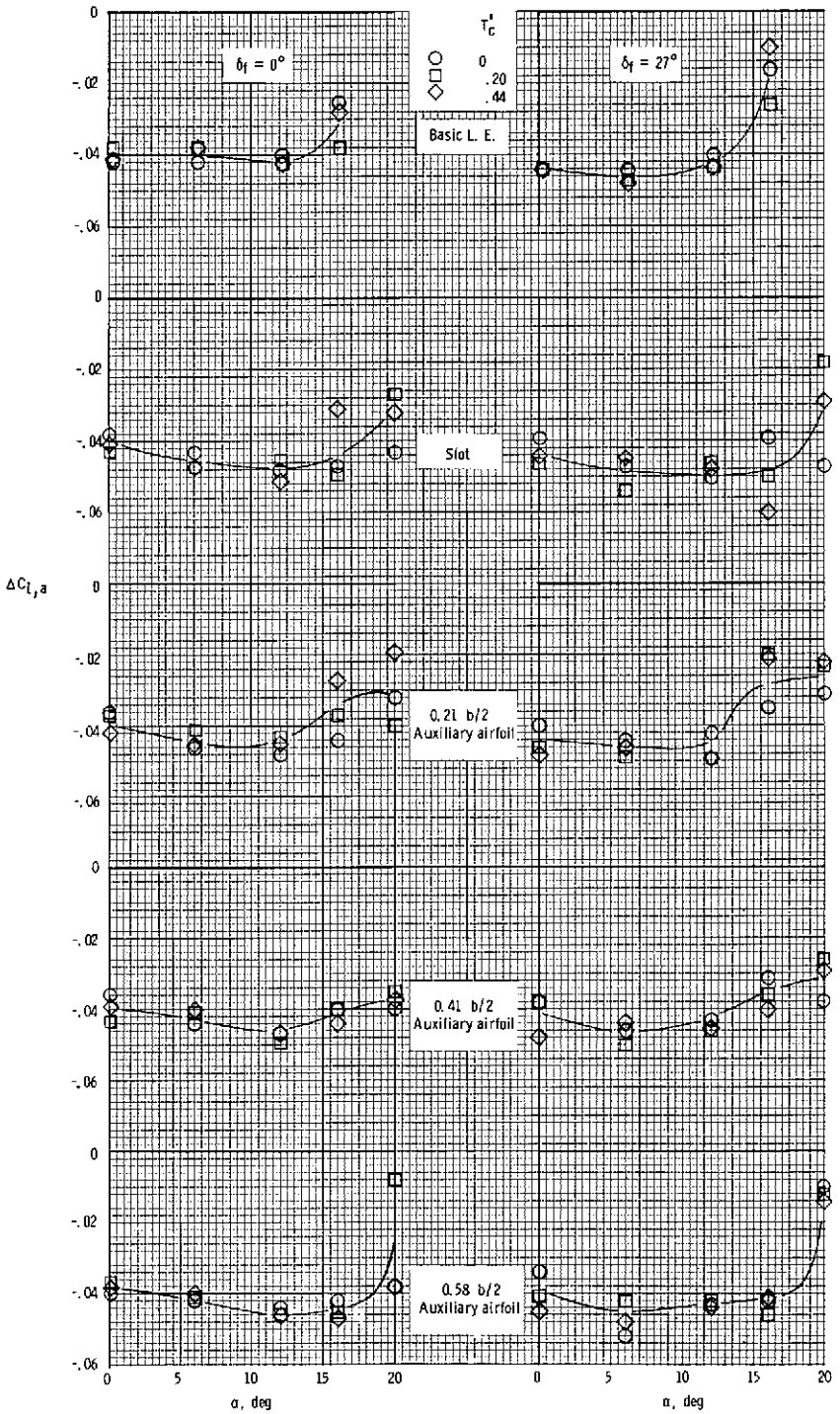

Figure 53.- Rolling moment due to full aileron deflection $\left(\delta_a = 15^o \text{ and } -19^o\right)$.